Journal of the American Society of Trace Evidence Examiners

Volume Number Six
Issue Number One
JANUARY 2015

www.asteetrace.org

JOURNAL OF AMERICAN SOCIETY OF TRACE EVIDENCE EXAMINERS

www.asteetrace.org
Volume Number Six, Issue Number One
January 2015
ISSN: 2156-9797

Robyn Weimer, M.S.
ASTEE Journal Editor
c/o Virginia Department of Forensic Science
700 North Fifth Street
Richmond, VA 23219
robyn.weimer@dfs.virginia.gov

The mission of ASTEE is to encourage the exchange and dissemination of ideas and information within the field of trace evidence through improved contacts between persons and laboratories engaged in trace evidence analysis. The journal of the American Society of Trace Evidence Examiners is a peer reviewed journal dedicated to the analysis of trace evidence. All original articles published in JASTEE have been subject to double-blind peer review.

INSIDE THIS ISSUE

JASTEE has established a working relationship with the Scientific Working Group for Materials Analysis (SWGMAT); whereby approved SWGMAT standards maybe published in *JASTEE*. These standards have been peer reviewed and approved by the SWGMAT group as a whole and thus were not subject to peer review through *JASTEE*.

JASTEE has also established a working arrangement with *The Microscope*, the journal established and edited by the McCrone Institute. Under this arrangement, articles published in *JASTEE* may be selected for publication in *The Microscope*, and vice versa.

Anne E. Kisler-Rao,[1] M.S.

Comparison of Nylon, Polyester, and Olefin Fibers Using FTIR and Melting Point Analysis

ABSTRACT

The primary goal of this study was to investigate whether Fourier transform infrared spectroscopy (FTIR) or melting point analysis provides higher discrimination of fibers when used for comparative purposes. Nylon, Polyester, and Olefin fibers from a reference collection were compared using both FTIR and melting point analysis and determinations were made as to which fibers within each generic class could be distinguished from one another using both techniques. Within each generic class, some fiber pairs were found to be distinguishable from each other using FTIR and not melting point and others using melting point and not FTIR. As these techniques are typically the last step in an analytical procedure, fibers found to be distinguishable by one technique and not the other were examined microscopically to determine if these fibers would have been distinguished from one another before reaching that point of the examination. The majority of fibers distinguishable by FTIR and not melting point or vice versa were found to be readily distinguishable using microscopy, with only one pair of colorless fibers possessing only minor differences in optical properties. This shows that while microscopy is typically the most useful technique for comparative analysis, it may be important to consider using both techniques of FTIR and melting point for comparative purposes as well.

Keywords: Fiber, Nylon, Polyester, Olefin, FTIR, melting point

INTRODUCTION

A typical fiber comparison involves going through a series of analytical steps to determine whether or not a questioned fiber could have come from a known source. The Scientific Working Group for Materials Analysis (SWGMAT) recommends the

[1] Georgia Bureau of Investigation, Division of Forensic Sciences, 3121 Panthersville Rd, Decatur, GA 30034

completion of at least two analytical techniques for each of the categories of generic class, physical characteristics, and color when performing a comparison (1). Analytical techniques to determine generic class include microscopic properties, polarized light microscopy, Fourier transform infrared spectroscopy (FTIR), thermal analysis, and a number of other miscellaneous techniques (1). This study intends to focus on two of these techniques, FTIR and thermal analysis. Both thermal microscopy and FTIR can be used for comparative purposes as well as determining generic class and subclass. While use of FTIR is widespread, thermal microscopy has been removed from many laboratories' schemes of analysis. As seen on a recent proficiency test administered by Collaborative Testing Services (CTS), only 10% of laboratories used melting point for the analysis of olefin and polyester fibers, while 95% used FTIR (6).

It is important to consider the destructive nature as well as discriminatory power of a technique when deciding what techniques to use in an analytical scheme. With regards to destructive nature, both FTIR and melting point require removing small portions of a fiber for analysis. With FTIR, the portion of fiber is typically flattened, and while the fiber could potentially be analyzed by FTIR again, comparative features such as cross section and diameter of the portion are destroyed. With melting point, once the portion of fiber is melted, this test cannot be performed on the portion of fiber again. Concerning discriminatory power, melting point can be of use when a fiber contains both nylon 6 and 6,6 (2) or both polypropylene and polyethylene (3), which can make interpretation of the FTIR spectrum difficult. Melting point can also differentiate between high density and low density polyethylene fibers (4). While both FTIR and melting point can be used to classify nylon fibers into subgroups such as nylon 6 and 6,6, melting point can further sub classify nylon fibers beyond 6 and 6,6, and thus can be used to supplement FTIR spectra (5).

The aim of this study is to determine if melting points can provide higher discriminating power than FTIR for certain fiber comparisons and evaluate whether forensic laboratories should consider including melting point in their analytical scheme. Conversely, this study will also provide additional data that FTIR has higher discriminating power than melting points in analysis of other types of fibers. Furthermore, if melting points are able to discriminate fibers not discriminated by FTIR (or vice versa), the question is asked if these fibers would have been discriminated by microscopy alone, as FTIR and thermal microscopy are often the last step in an analytical scheme.

METHODS AND MATERIALS

Nylon, polyester, and olefin samples from the Microtrace Forensic Fiber Reference Collection (5) were used for this study. A total of 46 nylon fibers, 52 polyester fibers, and 8 olefin fibers were compared. The fibers contained various levels of delustrant,

ranging from none to high levels. Various cross sections as well as diameters of fibers were represented. There were a limited number of dyed fibers present, with the majority of fibers being undyed.

Thermal Microscopy

Melting points were determined for all reference fiber samples using a Mettler FP82HT hotstage and FP90 processor (Mettler-Toledo, Inc, Columbus, OH). For each sample, a short length (up to a few millimeters) of the fiber was placed on a slide with a coverslip, inserted into the hotstage, and observed under crossed polars. Temperature was increased until a complete loss of interference colors was observed, and this was noted as the final melting point. Each fiber sample was run in triplicate and the results were recorded as a melting range for that sample.

The melting range for each fiber sample was compared to every other fiber sample in the same generic class (nylon, polyester, or olefin) to determine whether or not the ranges overlapped. The instrumental accuracy of $\pm$ 0.8ºC between 200 and 300ºC and $\pm$ 0.6ºC between 100 and 200ºC was accounted for when determining whether fibers were distinguishable. Fibers that had overlapping melting ranges (melting range of fiber $\pm$ 0.8ºC or $\pm$ 0.6ºC as appropriate) were categorized as indistinguishable by melting point, and results were recorded.

FTIR

FTIR analysis was performed on all reference fiber samples using a Nicolet 4700 FTIR spectrometer with a Continuum microscope (Thermo Nicolet, Madison, WI). Each sample was flattened and placed on a KBr substrate for FTIR analysis. The spectra were collected using 64 scans at 4 cm^{-1} resolution with a MCT/A detector. A minimum of three spectra were collected for each reference sample.

FTIR spectra for each fiber sample were compared to every other fiber sample in the same generic class to determine if they could be distinguished from one another and results were recorded.

Microscopy

After thermal microscopy and FTIR were complete, fibers which were distinguishable by one method but not the other were further examined using transmitted light and polarized light microscopy. Color, cross section, relative amount of delustrant (none, low, medium, high), and diameter were recorded for each fiber sample. Fiber samples that were close in all four categories were examined together using comparison microscopy to determine if they could be distinguished from one another.

Fibers that were indistinguishable using transmitted light microscopy were compared using polarized light microscopy followed by fluorescence microscopy. Three different fluorescence cubes were used for this analysis: UV, UV/VIO and BLUE.

RESULTS

Information provided by the reference collection (5) is listed in Table 1 along with melting points that were determined for each fiber sample.

Table 1 Sample Information and Melting Points

Microtrace Sample #	Class or subclass	Manufacturer, Trade Name	Remarks	Melting Point (°C)
74	Nylon 6	Allied Signal fibers, 1392 MBX	PA-6 Non-textured feeder yarn. It has not been cabled twisted or heat set. 1 of 7 in a series of fiber processing techniques.	221.2-222.2
75	Nylon 6	Allied Signal fibers, 1392 MBX	PA-6 2-ply cabled yarn. It has not been heat set. 2 of 7 in a series of fiber processing techniques.	221-223.8
76	Nylon 6	Allied Signal fibers	PA-6 2-ply cabled and autoclave heat set yarn. 3 of 7 in a series of fiber processing techniques.	221.4-223.5
77	Nylon 6	Allied Signal fibers	PA-6 Superba heat set 1190d. Carpet yarn. No after treatment. 4 of 7 in a series of fiber processing techniques.	219.9-222.6
78	Nylon 6	Allied Signal fibers	PA-6 Superba heat set 1190d. Carpet yarn, dyed w/ a typical acid dye. 5 of 7 in a series of fiber processing techniques.	222.1-223.0
79	Nylon 6	Allied Signal fibers	PA-6 Superba heat set 1190d. Carpet yarn. Dyed, treated w/ stainblocker. 6 of 7 in a series of fiber processing techniques.	221.9-222.2
80	Nylon 6	Allied Signal fibers	PA-6 Superba heat set 1190d. Carpet yarn. Dyed, treated w/ stainblocker, fluorocarbon process. 7 of 7 in a series of fiber processing techniques.	222.0-222.4
81	Nylon 6	Allied Signal fibers, 1220 MBX	PA-6 Trilobal w/ 3 holes. BCF	221.3-222.5
82	Nylon 6	Allied Signal fibers, Hydrofil®	PA-6 A highly absorbent, quick drying fiber used for outerwear, gloved, hats, activewear	215.2-217.8
83	Nylon 6	Allied Signal fibers, Patina™	PA-6Pentalobal X.S. 20d./12fils. Use: lingerie. Fabric	220.6-221.7
84	Nylon 6	Allied Signal fibers, T-260	PA-6 Trilobal X.S.	221.1-222.0
85	Nylon 6	Allied Signal fibers, T-511	PA-6 Trilobal X.S.	221.1-222.0
86	Nylon 6	Allied Signal fibers, T-716	PA-6 Trilobal X.S.	220.9-221.6
87	Nylon 6	BASF	PA-6 Trilobal X.S. BASF Automotive Solution Dyed Nylon Staple. Pigments: carbazole red, perylene violet, carbon black	224.3-225.4
88	Nylon 6	BASF, H110S	PA-6 Solution dyed. Pentagonal, hollow, 6 hole X.S. 17.4dpf, BCF. Multicolor	220.9-222.7
117	Nylon 6	Shaw Industries	PA-6 Dyed Mauve. Trilobal X.S. 1452d. Yarn (64f)	222.4-222.6
118	Nylon 6	Snia, Lilion®	PA-6 Trilobal X.S. 9.3dtex x 165mm staple	221.0-222.8
89	Nylon 66	Du Pont 266AS	PA-66 Trilobal X.S. 1365d. BCF.	252.7-254.0
90	Nylon 66	Du Pont 426A	PA-66 Trilobal X.S. 1340d. BCF.	253.4-254.0
91	Nylon 66	Du Pont 496A	PA-66 Square 4 hole X.S. 1245d. BCF.	253.5-255.4
92	Nylon 66	Du Pont 566	PA-66 Trilobal X.S. 1005d. BCF.	253.9-257.7
93	Nylon 66	Du Pont 576	PA-66 Trilobal X.S. 1105d BCF.	252.9-254.0
94	Nylon 66	Du Pont 608	PA-66 "Michelin Man" trilobal X.S. 1405d. BCF	253.6-257.2
95	Nylon 66	Du Pont 696AS	PA-66 Trilobal X.S. 1150d. BCF.	254.2-255.1
96	Nylon 66	Du Pont 746	PA-66 Trilobal X.S. 1700d. BCF.	255.0-256.9

97	Nylon 66	Du Pont, Microsupplex™	PA-66 Microfiber. Dyed yellow. Fabric. Small denier allows for fabrics to be made with twice the wind resistance of standard nylon. Uses: rainwear, sports apparel	259.8-260.2
98	Nylon 66	Du Pont Optique™ Stainmaster™ Yarn	PA-66 DuPont color: Prairie. Carpet yarn with mixed X.S. and M.R. Smooth dull luster. Use: mid-high end marketing carpeting	257.0-257.7
99	Nylon 66	Du Pont P1136	PA-66 Trilobal "Jacks" X.S. 1400d BCF	253.0-255.3
100	Nylon 66	Du Pont P1232	PA-66 Trilobal "Jacks" X.S. Semi-dull 750d BCF	251.1-251.9
101	Nylon 66*	Du Pont P1237 Footlights™	PA-66 Trilobal X.S. w/ variable M.R. Zinc sulfide causes fiber to luminesces green. 1295d. BCF	220.9-221.3
102	Nylon 66	Du Pont P1261	PA-66 Trilobal X.S.1395d. BCF.	254.4-255.2
104	Nylon 66	ICI, Quintesse® T323	PA-66 Circular X.S. 3.3dtex. Staple. Outer Clothing	255.7-257.2
105	Nylon 66	ICI, Tactel® K000	PA-66 Trilobal X.S. BCF. Trade name now owned by DuPont	257.0-257.6
107	Nylon 66	Monsanto T0660	PA-66 Trilobal X.S. Staple	254.6-256.0
108	Nylon 66	Monsanto, T0802	PA-66 Trilobal X.S. Mixed denier and M.R. carpet yarn. Staple	254.1-255.8
109	Nylon 66	Monsanto, T0810	PA-66 Round X.S. Staple	261.8-262.9
110	Nylon 66	Monsanto, T0811	PA-66 Trilobal X.S. Staple	253.6-255.2
111	Nylon 66	Monsanto, T08DV	PA-66 Trilobal X.S. Staple	255.3-255.7
112	Nylon 66	Monsanto, T1184	PA-66 Trilobal X.S. Staple	255.7-256.7
113	Nylon 66	Monsanto, T1943	PA-66 Trilobal X.S. Staple	254.9-257.0
114	Nylon 66	Monsanto, T19DV	PA-66 Delta X.S. Staple	255.3-256.3
115	Nylon 66	Monsanto, T2082	PA-66 Trilobal X.S. Staple	256.2-256.7
116	Nylon 66	Monsanto, T2093	PA-66 Trilobal X.S. Staple	256.8-257.6
119	Nylon 66	Wellman, Inc.	PA-66 Round X.S. Semi-dull 18dpf. X 5.25" staple M.P. =255C	259.4-261.0
120	Nylon 66	Wellman, Inc.	PA-66 Round X.S. Semi-dull 18dpf. X 7.5" staple M.P. =255C	258.0-258.4
103	Nylon	Du Pont, Qiana® T472	Special PA. Dyed Orange. Trilobal w/ variable M.R. Fabric. Obsolete	273.6-277.0
106	Nylon	Monsanto, Monvelle®	PA/PU bicomponent. Staple. Obsolete	222.9-224.4
173	Nylon	ICI, Timbrelle®	Mélange dyed.	258.3-260.6
132	Polyester	Albany International, Primaloft®	PET-microfiber. Mixture of microfibers (0.5d.) and supporting macrofibers.	260.7-261.7
133	Polyester	Allied Signal Fibers, Poly(ethylene naphthenate)	Drawn PEN. Circular X.S. BCF.	278.0-279.8
135	Polyester	Bayer, Vestan® 16	PCDT. Staple	287.4-289.7
136	Polyester	Du Pont, Coolmax®	White. Tetra-channel X.S 100% Dacron	256.9-262.8
137	Polyester	Du Pont, Dacron® 242	Normal PET Elongated 35%. Octalobal X.S. Semi-dull. BCF	257.6-259.6
138	Polyester	Du Pont, Dacron® 50T	Normal PET Draw elongated 123%. Round X.S. Semi-dull BCF	263.4-265.1
139	Polyester	Du Pont, Dacron® 56T	Normal PET. Polygonal X.S. due to texturing process. POY. BCF	261.3-262.2
140	Polyester	Du Pont, Hollofil #76®	Not dyeable. 100% Dacron PE fiber. Hollow X.S. Staple Diameter larger than Hollofil II. Fiber fluoresces with UV excitation	258.7-260.1
141	Polyester	Du Pont, Hollofil 808®	4 hole X.S. 5.5d. X 2" staple. Made from 100% pre-consumer recycled PET	255.8-256.6
142	Polyester	Du Pont, Hollofil II®	Not dyeable. Hollow X.S. Staple. 100% Dacron PET fiber. Fiber fluoresces	260.0-261.1
143	Polyester	Du Pont, Quallofil®	4 hole X.S. 5.5d. X 3" staple	264.5-267.1

144	Polyester	Enka, Encron®	Plyloc process Texturized. Semi-dull. BCF	264.2-268.0
145	Polyester	Enka, Encron® 8	Plyloc process. Octalobal X.S. BCF	263.8-264.1
146	Polyester	Fiber Extrusion, F931	Clear 6d. X 2" staple	255.4-258.3
147	Polyester	Fiber Extrusion, F935	Black 6d. X 3" staple	251.6-257.5
148	Polyester	Fiber Extrusion, F939	Semi-dull. 6d. X 3" staple	257.0-258.0
149	Polyester	Grilon SA, Grilene® W	Normal PET. Raw White. Bright. 17dtex x 80mm staple. Wool type	256.5-257.5
150	Polyester	Grilon SA, Grilene® W	Normal PET. Raw White. Semi-dull. 4.4dtex. Staple	256.2-257.0
151	Polyester	Hoechst, Trevira® 120	Standard PET. Bright + Optical brightener. 1.2d. X 30mm staple.	260.3-265.1
152	Polyester	Hoechst, Trevira® 210	Carrier free deep dyeable. 3.6dtex. Staple. Modified wool type	259.7-261.2
153	Polyester	Hoechst, Trevira® 350	Modified PET. Staple. Low pill, low tenacity	237.3-239.9
154	Polyester	Hoechst, Trevira® 353	Normal PET. Trilobal X.S. Bright. 4dtex x 60mm staple.	263.3-264.2
155	Polyester	Hoechst, Trevira® 525	Special type PET (100%) from dull raw material. Octalobal X.S 167dtex	262.8-264.1
156	Polyester	Hoechst, Trevira® 550	Modified PET, high shrink. Dull. 3.6dtex. Staple. Low M.P.	237.0-237.9
157	Polyester	Hoechst, Trevira® 561	Normal PET. Jet set. Dyed Red. Trilobal X.S. 150dtex. F72.	266.9-270.3
158	Polyester	Hoechst, Trevira® 561	Jet set. Dyed red. 110dtex. Yarn(48f)	262.4-264.4
159	Polyester	Hoechst, Trevira® 610	Standard type. Dull	262.5-264.0
160	Polyester	Hoechst, Trevira® 630	Modified PET. Disperse dyeable. Dull. 150dtex. Low M.P. Z twist yarn(f20)	245.4-250.6
161	Polyester	Hoechst, Trevira® 640	Modified PET. Yarn. Cationic dyeable. Low M.P	248.6-249.4
162	Polyester	Hoechst, Trevira® 661	Normal PET. Dyed Red. Yarn	264.3-265.8
163	Polyester	Hoechst, Trevira® 684	Normal Pet. Cotton type. Yarn.	262.0-262.8
164	Polyester	Hoechst, Trevira® 810	PBT. 17dtex x 150mm staple.	225.1-225.9
165	Polyester	Hoechst, Trevira® 813	PBT. Trilobal X.S. 6.7d. X 150mm staple.	225.0-225.9
166	Polyester	Hoechst, Trevira	Normal PET. Texturized. Blue dyed. Yarn	262.2-262.5
167	Polyester	Hoechst Celanese, #2359 - Bicomponent	Polyester core, co-polyester sheath. 2.0d. X 1.5" staple	258.3-264.8
168	Polyester	Hoechst Celanese, T295	Pentalobal. 6.0d. Staple	259.0-259.3
169	Polyester	ICI, Mitrelle® K1010	Normal PET. Filament	264.5-265.4
170	Polyester	ICI, Mitrelle® silk fabric	Normal PET. Dyed Purple. Yarn	267.8-268.3
171	Polyester	ICI, Terinda® Suede Fabric	Normal PET. Dyed red. Fabric	259.1-261.6
172	Polyester	ICI, Terinda® T5001	Normal PET. Filament	256.7-257.6

174	Polyester	ICI Fibers, Epitropic® PET Type 745	Conductive fiber. Carbon coated. 3.3dtex x 75mm staple. Obsolete	257.9-260.4
175	Polyester	Shaw Industries	Griege. 1455d. Yarn(80f)	262.3-264.9
176	Polyester	Shaw Industries	Beige. 1460d. Yarn(80f)	260.0-260.4
177	Polyester	Snia, Wistel® C	Normal PET. 13.2dtex x 60mm staple	261.2-262.0
178	Polyester	Snia, Wistel® S	Normal PET. 13.2dtex x 60mm staple	260.7-261.4
179	Polyester	Unitika, A-Telluna®	Copolymer terephthalic acid + ethylene glycol + p-hydroxybenzoic acid. Staple	233.5-234.0
180	Polyester	Unitika, H 38	Conjugate: 2 types of PET. Hollow X.S. Staple for wadding	260.3-261.6
181	Polyester	Unitika, P 68	Conjugate: 2 types of PET. Trilobal X.S. Staple	260.5-261.9
182	Polyester	Wellman, Heptalobal	Heptalobal X.S. POY. BCF	259.9-260.7
183	Polyester	Wellman, PET	Recycled polyester	254.7-255.6
184	Polyester	Wellman, Inc.	Non-carrier dye. Bright. Trilobal X.S. 12dpf. Staple	255.2-255.6
185	Polyester	Wellman, Inc.	Bright. Trilobal X.S. 15dpf. X 7.5 staple. M.P 250C	255.3-256.5
121	Olefin PP	Hercules Inc., T-150	Polypropylene. Gray. Swollen Delta X.S. 20dpf. Staple	167.6-168.9
122	Olefin PE	Hoechst Celanese, Certran® HMPE	High Molecular Weight Polyethylene. High strength, high crystallinity. BCF	140.3-141.0
123	Olefin PP	Phillips, Marvess®	Polypropylene. White. Delta X.S. 300d. BCF	165.7-166.4
124	Olefin PP	Phillips, Marvess®	Polypropylene. Textured. Round X.S 420d. Actual X.S. is polygonal due to the false twist texturing process. BCF.	165.5-166.3
125	Olefin PP	Phillips, Marvess®	Polypropylene. Phillips color: natural. Y modified X.S. 300d. BCF	165.1-166.7
126	Olefin PP	Shaw Industries	Polypropylene. Solution dyed green. Delta X.S. 1802 X.S. Yarn(120f)	167.6-169.8
127	Olefin PP	Shaw Industries	Polypropylene. White. Delta X.S. 2600d. Yarn(120f)	168.9-170.0
128	Olefin PP	Shaw Industries, Type 079	Polypropylene. Solution dyed blue. Delta X.S. 1100d. Yarn(60f)	168.2-169.7

** Fiber 101 was indicated to be Nylon 66 by the reference material, however, both melting point and FTIR corresponded more closely with Nylon 6. Therefore, 101 will be grouped with Nylon 6 in future discussion.*

Nylon

The nylon fibers were grouped into five groups based on their FTIR spectra. Within each group spectra were indistinguishable from one another, allowing for a 4 cm^{-1} variation in peak location due to the resolution of the instrument (Two fibers, 97, and 83 gave inconclusive results with regards to the FTIR spectra due to small diameter, and were not included in the results.).

Group A – 74–81, 84–88, 101, 117, 118
Group B – 89–96, 98–100, 102, 104, 105, 107–116, 119, 120, 173
Group C – 82
Group D – 103
Group E – 106

The melting range of each sample was then compared to that of every other sample. All members of group A were distinguishable from members of group B by both FTIR and melting point. Within group A, sample 87 could be further distinguished from 10 other

members of the group by melting point analysis (Table 2). Within group B, a number of samples could be distinguished from other members of the group by melting point analysis for a total of 116 pairs of fibers that did not have overlapping melting ranges with one another (Table 3). Groups C, D, and E each consisted of one fiber sample. The samples in groups C and D could be distinguished from all other samples by both FTIR and melting point. The sample in group E could be distinguished from all other samples by FTIR, and only 29 of the other nylon samples by melting point.

Table 2 Nylon Group A. Pairs marked with a Y indicate they are distinguishable by melting point.

#	75	76	77	78	79	80	81	84	85	86	87	88	101	117	118
74	N	N	N	N	N	N	N	N	N	N	Y	N	N	N	N
75		N	N	N	N	N	N	N	N	N	N	N	N	N	N
76			N	N	N	N	N	N	N	N	N	N	N	N	N
77				N	N	N	N	N	N	N	Y	N	N	N	N
78					N	N	N	N	N	N	N	N	N	N	N
79						N	N	N	N	N	Y	N	N	N	N
80							N	N	N	N	Y	N	N	N	N
81								N	N	N	Y	N	N	N	N
84									N	N	Y	N	N	N	N
85										N	Y	N	N	N	N
86											Y	N	N	N	N
87												Y	Y	N	N
88													N	N	N
101														N	N
117															N

A total of 46 nylon fibers were compared, resulting in 1035 pairwise comparisons. When looking at all of the nylon fibers together, 16 of these pairs were distinguishable by FTIR and not melting point, 126 pairs were distinguishable by melting point and not FTIR, and 564 pairs were distinguishable by both FTIR and melting point.

The majority of fibers distinguishable by melting point and not FTIR are in group B and belong to the nylon 6,6 subtype, with sample 87 being the only nylon 6 fiber differentiated from more than 1 other sample in this manner. The FTIR spectrum of sample 87 is shown alongside the FTIR spectrum of one of the fiber samples differentiated by melting point but not FTIR (Fig. 1). The nylon 6,6 fiber, sample 109, was distinguishable by melting point and not FTIR from 24 other samples, more than any other nylon fiber in the collection. The FTIR spectrum of sample 109 is shown alongside the FTIR spectrum of one of the fiber samples differentiated by melting point but not FTIR (Fig. 2).

Table 3 Nylon Group B. Pairs marked with a Y indicate they are distinguishable by melting point.

#	90	91	92	93	94	95	96	98	99	100	102	104	105	107	108	109	110	111	112	113	114	115	116	119	120	173
89	N	N	N	N	N	N	N	Y	N	N	N	Y	Y	N	N	Y	N	N	Y	N	N	Y	Y	Y	Y	Y
90		N	N	N	N	N	N	Y	N	N	N	Y	Y	N	N	Y	N	N	Y	N	N	Y	Y	Y	Y	Y
91			N	N	N	N	N	Y	N	N	N	N	N	N	N	Y	N	N	N	N	N	N	N	Y	Y	Y
92				N	N	N	N	N	N	Y	N	N	N	N	N	Y	N	N	N	N	N	N	N	N	N	N
93					N	N	N	Y	N	N	N	Y	Y	N	N	Y	N	N	Y	N	N	Y	Y	Y	Y	Y
94						N	N	N	N	Y	N	N	N	N	N	Y	N	N	N	N	N	N	N	Y	N	N
95							N	Y	N	Y	N	N	Y	N	N	Y	N	N	N	N	N	N	Y	Y	Y	Y
96								N	N	Y	N	N	N	N	N	Y	N	N	N	N	N	N	N	Y	N	N
98									Y	Y	Y	N	N	N	N	Y	Y	N	N	N	N	N	N	Y	N	N
99										N	N	N	Y	N	N	Y	N	N	N	N	N	N	N	Y	Y	Y
100											Y	Y	Y	Y	Y	Y	Y	Y	Y	Y	Y	Y	Y	N	Y	Y
102												N	Y	N	N	Y	N	N	N	N	N	N	N	Y	Y	Y
104													N	N	N	Y	N	N	N	N	N	N	N	Y	N	N
105														N	N	Y	Y	N	N	N	N	N	N	Y	N	N
107															N	Y	N	N	N	N	N	N	N	Y	Y	Y
108																Y	N	N	N	N	N	N	N	Y	Y	Y
109																	Y	Y	Y	Y	Y	Y	Y	N	Y	N
110																		N	N	N	N	N	N	Y	Y	Y
111																			N	N	N	N	N	Y	Y	Y
112																				N	N	N	N	Y	N	N
113																					N	N	N	Y	N	N
114																						N	N	Y	Y	Y
115																							N	Y	N	N
116																								Y	N	N
119																									N	N
120																										N

All 16 pairs distinguishable by FTIR and not melting point can be attributed to a single sample, 106, which was identified as a bicomponent fiber. The FTIR spectrum differs significantly from a typical Nylon 6 or Nylon 6,6 spectrum (Fig. 3), however, the melting point overlapped with a number of the nylon 6 fibers.

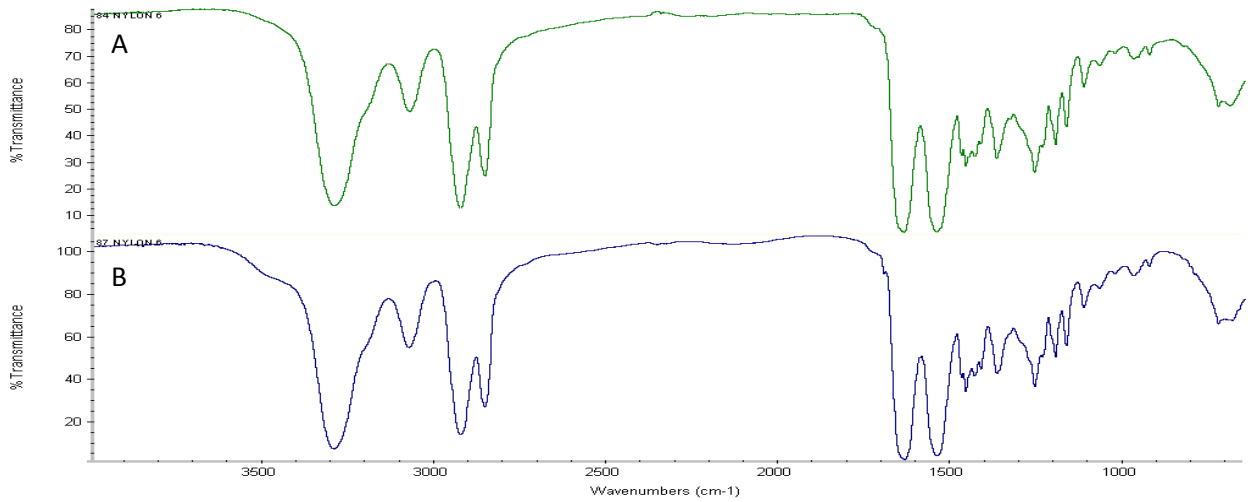

Figure 1 FTIR spectra of nylon 6 fibers: (A) sample 84 and (B) sample 87.

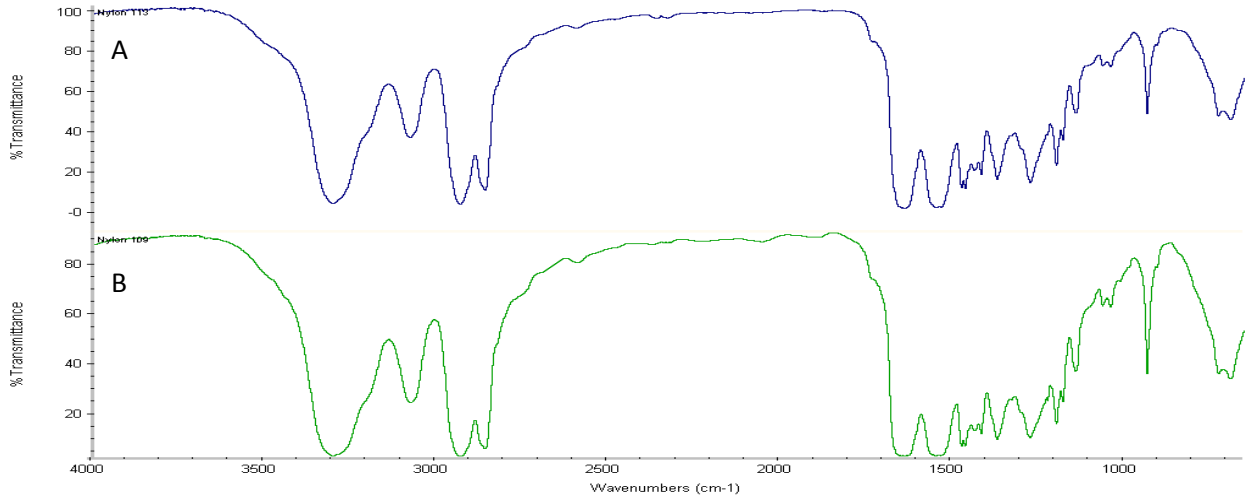

Figure 2 FTIR spectra of nylon 6,6 fibers: (A) sample 119 and (B) sample 109.

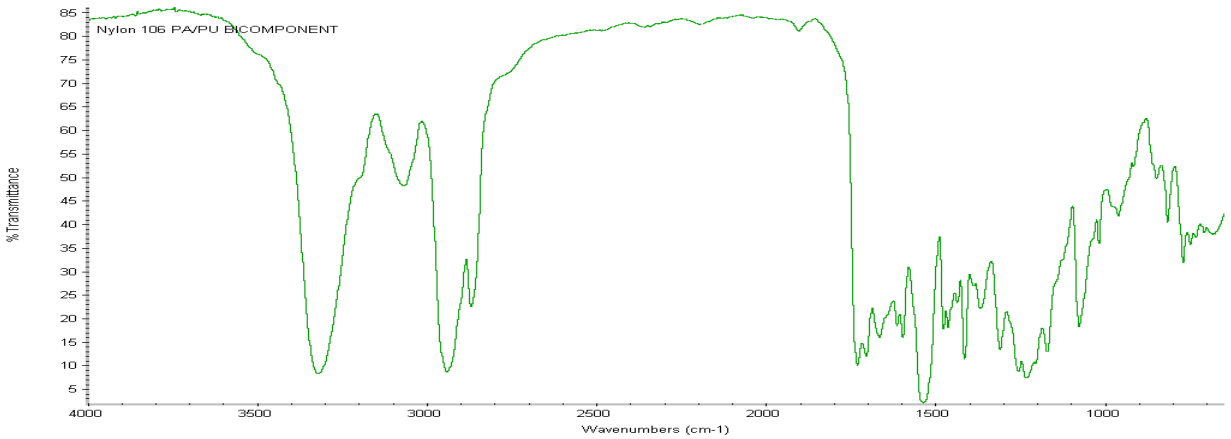

Figure 3 FTIR spectrum of bicomponent nylon fiber sample 106.

Polyester

The polyester fibers were grouped into eight groups based on their FTIR spectra. Within each group spectra were indistinguishable from one another, allowing for a 4 cm^{-1} variation in peak location due to the resolution of the instrument.

Group A – 132, 136-147, 149-163, 168, 169, 171, 172, 174-178, 180-185
Group B – 164, 165
Group C – 133
Group D – 135
Group E – 148
Group F – 167
Group G – 170
Group H – 179

Within group A, a number of samples could be distinguished from other members of the group by melting point analysis for a total of 569 pairs of fibers that did not have overlapping melting ranges with one another (Table 4). The two samples in group B could not be distinguished from one another by FTIR or melting point, however, they could be distinguished from all other samples by both FTIR and melting point. Groups C, D, and H each consisted of one fiber sample which could be distinguished from all other samples by both FTIR and melting point. The samples in groups E, F, and G could be distinguished from all other samples by FTIR. The sample in group E could be distinguished from 35 samples in other groups by melting point, the sample in group F from 15 samples, and the sample in Group G from 48 samples. The remaining 55 pairs compared with groups E, F, and G were distinguishable by FTIR and not melting point.

In summary, a total of 52 polyester fibers were compared with each other for a total of 1326 pairwise comparisons. Fifty-five of the pairs were distinguishable by FTIR and not melting point, 569 pairs were distinguishable by melting point and not FTIR, and 322 pairs were distinguishable by both FTIR and melting point.

A large portion of the 569 pairs distinguishable by melting point and not FTIR can be attributed to 4 fiber samples: 153, 156, 160, and 161. These samples were identified as modified PET and had FTIR spectra that were indistinguishable from the FTIR spectra of all other samples in group A, regular PET fibers. In contrast, these samples possessed lower melting points than most other regular PET samples in the collection. Sample 156 melted from 237.0-237.9ºC, the lowest of the modified PETs, and sample 160 melted from 245.4-250.6ºC, the highest of the modified PETs. The only polyester fiber in the

Table 4 Polyester Group A. Pairs marked with a Y indicate they are distinguishable by melting point.

#	136	137	138	139	140	141	142	143	149	150	151	154	155	157	162	163	166	169	171	172	177	178	180	181	153	156	160	161	144	145	146	147	152	158	159	168	174	175	176	182	183	184	185
132	N	N	Y	N	N	Y	N	Y	Y	Y	N	N	N	Y	Y	N	N	Y	N	Y	N	N	Y	N	Y	Y	Y	Y	Y	Y	Y	N	N	N	N	N	N	N	N	Y	Y	Y
136		N	N	N	N	N	N	Y	N	N	N	N	N	Y	N	N	N	Y	N	N	N	N	N	N	Y	Y	Y	Y	N	N	N	N	N	N	N	N	N	N	N	N	N	N	N
137			Y	Y	N	N	N	Y	N	N	N	Y	Y	Y	Y	Y	Y	Y	N	N	N	N	N	N	Y	Y	Y	Y	Y	Y	N	N	N	Y	Y	N	N	Y	N	N	Y	Y	N
138				N	Y	Y	Y	N	Y	Y	N	N	N	Y	N	N	N	N	Y	Y	N	Y	Y	N	Y	Y	Y	Y	N	N	Y	Y	Y	N	N	Y	Y	N	Y	Y	Y	Y	Y
139					N	Y	N	Y	Y	Y	N	N	N	Y	Y	N	N	Y	N	Y	N	N	N	N	Y	Y	Y	Y	Y	N	Y	Y	N	N	N	Y	N	N	N	N	Y	Y	Y
140						Y	N	Y	N	Y	N	Y	Y	Y	Y	Y	Y	Y	N	N	N	N	N	N	Y	Y	Y	Y	Y	Y	N	N	N	Y	Y	N	N	Y	N	N	Y	Y	Y
141							Y	Y	N	N	Y	Y	Y	Y	Y	Y	Y	Y	Y	N	Y	Y	Y	Y	Y	Y	Y	Y	Y	Y	N	N	Y	Y	Y	Y	N	Y	Y	Y	N	N	N
142								Y	Y	Y	N	Y	Y	Y	Y	N	N	Y	N	Y	N	N	N	N	Y	Y	Y	Y	Y	Y	Y	Y	N	N	N	N	N	N	N	N	Y	Y	Y
143									Y	Y	N	N	N	N	N	Y	Y	N	Y	Y	Y	Y	Y	Y	Y	Y	Y	Y	N	N	Y	Y	Y	N	N	Y	Y	N	Y	Y	Y	Y	Y
149										N	Y	Y	Y	Y	Y	Y	Y	Y	N	N	Y	Y	Y	Y	Y	Y	Y	Y	Y	N	N	Y	Y	Y	N	N	Y	N	Y	N	N	N
150											Y	Y	Y	Y	Y	Y	Y	Y	Y	N	Y	Y	Y	Y	Y	Y	Y	Y	Y	N	N	Y	Y	Y	Y	N	Y	Y	Y	N	N	N
151												N	N	Y	N	N	N	N	N	Y	N	N	N	N	Y	Y	Y	Y	N	N	Y	Y	N	N	N	N	N	N	N	Y	Y	Y
154													N	Y	N	N	N	N	N	Y	N	Y	Y	N	Y	Y	Y	Y	N	N	Y	Y	Y	N	N	Y	Y	N	Y	Y	Y	Y	Y
155														Y	N	N	N	N	N	Y	N	N	N	N	Y	Y	Y	Y	N	N	Y	Y	N	N	N	Y	Y	N	Y	Y	Y	Y	Y
157															N	Y	Y	N	Y	Y	Y	Y	Y	Y	Y	Y	Y	Y	N	Y	Y	Y	Y	Y	Y	Y	Y	Y	Y	Y	Y	Y
162																N	Y	N	Y	Y	Y	Y	Y	Y	Y	Y	Y	Y	N	N	Y	Y	Y	N	N	Y	Y	N	Y	Y	Y	Y	Y
163																	N	Y	N	Y	N	N	N	N	Y	Y	Y	Y	N	N	Y	Y	N	N	N	Y	N	N	N	N	Y	Y	Y
166																		Y	N	Y	N	N	N	N	Y	Y	Y	Y	N	Y	Y	N	N	N	Y	Y	N	Y	N	Y	Y	Y
169																			Y	Y	Y	Y	Y	Y	Y	Y	Y	Y	N	N	Y	Y	Y	N	N	Y	Y	N	Y	Y	Y	Y	Y
171																				N	N	N	N	N	Y	Y	Y	Y	Y	Y	N	N	N	N	N	N	N	N	N	N	Y	Y	Y
172																					Y	Y	Y	Y	Y	Y	Y	Y	Y	Y	N	N	Y	Y	Y	N	N	Y	Y	Y	N	N	N
177																						N	N	N	Y	Y	Y	Y	Y	Y	Y	Y	N	N	N	Y	N	N	N	N	Y	Y	Y
178																							N	N	Y	Y	Y	Y	N	Y	Y	Y	N	N	N	N	N	N	N	N	Y	Y	Y
180																								N	Y	Y	Y	Y	Y	Y	Y	Y	N	N	N	N	N	N	N	N	Y	Y	Y
181																									Y	Y	Y	Y	Y	Y	Y	Y	N	N	N	N	N	N	N	N	Y	Y	Y
153																										N	Y	Y	Y	Y	Y	Y	Y	Y	Y	Y	Y	Y	Y	Y	Y	Y	Y
156																											Y	Y	Y	Y	Y	Y	Y	Y	Y	Y	Y	Y	Y	Y	Y	Y	Y
160																												N	Y	Y	Y	N	Y	Y	Y	Y	Y	Y	Y	Y	Y	Y	Y
161																													Y	Y	Y	Y	Y	Y	Y	Y	Y	Y	Y	Y	Y	Y	Y
144																														N	Y	Y	Y	N	N	Y	Y	N	Y	Y	Y	Y	Y
145																															Y	Y	Y	N	N	Y	Y	N	Y	Y	Y	Y	Y
146																																N	N	Y	Y	N	N	Y	Y	N	N	N	N
147																																	Y	Y	Y	N	N	Y	Y	Y	N	N	N
152																																		N	N	N	N	N	N	N	Y	Y	Y
158																																			N	Y	Y	N	Y	Y	Y	Y	Y
159																																				Y	Y	N	Y	Y	Y	Y	Y
168																																					N	Y	N	N	Y	Y	Y
174																																						Y	N	N	Y	Y	N
175																																							Y	N	Y	Y	Y
176																																								N	Y	Y	Y
182																																									Y	Y	Y
183																																										N	N
184																																											N

collection that had an overlapping melting range with one of these four samples (once instrumental accuracy was taken into account) was 147, which had a melting range that

overlapped with sample 160. The majority of other samples in group A did not start melting until 255ºC or higher, which is much higher than the modified PET samples, beyond any variations that could be attributed to instrumental accuracy. This shows that melting point provides better discrimination than FTIR in this case. FTIR spectra of samples 153, 156, 160, and 161 are shown alongside one of the fibers they were distinguished from using melting point and not FTIR (Fig. 4).

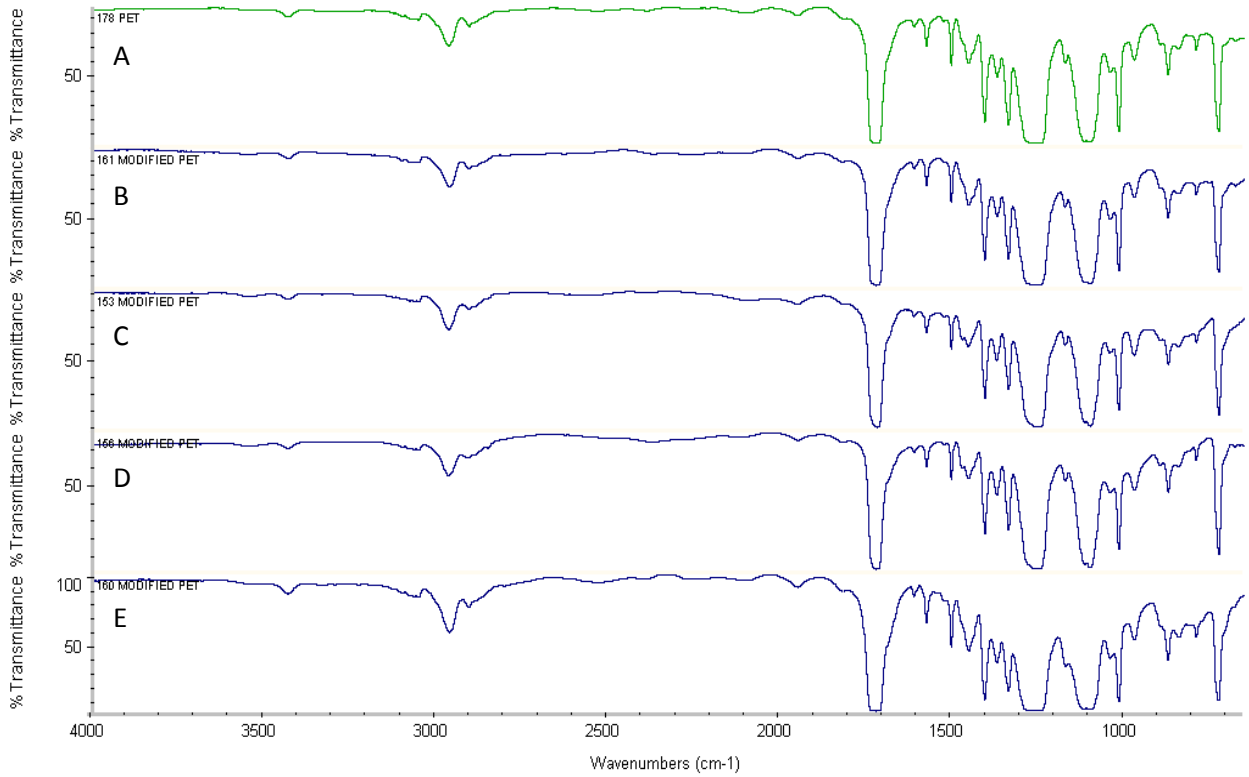

Figure 4. FTIR spectra of (A) sample 178, PET, (B) sample 161, modified PET, (C) sample 153, modified PET, (D) sample 156, modified PET, and (E) sample 160, modified PET.

Sample 167, identified as having a polyester core and co-polyester sheath, and sample 148, only identified as polyester, had different FTIR spectra from every other polyester sample examined. Sample 167 has an extra peak around 932cm^{-1}, while sample 148 has a shifting of the peak around 2908 cm^{-1} to 2916 cm^{-1} (Fig. 5). While some of the other samples also had different melting ranges when compared to these two samples, 36 samples had melting ranges that overlapped with sample 167, and 16 samples had melting ranges that overlapped with sample 148. Therefore, FTIR is of much more value than melting point for comparative purposes regarding these samples.

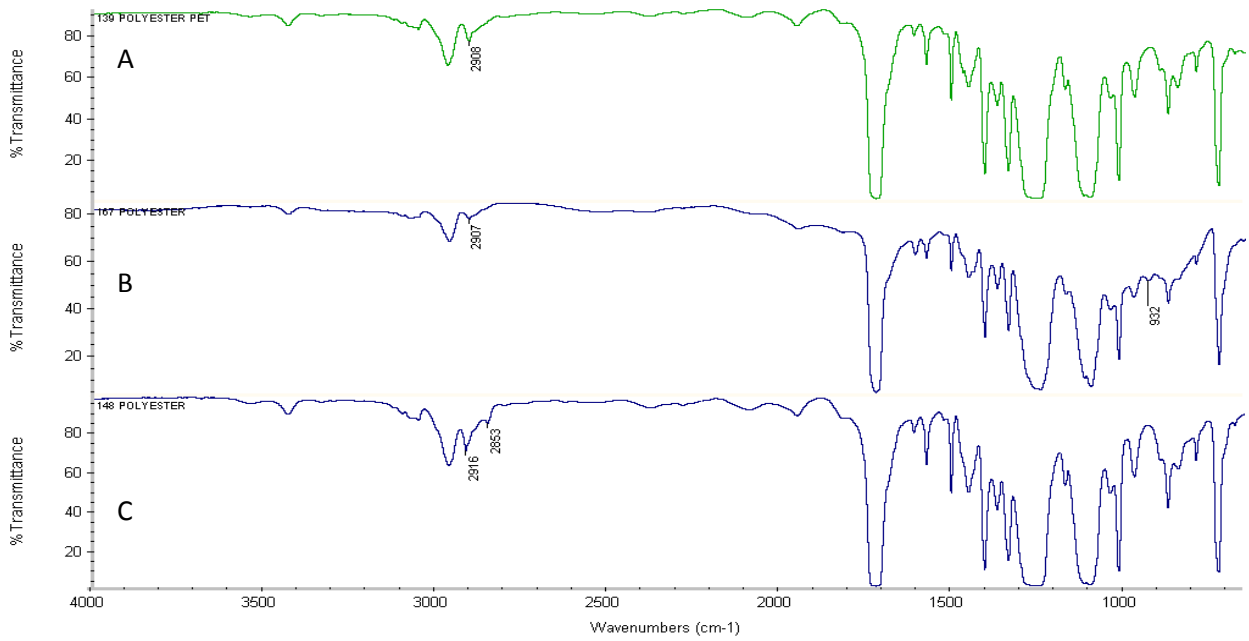

Figure 5. FTIR spectra of polyester fibers: (A) sample 139, (B) sample 157, and (C) sample 148. Sample 157 has an extra peak at 932 cm^{-1}, while sample 148 has a peak at 2916 cm^{-1} not present in typical PET fiber spectra.

Olefin

The Olefin fibers were grouped into three groups based on their FTIR spectra. Within each group spectra were indistinguishable from one another, allowing for a 4 cm^{-1} variation in peak location due to the resolution of the instrument.

Group A – 121, 123, 124, 125, 127, 128
Group B – 122
Group C – 126

Within group A, 7 pairs out of a possible 15 pairs could be distinguished from each other by melting point analysis (Table 5). Groups B and C each consisted of one fiber sample that could be distinguished from all other samples by FTIR. The sample in group B could also be distinguished from all other samples by melting point, while the sample in group C could only be distinguished from two of the other samples by melting point.

In summary, a total of 8 olefin fibers were compared for a total of 28 pairwise comparisons. Five of the olefin pairs were distinguishable by FTIR and not melting point, 7 pairs were distinguishable by melting point and not FTIR, and 8 pairs were distinguishable by both FTIR and melting point.

Table 5 Olefin Group A. Pairs marked with a Y indicate they are distinguishable by melting point.

#	123	124	125	127	128
121	N	Y	N	N	N
123		N	N	Y	Y
124			N	Y	Y
125				Y	Y
127					N
128					

Sample 126, identified as polypropylene, was distinguishable from other samples by the presence of a peak around 731 cm^{-1} in its FTIR spectrum (Fig. 6), which could be due to some polyethylene being present in the sample (3). The melting range of sample 126 overlapped with most of the other samples, showing the higher discrimination power of FTIR in this case. For other samples, the contrary was true, with samples 124, 127, and 128 being distinguished from more samples by melting point and not FTIR than the converse. The FTIR spectrum of sample 128 is shown alongside the FTIR spectrum of one of the fiber samples differentiated by melting point but not FTIR (Fig. 6).

Microscopic Examinations

In a typical fiber examination, microscopy is performed before other examinations. While this study pertains primarily to melting point and FTIR analysis, it was also of interest to determine whether or not the findings would further discriminate fibers that had also been examined using microscopy. The question was asked if fibers found to be distinguished by FTIR but not melting point or vice versa would have been distinguished by microscopy before they even got to that point of the examination. All fibers that could be distinguished by FTIR but not melting point and vice versa were examined using transmitted light microscopy and categorized as described in the methods section. All except for one pair of fibers could be distinguished by transmitted light microscopy. This pair, samples 159 (standard PET) and 161 (modified PET), was further examined using polarized light microscopy and fluorescence microscopy. Only slight differences were noted under polarized light as well as the intensity of the fluorescence using the BLUE cube (Fig. 7).

CONCLUSIONS

In conducting a fiber examination is it important to consider the value of techniques that can be used to distinguish different fibers. Both FTIR and melting point can be used not only to verify a fiber type, but also for comparative purposes. Both techniques have the potential to distinguish fibers that the other method cannot.

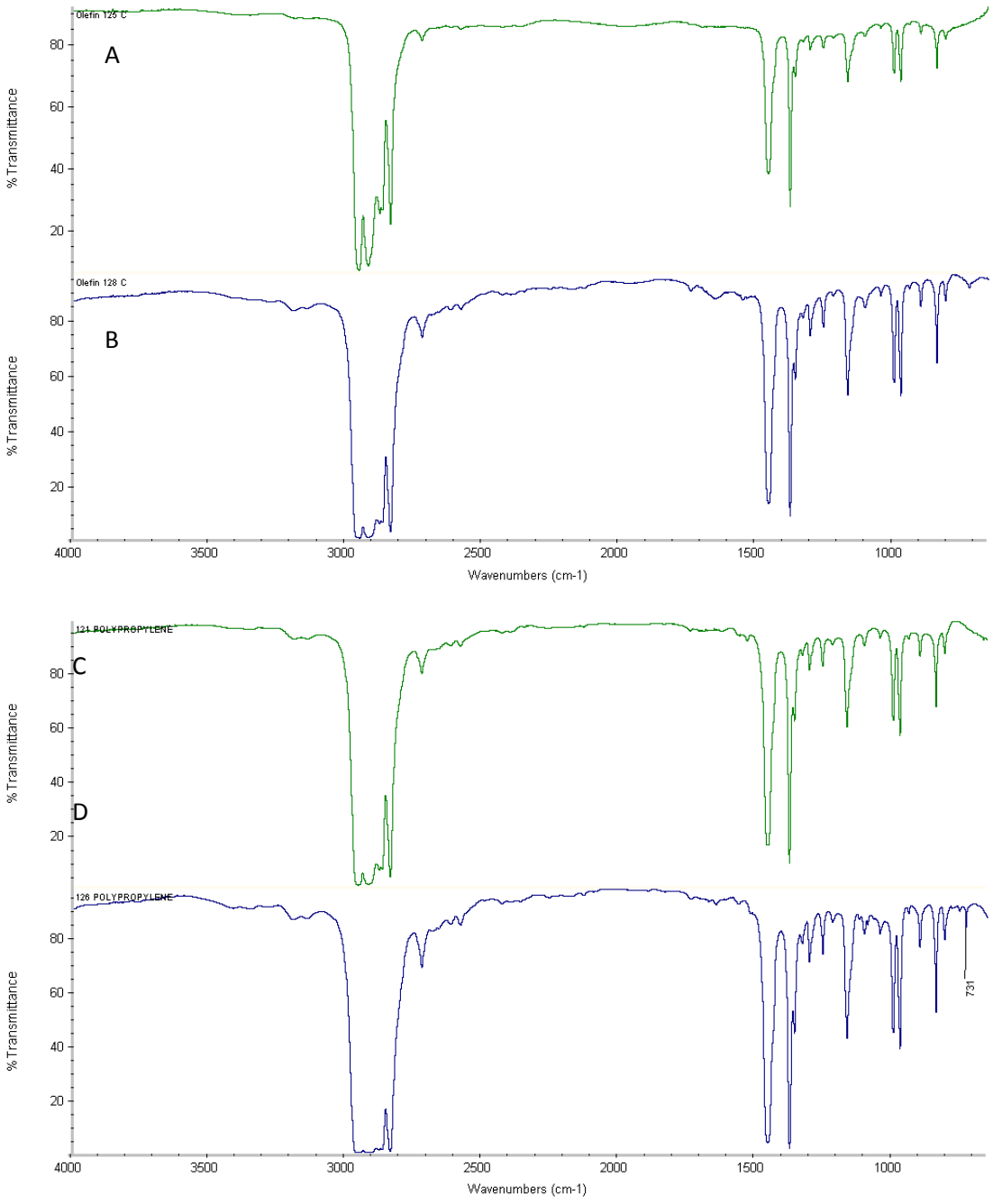

Figure 6. FTIR spectra of olefin fibers: (A) sample 125 and (B) sample 128, (C) sample 121 and (D) sample 126. (A) and (B) are distinguishable by MP but not FTIR. (D) has an extra peak at 731 cm^{-1} that was not seen in the spectra of other olefin fibers.

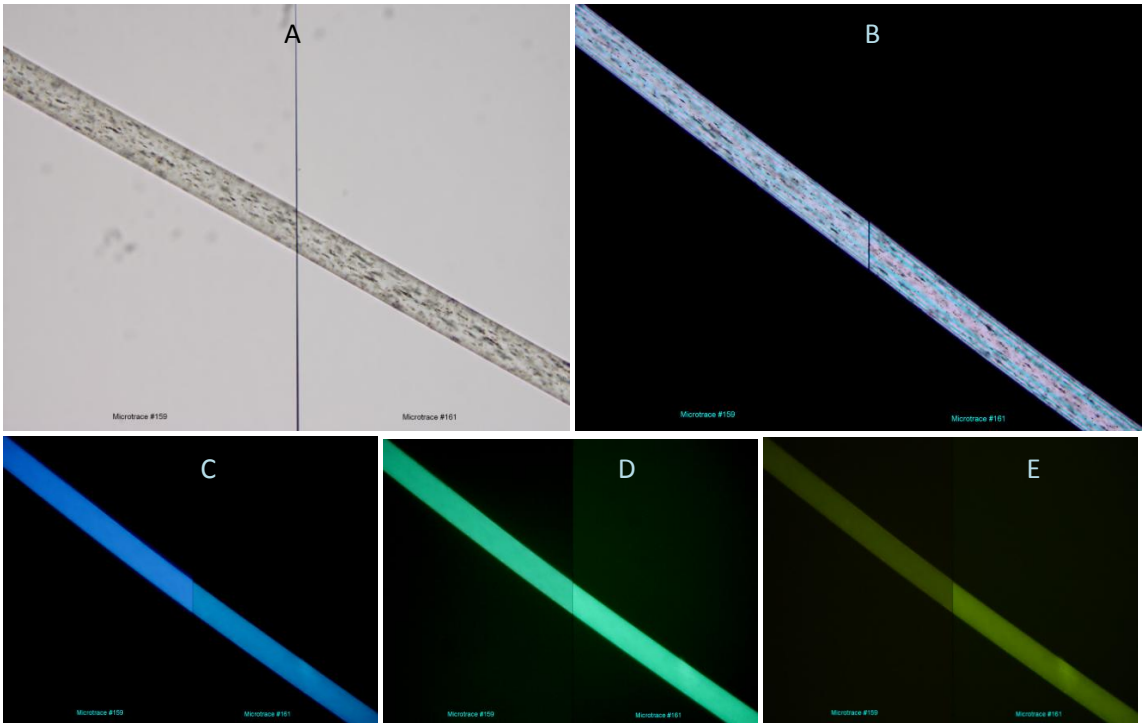

Figure 7. Microscopical examination of samples 159 (left) and 161 (right). (A) Transmitted light. (B) Polarized light. (C) Fluorescence with UV cube. (D) Fluorescence with UV/VIO cube. (E) Fluorescence with BLUE cube.

In a typical fiber comparison, thermal microscopy and FTIR are often the last methods to be used. Oftentimes, fiber matches will be eliminated using other methods such as transmitted light microscopy, polarized light microscopy, fluorescence microscopy, and microspectrophotometry (MSP). The author has yet to complete a fiber comparison in which the fibers were consistent in the various microscopy and MSP techniques, but were found to be inconsistent in either FTIR or MP. Other laboratories have shown similar results with regards to IR (7).

While it might be rare to find two fibers that match optically but not with melting point or FTIR, in this study, there was one pair of fibers (samples 159 and 161) that could be distinguished readily by melting point with only minor differences in optical properties. As this pair consisted of two colorless fibers, MSP would be of limited value for a comparison. Using melting point analysis was helpful in this situation to more readily distinguish the fibers being compared. Therefore, in many cases, especially when dealing with colorless fibers, it may be important to consider using both techniques of FTIR and melting point when completing a comparative analysis.

ACKNOWLEDGEMENTS

The author would like to thank Natasha Wright for collecting FTIR spectra, Sarah Glenn for collecting thermal microscopy data, Tammy Jergovich for her review of the paper, and the Georgia Bureau of Investigation for the time and facilities needed to complete the project.

REFERENCES

1. Scientific Working Group on Materials Analysis (SWGMAT). (1999). Forensic Fiber Examination Guidelines. http://www.swgmat.org/fiber.htm
2. Palenik S.J. (1999). Microscopical Examination of Fibres, in J. Robertson & M. Grieve (Eds.) Forensic Examination of Fibres, 2nd ed., p. 154 & 171, Philadelphia: Taylor & Francis Inc.
3. Hartshorne A.W., Laing D.K.. The Identification of Polyolefin Fibres by Infrared Spectroscopy and Melting Point Determination. Forensic Science International 1984; 26: 45-52.
4. Wiggins K.G. (1999). Ropes and Cordage, in J. Robertson & M. Grieve (Eds.) Forensic Examination of Fibres, 2nd ed., p. 60, Philadelphia: Taylor & Francis Inc.
5. Microtrace Forensic Fiber Reference Collection (2008). p.8
6. Collaborative Testing Services, Inc, Test No. 12-539: Fibers Analysis, Summary Report.
7. Tungol M.W., et al. Analysis of Single Polymer Fibers by Fourier Transform Infrared Microscopy: The Results of Case Studies. Journal of Forensic Sciences 1991; 36(4): 1027-1043.

Andria H. Mehltretter,[1] M.S., Diana M. Wright,[2] Ph.D., Joshua R. Dettman,[3] Ph.D., and Michael A. Smith,[2] Ph.D.

Intra-Roll and Intra-Jumbo Roll Variation of Duct Tapes

ABSTRACT

In forming opinions regarding duct tape examinations, the forensic community has relied primarily upon empirical observations from analyzing case samples or reference rolls, information obtained from industry/manufacturing representatives, and research projects that were relatively limited in scope. This study was designed and undertaken to expand on this body of knowledge by 1) evaluating the within-roll variation of duct tapes, specifically the physical characteristics of scrim count, warp yarn offset, width, and thickness; as well as the chemical composition of the adhesives via Fourier transform infrared (FTIR) spectroscopy; 2) assessing whether rolls removed from the middle and both edges of a jumbo roll have any observable or measureable differences; and 3) determining the association/discrimination criteria that should be used for the forensic analysis of duct tapes. The results indicate that warp yarn offset should not be used to discriminate samples due to variations in this feature along the length of a roll, but that scrim count, width, thickness, and adhesive composition vary to a limited extent along the length of an individual roll of tape. Aside from width, minimal variation in these characteristics occurs between different rolls cut from the same jumbo roll. Statistical analysis of the thickness and adhesive composition via FTIR indicate that

[1] Corresponding Author: Federal Bureau of Investigation, Laboratory Division, Chemistry Unit, 2501 Investigation Parkway, Quantico, VA 22135
[2] Federal Bureau of Investigation, Laboratory Division, Chemistry Unit, 2501 Investigation Parkway, Quantico, VA 22135
[3] Oak Ridge Institute for Science and Education, Federal Bureau of Investigation, Laboratory Division, 2501 Investigation Parkway, Quantico, Virginia 22135

This is the FBI Laboratory Division's publication number 14-08. Names of commercial manufacturers are provided for identification only, and inclusion does not imply endorsement of the manufacturer, or its products or services, by the FBI. The views expressed are those of the authors and do not necessarily reflect the official policy or position of the FBI or the U.S. Government.

some statistically significant differences are observed, but these differences are minor and would not likely have resulted in an exclusion/elimination in a forensic comparison case.

Keywords: duct tape, variation, stereomicroscopy, scrim count, width, thickness, Fourier transform infrared spectroscopy, statistical analysis, jumbo roll

INTRODUCTION

Duct tapes are the most common type of tape submitted as evidence to forensic laboratories in North America, and the variations exhibited between duct tape products make the material amenable to comparative analyses. There are generally between five and ten duct tape manufacturers in North America at any given time, and the amount of duct tape produced between manufacturers can vary substantially. Each manufacturer makes a variety of duct tape products that meet certain specifications depending upon their intended/advertised use. Individual duct tape rolls are cut from a much larger roll, referred to as a jumbo roll, using slitting knives pre-set at fixed distances (nominally 2" apart for a standard-width duct tape). The number of jumbo rolls needed to make a given product depends on a variety of market-driven factors (e.g., anticipated demand).

Certain differences between two tape samples can indicate that they are not from the same product and therefore did not originate from the same roll. Similarities between tape samples may suggest commonalities in the manufacturing process. If there are no observed differences between two tape samples, an analyst can generally conclude that the two originated from the same roll or another roll manufactured in the same manner; for duct tapes, this generally indicates the same tape product (Mehltretter 2012). It can be concluded a piece of tape originated from a specific roll only when two pieces of tape physically refit to each other at their ends (i.e., an end match).

The results of a 2012 Forensic Testing Services (Williamston, MI) duct tape proficiency test highlighted the need for additional studies regarding the acceptable variations in the parameters routinely assessed in duct tape comparisons. For this test, the participants received three duct tape samples: Item 1 was a piece of duct tape representing the roll from the suspect's vehicle, Item 2 was a piece of tape from Victim A, and Item 3 was a partial piece (torn lengthwise) of duct tape from Victim B. Once the test was closed, the test provider indicated Items 1-3 were separate pieces of tape torn from the same roll of Duck® brand tape. All Item 1 samples were prepared sequentially, followed by Item 2 samples, and then Item 3 samples. Therefore, the samples for each individual test were yards away from each other on the original roll.

The test results for the comparison of Items 1 and 2 were as follows: of the 49 respondents, 42 (86%) correctly reported an association and seven (14%) incorrectly reported an elimination (exclusion). For the comparison of Items 1 and 3, 45 (92%) correctly reported an association, two (4%) incorrectly reported an elimination, and two (4%) reported an inconclusive. All four of the test takers that did not correctly report an association between Items 1 and 3 also eliminated Items 1 and 2 from sharing a common source roll. In examining the report wording for each of the incorrectly reported results, several themes emerged. Eliminations appeared to be reported based on scrim count, width, and warp yarn offset. These results suggest that there may be uncertainty in the community as to what constitutes a significant difference between duct tape samples, and further, what is typical for intra-roll variation within a commercial grade product.

According to discussions with industry representatives (Mehltretter 2012), scrim counts of ± 1 are generally acceptable in the manufacturing of duct tape products. Further, a significant difference between pristine tapes (not stretched, deformed, or highly contaminated) is generally considered to be a width difference greater than 1.0 mm or a thickness difference greater than 10%. These tolerances do not appear to have been explored by forensic scientists.

Few publications have addressed if physical and chemical properties are consistent throughout a roll of tape: one addressed electrical tapes (Keto 1984), one considered elemental analysis on duct tapes (Jenkins 1984), and one was a review article (Blackledge 1987), which referenced the other two. In Keto's work, three rolls from each of six different electrical tape manufacturers were examined by X-ray fluorescence and FTIR; no statistically significant differences were found within a roll or between rolls of the same manufacturer. All six of the analyzed brands were clearly different. Jenkins reported no significant variation in elemental composition between the beginning, middle, and end of a duct tape roll when analyzed by energy dispersive X-ray spectrometry. The number of rolls analyzed and the sampling procedure were not noted in this latter work.

To date, no studies have been found that address the intra-roll variation of the physical characteristics or chemical composition (via FTIR) of duct tapes. These analyses (physical and FTIR) are the most widely used techniques for the analysis of duct tapes and have been found to yield a very high degree of discrimination between duct tape products (Mehltretter 2012). Additionally, no studies have been found which examined the variation between different rolls produced from the same jumbo roll or manufacturing batch.

This study was designed and undertaken to address this knowledge gap through 1) evaluation of the within-roll variation of duct tapes, specifically documenting the observed and measured physical characteristics as well as the chemical composition via FTIR spectroscopy, 2) assessment of whether rolls removed from the middle and both edges of a jumbo roll have any observable or measureable differences, and 3) determination of the appropriate association/discrimination criteria for the forensic analysis of duct tapes.

MATERIALS AND METHODS

Tape Collection

The major North American manufacturers of duct tape were contacted and asked to submit three rolls of a popular, commodity-grade duct tape product. These three rolls were to come from the left, middle, and right side of the same jumbo roll of their selected product. In total, five products were received from four different manufacturers, totaling 15 rolls of tape. All were silver-backed, nominally two inches wide, placed on manufacturer or brand name labeled cores, and 55 or 60 yards in length.

These rolls were unwound, cut into five yard increments, and placed on plastic tubular roll stock. This process resulted in twelve or thirteen pieces of tape for each roll.

The nomenclature used for each piece of tape was as follows:

Character	Comments
1	Product identifier (B, C, I, M, or S)
2	Collection time (0 indicates time=0, a single collection time)
3	Individual roll (A=left, B=middle, C=right)
4-5	Number of yards cut from the leading edge of the tape roll.

For instance, B0B15 indicates that this particular piece of tape originated from product B, at the initial collection time (this study represents only a single collection time for each product), from the middle roll on the jumbo roll, and that the piece was cut beginning at 15 yards from the leading edge of the roll. Each piece was then prepared and analyzed as described herein.

Scrim Count

A portion of the adhesive was removed as needed with suitable solvent and cotton swabs/Kimwipes® to expose enough of the fabric to measure one square inch. The

scrim count was measured using an English/Imperial ruler, in which the number of warp yarns (machine direction) and the number of fill or weft yarns (cross direction) were counted per inch in each direction, and recorded as a measure of warp/fill (w/f). To ensure consistency of measurement, the zero point of the ruler was lined up with a yarn, and that yarn was not counted. If a yarn lined up with the 1" point of the ruler, that yarn was counted. Since variations in scrim count are expected to be minimal at any given location, one measurement was taken near the leading end of each five yard piece of tape. Any variations in scrim count values over the length of the tape were noted.

Warp Yarn Offset

The warp yarn offset is defined as the distance from the machine edge of the tape to the first warp/machine-direction yarn. This offset was evaluated one of two ways for each product, depending on what was most amenable for a particular tape. One method was to examine the warp yarn closest to the machine edge of the tape and follow it along the length of the tape to determine whether the offset changed in an observable way (e.g., from at-edge to off-edge). The second method was to visually examine the piece of tape at various points along its length and observe whether there were noticeable variations in offset (e.g., from at-edge to off-edge).

Width

With a metric ruler, a single width measurement (again because variation at a given location is expected to be minimal) was taken at each five yard increment and recorded to the nearest 0.5 mm (ruler gradations were 1 mm). Any variations in width over the length of the tape were noted.

Thickness (Overall and Film)

For thickness measurements, the sample was placed between the two faces of a Mitutoyo digital micrometer, model number 293-348 (Mitutoyo, Aurora, IL). For film thickness measurements, the adhesive and fabric were first removed with hexane or chloroform. Five overall thickness and five film thickness measurements were taken within approximately the first two inches of each five yard piece, and the values were recorded to the nearest 0.05 mil (1 mil = 1/1000 inch). To avoid possible drift of the mean measurement from one piece to the next, one measurement of each piece from a roll was taken before taking the second measurement of each piece, and so forth. All measurements for a particular product were taken on the same day.

Repeat film thickness and overall thickness measurements were taken for each piece in order to subject the results to statistical analyses using an Analysis of Variance (ANOVA) scheme. Because the tape samples necessarily followed each other sequentially and came from the same individual and jumbo roll of tape, the sampling design was not fully

randomized. Rather, the sampling methodology employed approximated a standard, Two-Way, Repeated Measures ANOVA design. Accordingly, that model was assumed and was used to perform the initial ANOVA analysis using MINITAB (State College, PA) Version 13 software.

In addition, a One-Way ANOVA analysis was conducted and Tukey's Honestly Significant Difference (HSD) test (with overall $\alpha=0.05$) was applied to the individual rolls to conduct pairwise comparisons among all of the tape samples known to be from the same individual roll. Similarly, Tukey's HSD test with overall $\alpha=0.05$ was applied to identify significant differences in mean thickness among the set of three rolls that originated from the same jumbo roll.

FTIR

Between five and seven adhesive samples were physically removed with a scalpel at each five yard increment. They were smeared onto a KBr disc and analyzed in the transmission mode using a Continuum microscope attached to a Nicolet Nexus 6700 FTIR E.S.P. spectrometer with a MCT/A detector (4000-650 cm^{-1}) (Thermo Nicolet, Madison, WI). The resolution was 4 cm^{-1}, the aperture was approximately 100x100 µm, and the number of scans was 128. Intensity was recorded at a total of 1738 wavenumbers.

Raw spectra were first normalized to a common baseline by taking the first derivative. MATLAB (The MathWorks, Inc., Natick, MA) was used to generate a heat map image of the first derivative spectra. To identify outlying samples for visual comparison, statistical analysis of the FTIR spectra (made possible through the replicate analyses) was conducted by first reducing the number of variables (wavenumbers) to a few principal components (PCs), which describe a large portion of the information contained in the spectra. Unscrambler X (CAMO Software, Oslo, Norway) was used to perform principal component analysis (PCA) for reduction of the number of variables to a few important PCs. A multivariate form of ANOVA, multivariate analysis of variance (MANOVA), was used with the values of the first four PCs in JMP Pro (SAS, Cary, NC) to separately detect statistically significant differences 1) along the length of a single roll and 2) across the width of a jumbo roll. Pillai's Trace was used as the p-value estimate as recommended in the JMP Pro software documentation. If statistically significant differences were detected, visual comparison of the spectra that appeared most different was conducted by an experienced duct tape examiner to determine if the difference would lead to an exclusion in a forensic examination.

RESULTS

Scrim Count

Table 1 provides the scrim count measurements for each piece of tape. Within a single roll of tape, scrim count did not vary on most rolls. However, exceptions did occur in rolls from two of the products. For product C, the warp count varied on one of the rolls (roll A) up to two yarns per inch ranging from 19 to 21 (there was no variation in the fill yarns). The other two rolls from the same jumbo roll did not demonstrate this variation. For the roll with variation, however, it was observed that there was an unusual pattern to the fabric (see Figure 1a). The fill yarns were curved across the tape width rather than perpendicular to the warp yarns, and the warp yarn count appeared higher on one side of the tape than on the other. For product I, the fill count varied between 11 and 12 for two of three rolls (rolls B and C); however, for those with an 11 count, the 12th yarn was located just outside of the measurement window.

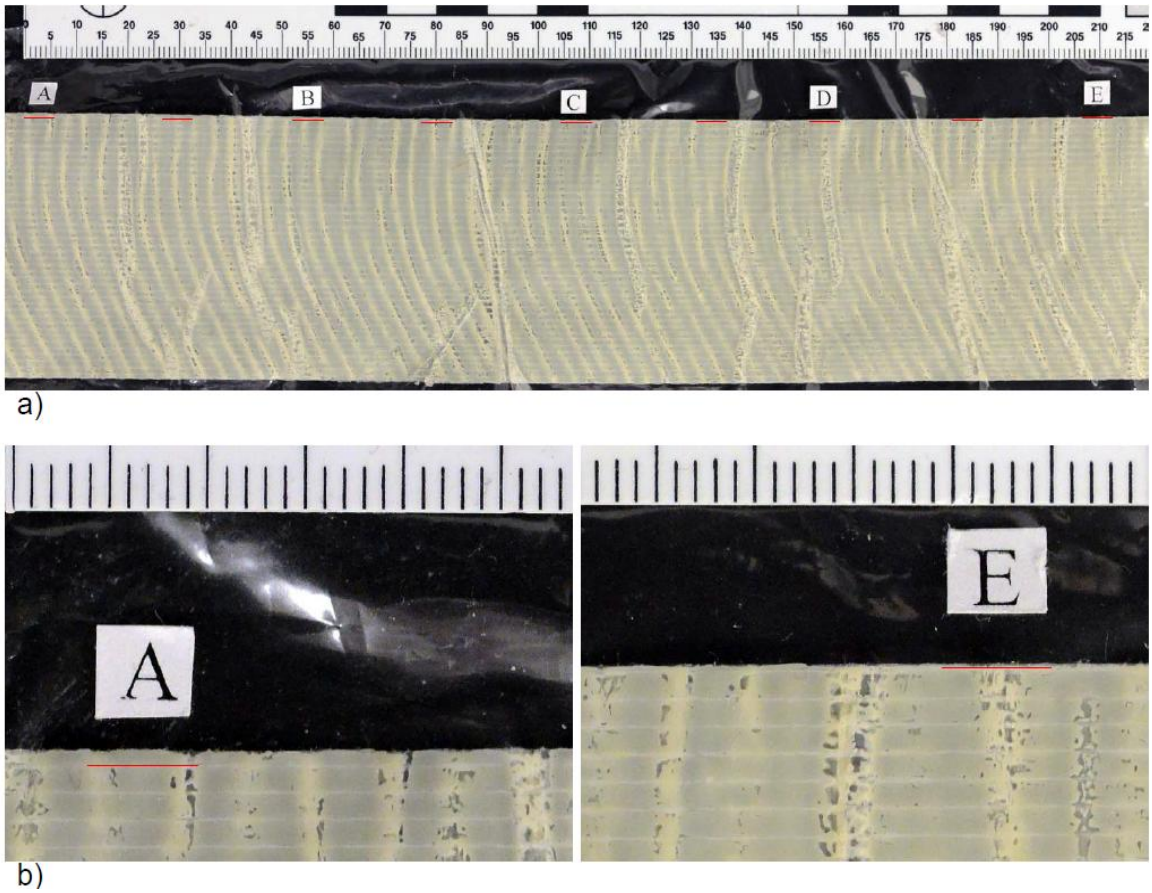

Figure 1 a) Photograph depicting how the fill yarns curve across the width of the tape piece and how the edge warp yarn shifts along the length of the piece. In this example, the shift is observed over approximately 8" in length, and the warp yarn of interest is emphasized with a recurring thin red line. b) Higher magnification photographs of areas A and E.

Table 1 Scrim count and width measurements for each piece of tape.

Piece	Scrim Count	Width (mm)	Piece	Scrim Count	Width (mm)	Piece	Scrim Count	Width (mm)	Piece	Scrim Count	Width (mm)	Piece	Scrim Count	Width (mm)
B0A00	17/5	48.0	C0A00	20/7	49.0	I0A00	18/11	50.0	M0A00	29/8	47.5	S0A00	19/7	49.0
B0A05	17/5	48.0	C0A05	20/7	49.0	I0A05	18/11	50.0	M0A05	29/8	47.5	S0A05	19/7	49.0
B0A10	17/5	48.0	C0A10	20/7	49.0	I0A10	18/11	49.5	M0A10	29/8	47.5	S0A10	19/7	49.0
B0A15	17/5	48.0	C0A15	20/7	49.0	I0A15	18/11	49.5	M0A15	29/8	47.5	S0A15	19/7	49.0
B0A20	17/5	48.0	C0A20	20/7	49.0	I0A20	18/11	49.5	M0A20	29/8	47.5	S0A20	19/7	49.0
B0A25	17/5	48.0	C0A25	21/7	49.0	I0A25	18/11	49.5	M0A25	29/8	47.5	S0A25	19/7	49.0
B0A30	17/5	48.0	C0A30	20/7	49.0	I0A30	18/11	49.5	M0A30	29/8	47.5	S0A30	19/7	49.0
B0A35	17/5	48.0	C0A35	21/7	49.0	I0A35	18/11	49.5	M0A35	29/8	47.5	S0A35	19/7	49.0
B0A40	17/5	48.0	C0A40	20/7	49.0	I0A40	18/11	49.5	M0A40	29/8	47.5	S0A40	19/7	49.0
B0A45	17/5	48.0	C0A45	21/7	49.0	I0A45	18/11	50.0	M0A45	29/8	47.5	S0A45	19/7	49.0
B0A50	17/5	48.0	C0A50	19/7	48.5	I0A50	18/11	50.0	M0A50	29/8	47.5	S0A50	19/7	49.0
B0A55	17/5	48.0	C0A55	20/7	48.5	I0A55	18/11	49.5	M0A55	29/8	47.5	S0A55	19/7	49.0
			C0A60	20/7	48.5	I0A60	18/11	50.0	M0A60	29/8	47.5	S0A60	19/7	48.5
B0B00	17/5	48.5	C0B00	19/7	48.0	I0B00	18/11	47.5	M0B00	29/8	47.5	S0B00	19/7	48.5
B0B05	17/5	48.5	C0B05	19/7	48.0	I0B05	18/11	47.5	M0B05	29/8	47.5	S0B05	19/7	48.5
B0B10	17/5	48.5	C0B10	19/7	48.0	I0B10	18/11	47.5	M0B10	29/8	47.5	S0B10	19/7	48.5
B0B15	17/5	48.5	C0B15	19/7	48.0	I0B15	18/11	47.5	M0B15	29/8	47.5	S0B15	19/7	48.5
B0B20	17/5	48.5	C0B20	19/7	48.0	I0B20	18/11	47.5	M0B20	29/8	47.5	S0B20	19/7	48.5
B0B25	17/5	48.5	C0B25	19/7	48.0	I0B25	18/11	47.5	M0B25	29/8	47.5	S0B25	19/7	48.5
B0B30	17/5	48.5	C0B30	19/7	48.0	I0B30	18/12	47.5	M0B30	29/8	47.5	S0B30	19/7	48.5
B0B35	17/5	48.5	C0B35	19/7	48.0	I0B35	18/11	47.5	M0B35	29/8	47.5	S0B35	19/7	48.5
B0B40	17/5	48.5	C0B40	19/7	48.0	I0B40	18/12	47.5	M0B40	29/8	47.5	S0B40	19/7	48.5
B0B45	17/5	48.5	C0B45	19/7	48.0	I0B45	18/11	47.5	M0B45	29/8	47.5	S0B45	19/7	48.5
B0B50	17/5	48.5	C0B50	19/7	48.0	I0B50	18/11	47.5	M0B50	29/8	47.5	S0B50	19/7	48.5
B0B55	17/5	48.5	C0B55	19/7	48.0	I0B55	18/12	47.5	M0B55	29/8	47.5	S0B55	19/7	48.5
			C0B60	19/7	48.0	I0B60	18/12	47.5	M0B60	29/8	47.5	S0B60	19/7	48.5
B0C00	17/5	47.5	C0C00	19/7	48.0	I0C00	18/11	48.5	M0C00	29/8	48.0	S0C00	19/7	47.5
B0C05	17/5	47.0	C0C05	19/7	48.0	I0C05	18/11	48.5	M0C05	29/8	48.0	S0C05	19/7	47.5
B0C10	17/5	47.0	C0C10	19/7	48.0	I0C10	18/12	48.5	M0C10	29/8	48.0	S0C10	19/7	47.5
B0C15	17/5	47.0	C0C15	19/7	48.0	I0C15	18/11	48.5	M0C15	29/8	48.0	S0C15	19/7	47.5
B0C20	17/5	47.5	C0C20	19/7	48.0	I0C20	18/11	48.5	M0C20	29/8	48.0	S0C20	19/7	47.5
B0C25	17/5	47.0	C0C25	19/7	48.0	I0C25	18/12	48.5	M0C25	29/8	48.0	S0C25	19/7	47.5
B0C30	17/5	47.5	C0C30	19/7	48.0	I0C30	18/12	49.0	M0C30	29/8	48.0	S0C30	19/7	47.5
B0C35	17/5	47.0	C0C35	19/7	48.0	I0C35	18/11	48.5	M0C35	29/8	48.0	S0C35	19/7	47.5
B0C40	17/5	47.0	C0C40	19/7	48.0	I0C40	18/12	48.5	M0C40	29/8	48.0	S0C40	19/7	47.5
B0C45	17/5	47.5	C0C45	19/7	48.0	I0C45	18/11	48.5	M0C45	29/8	48.0	S0C45	19/7	47.5
B0C50	17/5	47.0	C0C50	19/7	48.0	I0C50	18/11	48.5	M0C50	29/8	48.0	S0C50	19/7	47.5
B0C55	17/5	47.5	C0C55	19/7	48.0	I0C55	18/12	48.5	M0C55	29/8	48.0	S0C55	19/7	48.0
			C0C60	19/7	48.0	I0C60	18/12	49.0	M0C60	29/8	48.0	S0C60	19/7	47.5

Warp Yarn Offset

For all the rolls in the study, the warp yarn offset was observed to vary along the length of the roll. For example, using the first method described earlier, roll C0A's warp yarn offset was observed to have an obvious shift in the position of the first warp yarn over a distance of approximately 8¼ inches (see Figure 1b). Using the second observation method, the offset for roll S0B was observed to change along the length of the roll (see Figure 2).

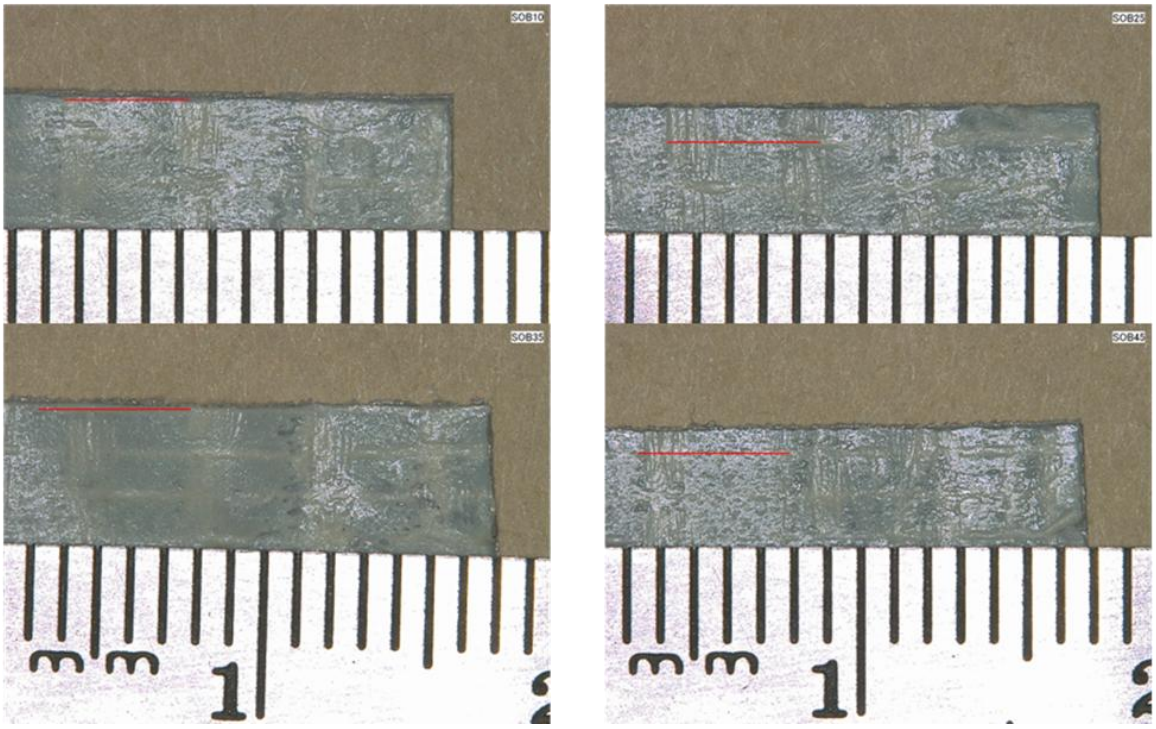

Figure 2 Four different pieces of tape from the same individual roll of tape depicting a variation in warp yarn offset along the length of a roll (clockwise from top left: S0B10, S0B25, S0B45, and S0B35). The warp yarn closest to the tape's machine edge is marked by a red line.

Width

Table 1 provides the width measurement for each piece of tape. The largest difference in width observed along the length of a single roll was 0.5 mm, which was observed in six of the 15 rolls included in the study (four different manufacturers). For a majority of the rolls, the width did not vary when recorded to the nearest 0.5 mm. The largest difference in width observed between pieces cut from the same jumbo roll of tape from the same product was observed for product I and was 2.5 mm (47.5 mm versus 50.0 mm).

Thickness (Overall and Film)

The results of thickness measurements on the individual rolls and pieces of tape are summarized in Table 2. Measurements of the mean overall thickness of individual tape pieces taken from the same roll showed maximum relative differences that ranged from 3.0%–19.3% depending upon the roll (Table 3). Similarly, measurements of the mean film thickness of individual tape pieces taken from the same roll showed maximum relative differences that ranged from 1.9% – 12.7% depending on the roll (Table 3). In general, the Two-Way Repeated Measures ANOVA analysis results revealed statistically significant effects on tape thickness (both film and overall) as a function of position along the length of the individual rolls. Likewise, Two-Way Repeated Measures ANOVA revealed statistically significant effects on tape thickness as a function of roll position (left, right or center of a jumbo roll).

Table 2 Mean (n=60 or 65) thickness by roll with the minimum and maximum mean (n=5) thicknesses for tape pieces taken from the same roll.

Roll	Overall Thickness (mils)				Film Thickness (mils)		
	Mean	Minimum	Maximum		Mean	Minimum	Maximum
B0A	8.42	8.24	8.52		5.07	5.00	5.13
B0B	8.60	8.40	8.91		5.26	5.20	5.33
B0C	8.36	8.22	8.47		5.21	5.16	5.26
C0A	7.00	6.76	7.14		2.07	1.99	2.20
C0B	6.91	6.63	7.23		2.08	1.99	2.23
C0C	7.33	6.98	7.99		2.13	2.06	2.25
I0A	8.70	8.55	8.91		3.08	2.99	3.16
I0B	8.96	8.69	9.12		3.11	3.01	3.21
I0C	8.68	8.53	8.80		3.19	3.12	3.32
M0A	8.66	8.52	9.03		2.56	2.44	2.66
M0B	8.53	8.29	8.82		2.61	2.45	2.76
M0C	8.41	8.23	8.77		2.58	2.48	2.68
S0A	8.31	7.84	8.79		3.98	3.92	4.03
S0B	8.41	7.76	9.26		3.97	3.89	4.06
S0C	8.25	7.75	8.69		3.97	3.92	4.02

Tukey's HSD test was used to conduct pairwise comparisons of the mean overall thickness (i.e., the average of all of the overall thickness measurements made on a given roll) amongst rolls from the same product. The comparisons demonstrated that these rolls often had statistically significant differences in this parameter. For example, the center roll of product B differs significantly in mean overall thickness from both the left and right rolls. However, the difference between the left and right rolls was not statistically significant (Figure 3). Of the tapes examined, only product S had no

statistically significant difference in mean overall thickness between any of the pairs (left-center, left-right, center-right). The largest relative differences in mean overall thickness between rolls from the same product ranged from 1.9%-6.0% (Table 4).

Table 3 Maximum relative difference in mean thickness among tape pieces taken from the same roll

Roll	Overall Thickness	Statistically Significant at α=0.05?		Film Thickness	Statistically Significant at α=0.05?
B0A	3.4%	No		2.6%	No
B0B	6.1%	Yes		2.5%	No
B0C	3.0%	No		1.9%	No
C0A	5.6%	No		10.6%	Yes
C0B	9.0%	Yes		12.1%	Yes
C0C	14.5%	Yes		9.2%	Yes
I0A	4.2%	Yes		5.7%	No
I0B	4.9%	Yes		6.6%	Yes
I0C	3.2%	Yes		6.4%	Yes
M0A	6.0%	Yes		9.0%	Yes
M0B	6.4%	Yes		12.7%	Yes
M0C	6.6%	Yes		8.0%	Yes
S0A	12.1%	Yes		2.8%	No
S0B	19.3%	Yes		4.4%	No
S0C	12.1%	Yes		2.6%	No

Table 4 Maximum relative difference in mean thickness among individual rolls from the same jumbo roll/product

Product	Mean Overall Thickness	Statistically Significant at α=0.05?		Mean Film Thickness	Statistically Significant at α=0.05?
B	2.81%	Yes		3.63%	Yes
C	6.02%	Yes		2.98%	Yes
I	3.22%	Yes		3.52%	Yes
M	2.91%	Yes		1.86%	Yes
S	1.87%	No		0.21%	No

Similarly, the results of Tukey's HSD test determined that again only product S had no statistically significant difference in mean film thickness between any of the rolls. At least one pair of rolls from the other four products had a statistically significant difference in mean film thickness. It was also observed that all of the products contained at least one pair of rolls that did not differ significantly in mean film thickness. The

largest relative differences in mean film thickness between two rolls from the same product ranged from 0.21% -3.63% (Table 4).

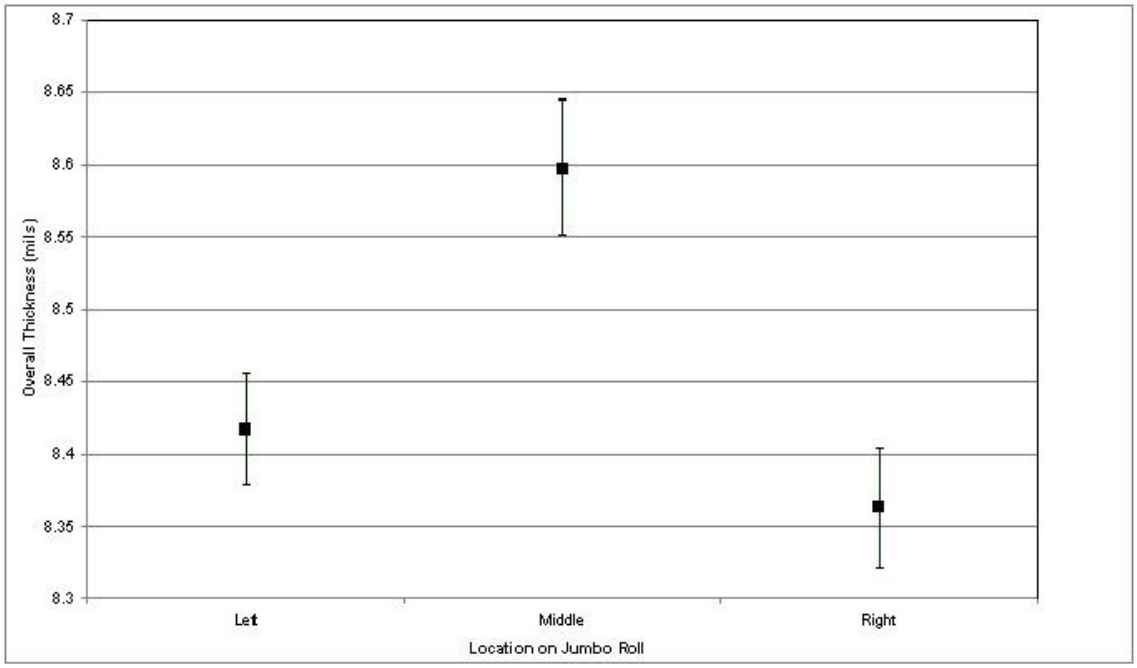

Figure 3 95% confidence intervals for mean overall thickness by roll location for product B. For this product, the left and right side rolls are statistically indistinguishable but both are significantly thinner than the center roll.

Pairwise comparisons performed with Tukey's HSD test on tape pieces taken from the same individual roll revealed statistically significant differences in overall thickness for at least one pair of samples in 12 of the 15 rolls examined. An example of this is shown in Figure 4. Under the assumption that the thickness of samples taken from a given roll is homogeneous, one might choose to conclude that two samples do not share a common origin if they differ significantly in overall thickness. However, for the 12 rolls for which significant differences are observed, the pairwise comparisons would lead to unwarranted exclusions between pairs of samples in as many as 78% of the comparisons under this scenario. The pairwise comparison data from all of the rolls are summarized in Table 5.

Similarly, pairwise comparisons performed with Tukey's HSD test of tape pieces taken from the same individual roll revealed statistically significant differences in mean film thickness for at least one pair of samples in seven of 15 rolls examined. Among these seven rolls, pairwise comparisons would lead to unwarranted exclusions from 1.3% to 18% of the time. No significant difference in film thickness was found in pairwise

comparisons of tape pieces from the same roll for any of the rolls from products B and S. The pairwise comparison data from all of the rolls are summarized in Table 5.

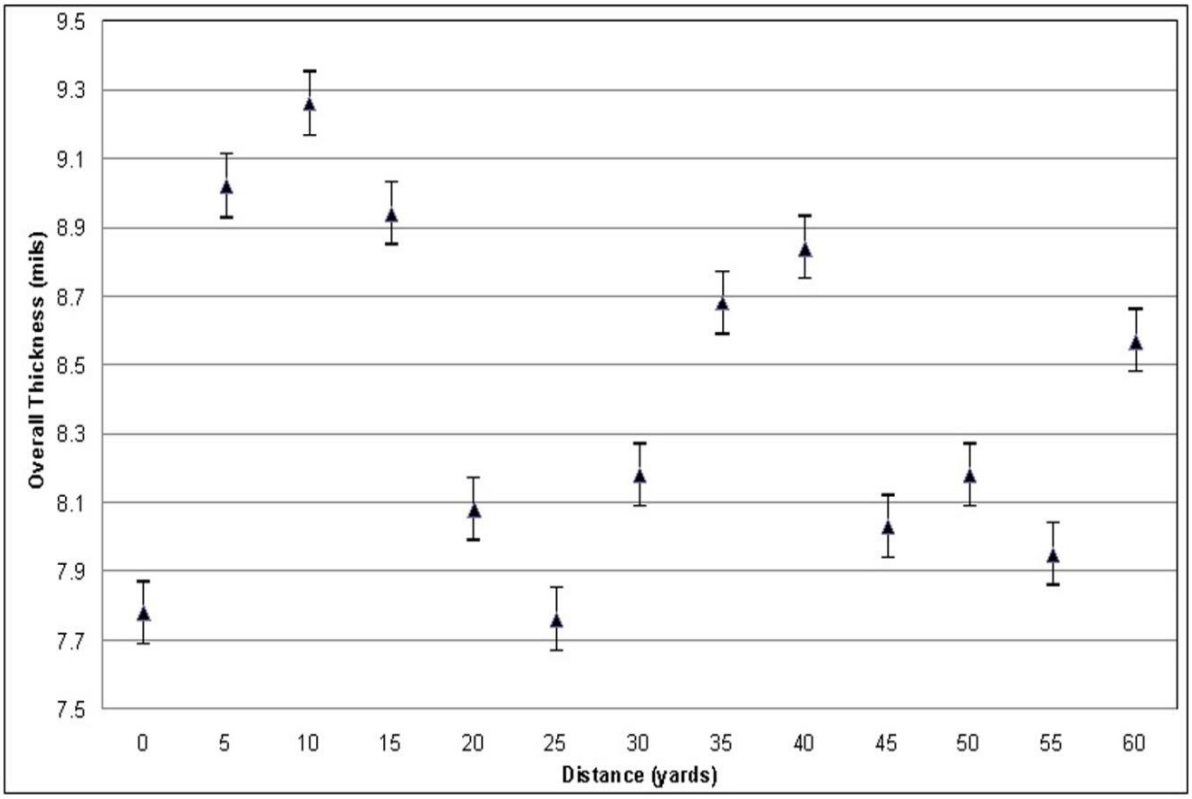

Figure 4 Individual 95% confidence intervals for mean overall thickness as a function of location on a single roll of tape from product S. Many of the pieces are statistically distinguishable in thickness.

In general, the results of the Two-Way Repeated Measures ANOVA and the One-Way ANOVA tests reported were found to yield comparable conclusions. Interaction effects between the length and the roll position factors also tended to be statistically significant but no clear trend was evident that would permit the interaction to be straightforwardly interpreted.

FTIR

The average first derivative FTIR spectra are plotted in Figure 5 as a heat map. Visual inspection of the roll homogeneity shows that differences between rolls (both along the length of a single roll and across the width of a jumbo roll) are much smaller than differences between products. However, potential differences along the length of the individual rolls and across the width of the jumbo rolls may be present even if not

Table 5: Tukey HSD pairwise comparisons results for tape pieces from the same roll

Roll	Unwarranted Exclusions (Overall Thickness)	Unwarranted Exclusions (Film Thickness)
B0A	0 of 66	0 of 66
B0B	16 of 66	0 of 66
B0C	0 of 66	0 of 66
C0A	0 of 78	1 of 78
C0B	1 of 78	5 of 78
C0C	2 of 78	12 of 78
I0A	3 of 78	0 of 78
I0B	12 of 78	2 of 78
I0C	7 of 78	4 of 78
M0A	12 of 78	14 of 78
M0B	10 of 78	11 of 78
M0C	8 of 78	0 of 78
S0A	48 of 78	0 of 78
S0B	61 of 78	0 of 78
S0C	49 of 78	0 of 78

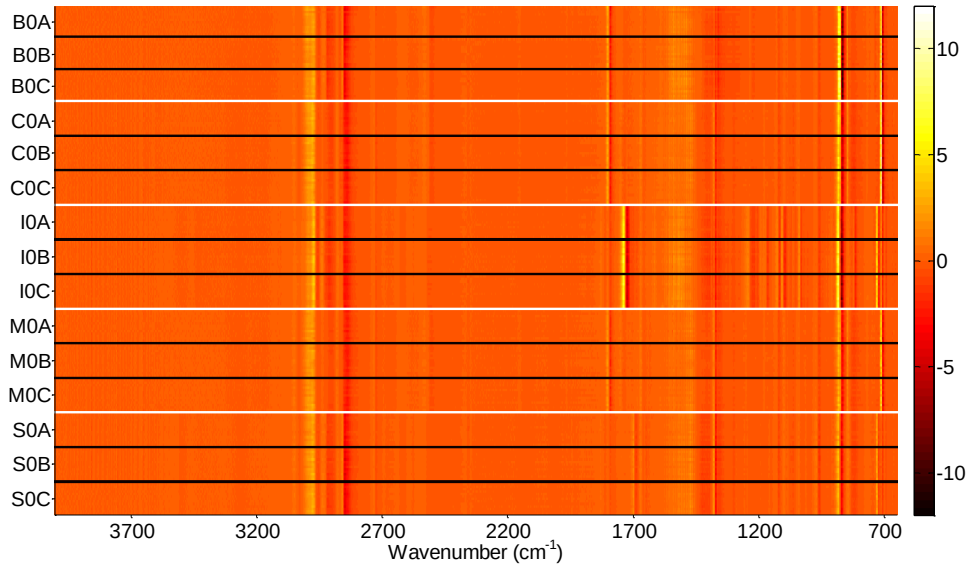

Figure 5 Heat map of average first derivative FTIR spectra. The color of each pixel corresponds to the intensity of the spectrum from each individual roll at each position along the roll length (stacked on the y axis) at the noted wavenumber (x axis) with a color scale given. Very close inspection will reveal minor differences for tape sections taken from the same roll.

visually apparent in the heat map. Therefore, the spectra were also compared statistically to identify potentially outlying samples for visual comparison.

To investigate potential differences along the length of each individual roll, the five to seven spectra from each piece of tape were used as replicate analyses and a separate PCA was performed for each individual roll. Initially, plots of the values of the first two PCs were used to identify potential outliers for visual comparison. None of the samples with the largest differences in PC1 by PC2 plots were distinguishable by spectral overlay when replicate analyses were taken into account. The values of the first 4 PCs were also used to conduct MANOVA analyses for each roll to determine if there were any statistically significant spectral differences along the length of any individual rolls. Statistically significant differences ($p \leq 0.05$) were detected within two rolls (one roll each of two different products): the left roll from product I and the center roll from product C (Table 6). Figure 6 shows the average spectra for the samples with the largest difference in replicate averaged PC values (the center roll from product C at 35 yards and at 60 yards). Although a possible difference in the average spectra occurs around 3600 cm^{-1}, this difference is not repeatable when the individual spectra are examined. Another possible explanation for the differences detected by the MANOVA tests for the samples in Figure 6 is prepared sample thickness, as the spectrum for one piece of tape indicates thicker samples than the spectrum of the other piece of tape. Other possible factors include spectral noise and unrepeatable peaks/ratios.

Because no differences were detected which would lead to an exclusion, the five to seven sample spectra from each piece of tape were averaged. The averaged spectra from each of the 12 or 13 locations along the length of each individual roll were then used as replicate analyses to compare differences across the width of each jumbo roll. A separate PCA was performed for each jumbo roll. The values of the first 4 PCs from each individual roll were compared to the values from the two other rolls arising from the same jumbo roll using a MANOVA test.

Table 6 p-values for a MANOVA test for comparison of FTIR spectra along the length of an individual roll

		Individual roll		
		A	B	C
Product	B	0.5307	0.0828	0.3827
	C	0.6152	0.0101	0.2232
	I	0.0338	0.2353	0.1154
	M	0.0537	0.8611	0.2217
	S	0.3734	0.0806	0.4622

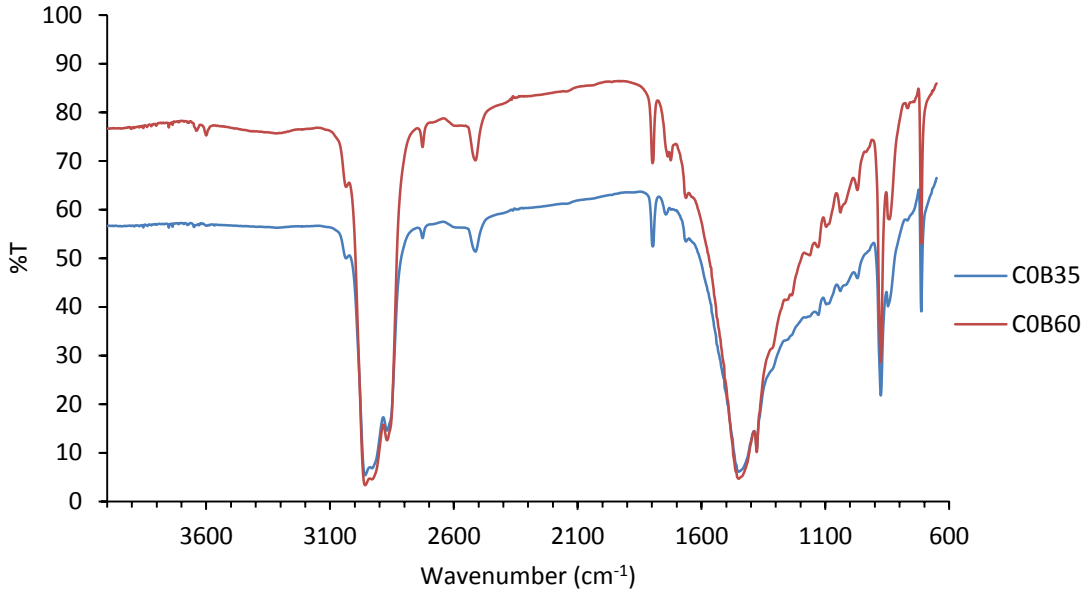

Figure 6 Product C FTIR spectra (average of six samples each) from the center roll at 35 yards (C0B35, blue trace, bottom spectrum) and at 60 yards (C0B60, red trace, top spectrum). These two average spectra had the largest difference between average PC scores for the two rolls (C0B and I0A) that showed a statistically significant difference along the roll length. The spectra are displayed on a common scale, in which the y-axis values are applicable to both spectra. The difference observed between these two spectra appears to be due primarily to the thickness of the samples analyzed. A doublet is observed at 3600 cm.-1 However, these peaks had a low intensity relative to background and were not sufficiently reproducible to call the spectra different when observing individual spectra (note: mean spectra are displayed for clarity).

Differences at $\alpha=0.05$ between individual rolls produced from the same jumbo roll were detected for four of the five jumbo rolls tested (Table 7). However, when the spectra with the largest difference between their PC values (the left roll at 20 yards and the right roll at 15 yards from product I) were compared visually no differences were detected (Figure 7). The difference between these two spectra could be due to the thickness of the samples analyzed (I0A20 appears to have been thicker than I0C15).

DISCUSSION

The scrim count measurements usually did not vary along the length of an individual roll or between rolls taken from the same jumbo roll. In rolls that did vary, additional observations (e.g., curved fill yarns) were made that should be considered when assessing whether two scrim counts are significantly different. In general, a tolerance of ± 1 yarn in either direction appears acceptable; however, analysis of a greater variety of tapes would be of benefit to establishing a specific criterion. Caution is advised in

casework samples when there is possible damage to the scrim (e.g., film deformation or a severely degraded adhesive).

Table 7 p-values for a MANOVA test for the comparison of individual rolls from within the same jumbo roll using the first 4 PCs from a separate PCA generated for each product using the 12 to 13 averaged spectra as replicate analyses

Product	p-value
B	0.0012
C	0.0015
I	<0.0001
M	0.6670
S	0.0012

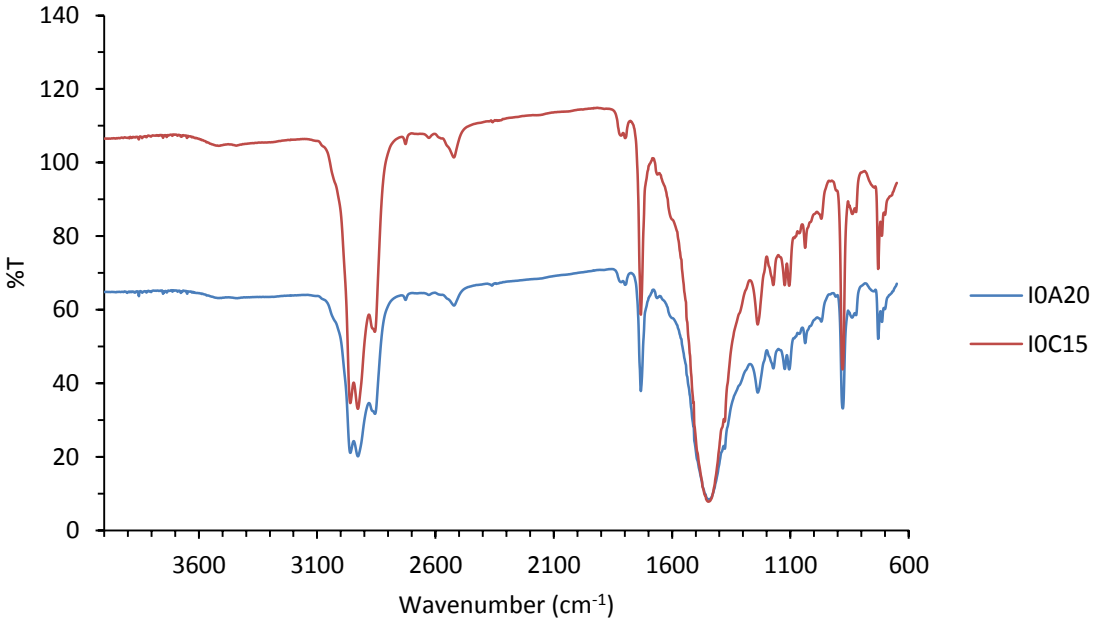

Figure 7. Product I FTIR spectra (average of six samples each) from the left roll at 20 yards (I0A20, blue trace, bottom spectrum) and the right roll at 15 yards (I0C15, red trace, top spectrum). These two average spectra had the largest difference between PC scores for product I (which had the most significant difference across a jumbo roll). The spectra are displayed on a common scale, in which the y-axis values are applicable to both spectra. The difference observed between these two spectra appears to be due to the thickness of the samples analyzed.

Since the warp yarn offset was observed to vary along the length of the individual rolls of tape, this examination should not be routinely conducted. A possible use of the

technique might be for end matching of tape pieces, since the fabric (and individual yarns) should be aligned when assessing whether an end match is possible.
In general, the widths of the examined tapes did not change or changed by only 0.5 mm within a single roll. Larger differences resulted between different rolls cut from the same jumbo roll. Since the sample set included only 15 rolls, a larger set of tapes should be analyzed before any broad statements are made regarding what criteria would result in an "exclusion". Additionally, the rolls examined were pristine and therefore not subjected to the effects of tearing or stretching. Any possible deformation should, therefore, be taken into account when assessing whether two widths are significantly different.

It is evident from the statistical evaluations performed that many of the individual rolls examined are neither statistically homogeneous in overall thickness nor in film thickness. Moreover, an overall evaluation of the tapes taken from the same jumbo roll shows that a particular tape piece will often be closer in thickness to pieces taken from another individual roll of the same jumbo roll than to some pieces taken from its parent individual roll (Figures 8 and 9). It is then obvious that pairwise comparisons of tape thickness using standard statistical methods will often lead to unacceptably high false exclusion rates due to inherent inhomogeneities within a given roll. Based on the limited number of rolls examined, the overall thickness appears to be of the greatest concern in this regard.

For these tape sets, empirically setting a maximum permissible difference in overall thickness of 15% would result in an overall false rejection rate of 0.5% for pairwise comparisons of tape pieces known to be from the same roll. Similarly, allowing a maximum difference of 15% for film thickness would result in no false rejections in pairwise comparisons of tape pieces known to be from the same roll. However, given the small sample of rolls examined and their pristine state, it is not obvious that a 15% maximum difference rule could be expected to perform well in all circumstances.

Two of 15 individual rolls of duct tape showed statistically significant variation in their FTIR spectra along the roll length. Visual inspection by spectral overlay of the statistically identified outlier samples showed differences that would not lead to an exclusion in a forensic examination. Similarly, the statistical differences detected across four of the five jumbo rolls would not lead to an exclusion by visual comparison of the spectra with the highest and lowest PC values.

In conclusion, this research indicates that scrim count does not vary to a great extent along the length of an individual pristine roll of tape nor between different rolls cut from the same jumbo roll. Width also does not vary to a great extent along the length of an

individual roll of tape, but it may differ between different rolls cut from the same jumbo roll. Warp yarn offset, however, should not be used to discriminate samples due to large variations in this feature along the length of a roll. Statistical analysis of the thickness and adhesive composition indicate that some statistically significant differences can be detected. However, these differences are not meaningful in the context of the forensic examination of mass-produced products. Notably, the thickness variation evident within a given roll means that relying on statistically significant thickness differences as a decision criterion can have a high probability of incorrectly excluding tape pieces that actually come from the same roll. As such, the finding of a relatively small but statistically significant difference in thickness cannot be used with high confidence to conclude that two tape pieces are from different rolls. Further, while there appear to be some statistically significant changes in chemical composition detected by FTIR along the length of an individual duct tape roll and more commonly across a jumbo roll for these samples, the changes are not large enough to cause an exclusion and are clearly much smaller than the changes in chemical composition between products.

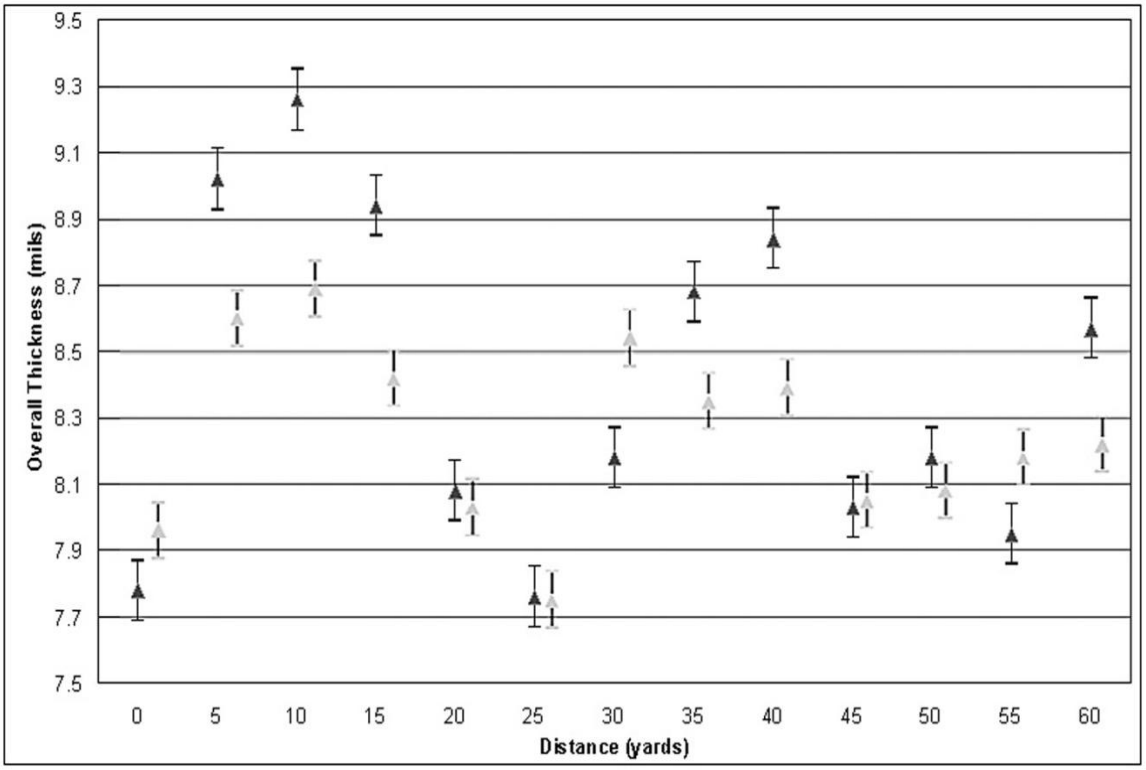

Figure 8 Individual 95% confidence intervals for mean overall thickness as a function of location for two different individual rolls of tape from product S. Often, a particular tape piece is closer in thickness to pieces taken from another roll from the same jumbo roll than to some pieces taken from its individual parent roll.

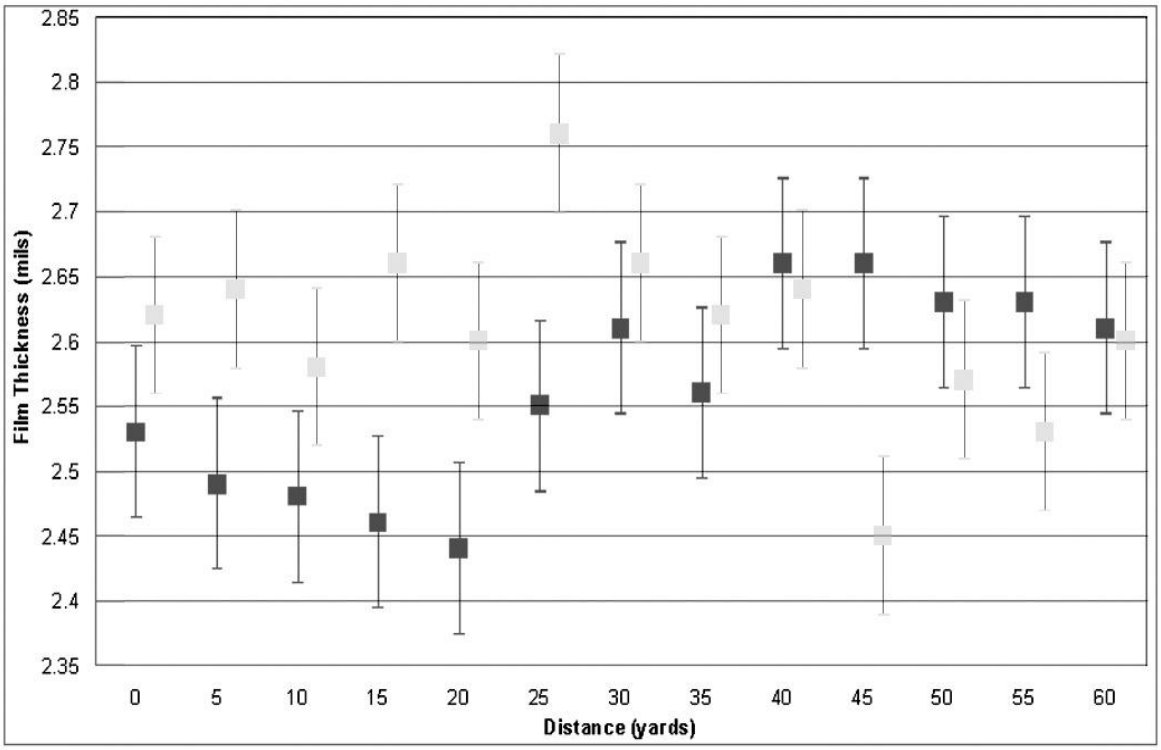

Figure 9 Individual 95% confidence intervals for mean film thickness as a function of location for two different individual rolls of tape from product M.

ACKNOWLEDGMENTS

The authors would like to thank the manufacturers who provided samples for the study. We also wish to thank Maureen Bradley for her assistance in preparing the samples, and Geoffrey Geberth for his assistance in analyzing them. Finally, we would like to thank Christopher Saunders for his fruitful discussions regarding the statistical analysis.

This research was supported in part by an appointment to the Visiting Scientist Program at the FBI Laboratory Division, administered by the Oak Ridge Institute of Science and Education, through an interagency agreement between the US Department of Energy and the FBI.

REFERENCES

1. Mehltretter A, Bradley M. Forensic analysis and discrimination of duct tapes. JASTEE 2012;3(1): 2-20.
2. Keto RO. Forensic characterization of black polyvinyl chloride electrical tape. *Proceedings of the International Symposium on the Analysis and Identification of Polymers*. Quantico, VA, July 31-August 2, 1984: 137-143.

3. Jenkins, Jr. TL. Elemental examination of silver duct tape using energy dispersive X-ray spectrometry. *Proceedings of the International Symposium on the Analysis and Identification of Polymers*. Quantico, VA, July 31-August 2, 1984: 147-149.
4. Blackledge, RD. Tapes with adhesive backings: their characterization in the forensic science laboratory. *Appl Polym Anal Charact* 1987: 413-421.

P. Gardner,[1] M.S., M.F. Bertino, [2] Ph.D., and Robyn Weimer,[3] M.S.

Differentiation between Lip Cosmetics Using Raman Spectroscopy

ABSTRACT

In this study, 34 lip glosses and 17 lip balms were analyzed using Raman spectroscopy. Samples that were not heavily colored had a high degree of spectral similarities within a product line. Product lines designed to impart color were found to differ between shades and brands. Though no individual peaks were found that could definitively categorize samples of lip cosmetics, it was possible to differentiate between brands and in some cases, between different colors within a product line. For lip glosses, all of the product lines and 59% of the samples examined could be differentiated. For lip balms, all of the product lines and 76% of samples examined could be differentiated.

Keywords: Cosmetics, Lip gloss, Lip balm, Raman

INTRODUCTION

In the course of laboratory casework, the analysis of cosmetic evidence may become necessary. Lipstick evidence in particular has been recovered on bedding and clothing in rape cases [1], as smears on car panels in hit and run cases or as smears on cigarettes, cups or glasses [2]. Mass production of cosmetic products makes individualization to a specific item impossible, but since cosmetics are diverse in brands, products and colors, they can often be useful as associative evidence. Extensive research has been done with respect to the forensic analysis of lipsticks [1-8], however there has been little investigation into other classes of lip cosmetics such as lip glosses and lip balms. These items are often used as an alternative to lipstick and may be found in similar places at a crime scene.

There have been many research articles discussing possible cosmetic analytical schemes. In the instance of lipsticks, a physical examination may be followed by thin layer chromatography (TLC) [2] or high performance liquid chromatography (HPLC) [1] to determine dye component contributions, scanning electron microscopy/energy

[1] Department of Forensic Science, Virginia Commonwealth University
[2] Corresponding Author: Department of Physics, Virginia Commonwealth University, Box 842000, Richmond, VA 23284
[3] Virginia Department of Forensic Science, 700 N. 5th Street, Richmond, VA 23219

dispersive X-ray spectroscopy (SEM/EDX) [1] to determine elemental composition, gas chromatography/mass spectrometry (GC/MS) for the identification of oils and waxes, fluorescence microscopy to screen based on fluorescence properties and [2] or infrared (IR) spectroscopy for comparison of molecular compositions [9]. Typically, a combination of these techniques is needed to achieve a high level of discrimination.

In recent years, Raman spectroscopy has been presented as a possible addition to the analytical scheme for lipsticks [5, 7, 10]. Raman is advantageous because it requires little sample preparation, is generally non-destructive, has a high discriminatory power, and can produce results within minutes. In a previous study by our group, we reported that when using a 780 nm laser source it was possible to differentiate 95% of 80 examined lipsticks using Raman spectroscopy alone [10].

In this study, the possibility of performing Raman analysis on lip glosses and lip balms was assessed. While in many cases the same company manufactures all three classes of products, there are several differences between them. Lip glosses have a more liquid character, have less contribution from waxes and produce a glossier appearance to lips. Lip balms have a similar waxy character to lipsticks but are typically used to sooth or protect lips rather than impart a visual effect. Both lip balms and lip glosses tend to be less colored than lipsticks.

MATERIALS AND METHODS

Samples of lip balms and lip glosses were obtained via donation. There were 34 samples of lip glosses and 17 lip balms examined. The lip glosses included 20 individual product lines from 16 different brands. The lip balms included eight different product lines from eight different brands. The outermost layer was removed from samples donated with prior use in order to maintain more consistent sample integrity. No information was available about date of manufacture, degree of use, or lot number. A list of lip glosses and lip balms analyzed are provided in Tables 1 and 2, respectively. Ingredients were obtained from either the company website or product packaging when available. Individual shades of lipsticks did not have specific ingredients, but rather were listed as part of a product line.

Two Raman spectrometers were used in this analysis: a Thermo Scientific DXR Smart Raman equipped with a 780 nm laser and a Horiba Labram HR800 confocal Raman microscope with a 532 nm laser. The Thermo Scientific instrument used a laser set to 50 mW with a 25 µm slit. The Horiba instrument used a 10x objective with a fixed laser output of 60 mW. Since aluminum foil has no Raman signal, it was used as the substrate during analysis of samples. Typically, a spectrum was collected using 10 two-second scans for a total exposure time of 20 seconds. Samples were scanned from 50-3400

cm^{-1} and compared via spectral overlay for chemical differences. No smoothing or corrections for background fluorescence were used on the spectra. Peak location, shape and band presence/absence were compared.

Table 1 Lip Gloss Samples Analyzed

Brand	Product Line	Color	Ingredients listed
Black Radiance	Liquid Lip Color	Coral Kiss	Not Available
Boots	Botanics Lip Gloss	Cherry	Pentaerythrityl Tetraisostearate, Lanolin, Polybutene, Cera Microcristallina (Microcrystalline Wax) (Microcrystalline Wax), Capric/Caprylic Stearic Triglyceride, Bis Diglyceryl Polyacyladipate 2, Octyldodecanol, Aroma (Fragrance) (Flavor), Propylene Glycol, Stearalkonium Hectorite, Cocos Nucifera (Coconut) Oil (Coconut), Mineral Oil (Paraffinum Liquidum) (Mineral oil), Propylene Carbonate, Ginkgo Biloba Leaf Extract, Hydroxyisohexl 3 Cyclohexene Carboxaldehyde, BHT, Phenoxyethanol, Methylparaben, Aloe Vera (Aloe Barbadensis) Leaf Juice, Butylparaben, Ethylparaben, Propylparaben, Isobutylparaben **May Contain**: Titanium Dioxide
Claire's Cosmetics	Square	Dark Pink	Beeswax, Butylene Glycol, Caprulic/Capric Triglyceride, Ceresin, Ethylhexyl Palmitate, Flavor, Hydrogenated Microcrystalline Wax, Iron Oxides, Isostearyl Isostearate, Mica, Petroleum, Polybutene, Propylparaben, Red 27 Lake, Red 6 Lake, Synthetic Fluorphlogopite, Titanium Dioxide, Tocopheryl Acetate
		Light Pink	
		Pink	
		White	
	Vial	Blue	Mineral Oil, Caprulic/Capric Triglyceride, Ethylene/Propylene/Stryene Copolymer, Butylene/Ethylene/Stryene Copolymer, Tocopheryl Acetate, Blue 1 Lake, Red 27 Lake, Red 6 Lake, Yellow 5 Lake
		Orange	
		Pink	
		Purple	
		Yellow	
Clarins	Prodige Lip Gloss	5 Grenadine	"The Suprashine Colour complex", "Maxi-Lip® peptide", "Radiance-boosting pearls", Raspberry seed oil
Clinique	Glosswear for Lips	Air Kiss	Lanolin, Aloe Barbadensis, Archidyl Propionate, BHT, Bismuth Oxychloride, Candelilla Wax, Caramine, Ceresin, Iron Oxides, Isopropyl Lanolate, Isopropyl Palmitate, Linoleic Acid, Manganese Violet, Mica, Microcrystalline Wax, Octyl Methoxycinnamate, Octyl Palmitate, Polybutene, Propylene Carbonate, Propylparaben , Red 30 Lake, Red 7 Lake, Stearalkonium Hectorite, Titanium Dioxide,
		Raspberry Jam	

			Tocopheryl Acetate
Covergirl	Outlast All Day Lip Color	553 597 807	**Basecoat**: Isododecane, Trimethylsiloxysilicate, Dimethicone, Disteardimonium Hectorite, PropyleneCarbonate, Propylparaben, Simmondsia Chinensis (Jojoba) Seed Oil, Camellia Sinensis LeafExtract, Tocopherol Acetate, Flavor **May Contain**: Mica, Iron Oxides, Titanium Dioxide, Yellow 5 Lake, Blue 1 Lake, Red 7 Lake,Red 30 Lake, Carmine **Topcoat**: Sucrose Polycottonseedate, Ozokerite, Beeswax, Tocopheryl Acetate, Tocopherol,Propylparaben, Propyl Gallate, Acetyl Glucosamine, Coco Nucifera (Coconut Oil)/ AloeBarbadensis Leaf Extract, Theobroma Cacao (Cocoa) Seed Butter, Butyrospermum Parkii (SheaButter), Sodium Saccharin, DL-Alpha Tocopheryl Acetate, Flavor
	Wetslick Lipgloss	415 Crush Eprise	Water, Propylene Glycol, Isopropyl Myristate, Mineral Oil, Talc, Cetyl Palmitate, Glyceryl Stearate, Fragrance, Stearic Acid, Eucalyptus Citriodora Oil, Sodium Lauryl Sulfate, Magnesium Aluminum Silicate, Triethanolamine, Trisodium EDTA, Cellulose Gum, Camphor, Menthol, Eugenia Caryophyllus (Clove) Flower Oil, Propylparaben, Methylparaben, Lithium Stearate, Titanium Dioxide, Iron Oxides **Dark Shades**: Water, Propylene Glycol, Isopropyl Myristate, Mineral Oil, Talc, Stearic Acid, Cetyl Palmitate, Polysorbate 60, Glyceryl Stearate, Fragrance, Eucalyptus Citriodora Oil, Magnesium Aluminum Silicate, Triethanolamine, Trisodium EDTA, Imidazolidinyl Urea, Camphor, Xanthan Gum, Menthol, Eugenia Caryophyllus (Clove) Flower Oil, Propylparaben, Methylparaben, Titanium Dioxide, Iron Oxides, Ultramarines
Estee Lauder	Purecolor Gloss	Hot Lava	Polybutene, Petrolatum, Polydecene, Microcrystalline Wax, Vitamin E, Lecithin, Ethylhexylglycerin, Vitamin C, Calcium Sodium Borosilicate, Poly(ethylene Terephthalate), Acrylates Copolymer, Simethicone, Silica, Butylated Hydroxytoluene, Tin Oxide, Fragrance, Mica, Titanium Dioxide, Bismuth Oxychloride, Red 7 Lake, Blue 1 Lake, Copper, Manganese Violet, Yellow 6 Lake, Bronze Powder, Red 33 Lake, Red 30 Lake, Carmine, Red 22 Lake, Red 28 Lake, Yellow 5 Lake, Orange 5, Red 6, Calcium Aluminum Borosilicate, Synthetic Fluorophlogopite, Iron Oxide
Loreal	Colour Riche LeGloss	Nude Touch	G849192:C18-36 Acid Triglyceride, Bis-iglyceryl Polyacyladipate-2, Pentaerythrityl Tetraisosterate, Polybutene, Tridecyl Trimellitate, Diisostearyl Malate, Silica Dimethyl Silylate, Pentylene Glycol, Caprylyl

			Glycol, Calcium Aluminum Borosilicate, Pentaerythrityl Tetra-Di-T-Butyl Hydroxyhydrocinnamate, Benzyl Alcohol, Alumina, Argania Spinosa Oil / Argania Spinosa Kernel Oil, Tocopheryl Acetate, Rosa Canina Fruit Oil, Isostearyl Alcohol, Sodium Saccharin, Calcium Sodium Borosilicate, Silica, Synthetic Fluorphlogopite, Polyethylene Terephthalate, Tin Oxide, Acrylates Copolymer, Parfum / Fragrance, May Contain Peut Contenir, Titanium Dioxide, Mica, Iron Oxides, Red 22 Lake, Red 28 Lake, Yellow 6 Lake, Red 7, Red 7 Lake, Yellow 5 Lake, Carmine, Blue 1 Lake
Mary Kate & Ashley	Liquid Color Ultra Wet Lip Gloss	Gorgeous	Not Available
Mary Kay	Nourishine Lip Gloss	Berry Sparkle Bronze Bliss Gold Rush	Hydrogenated Polyisobutene, Triisostearyl Citrate, C10-20 Cholesterol/Lanosterol Esters, Diisosteraryl malate, Ozokerite, Ethelyene/Propylene/Stryene Copolymer, Ricinus Communis (Castor) Seed Oil, Aluminium Calcium Sodium Silicate, Tocopherol, Shale Extract, Punica Granatum Sterols, Retinyl Palmitate, Tocopheryl Acetate, Aloe, Barbadensis Leaf Extract, Tetrahexyldecyl Ascorbate, Glycine Soja (Soybean) Oil, Octyldodecanol, Butylene/Ethylene/Stryene Copolymer, Calcium Sodium Borosilicate, Flavor, Calcium Aluminum Borosilicate, Silica, Synthetic Fluorphlogophite, BHT, Aluminium hydroxide, Alumina, Ascorbyl Palmitate, Mica, Tin Oxide
Max Factor	Colour	770	Not Available
Maybelline	Shinylicious	40 Lolly Pink	Not Available
NYX	Sheer Gloss	Not Available	Not Available
Revlon	Colorstay Mineral Lipglaze	Stay Ablaze	Styrene/Acrylates Copolymer, Phenyltrimethicone, Cetyl PEG/PPG 10/1 Dimethicone, Hexyl Laurate, Polyglyceryl 4 Isostearate, Trimethylsiloxyphenyl Dimethicone, Isododecane, PPG 51/SMDI Copolymer, Silica Silylate, Cera Microcristallina (Microcrystalline Wax), Parfum (Fragrance), Limonene, Benzyl Benzoate, Citral, Caprylyl Glycol, 1,2 Hexanediol **May Contain**: Mica, Titanium Dioxide, Iron Oxides, Yellow 5 Lake, Red 21, Red 7 Lake, Red 6 Lake, Red 33 Lake, Orange 5, Carmine
	Beyond Natural Cream Lipgloss	Berry	Not Available (Product Discontinued)
Ulta	Brilliant	Berry	Polybutene, Octyldodecanol, Petrolatum, Beeswax,

	Color	Pixie	Ozokerite, Trihydroxystearin, Ricinus Communis (Castor Oil) Seed Oil Flavor, Phenoxyethanol, BHT, Tocopheryl Acetate, Helianthus Annuus, (Sunflower) Seed Oil Retinyl Palmitate, Carthamus Tinctorius, (Safflower) Seed Oil, Aloe Barbadensis Leaf Extract **May Contain**: Iron Oxides, Titanium Dioxide, Red 7 Lake, Red 6, Red 33 Lake, Red 28 Lake, Yellow 5 Lake, Blue 1 Lake, Carmine, Mica, Calcium Aluminum Borosilicate,
	Super Shiny	Cutie	Polyisobutene, Hydrogenated Polyisobutene, Isohexadecane, Octyl Palmitate, Hydroxystearic Acid, Fragrance
		Siren	
Victoria's Secret	Sweet Talk	Sensual Strawberry	Not Available (Product Discontinued)

Table 2 Lip Balm Samples Analyzed

Brand	Product Line	Color	Ingredients
Alba Botanica	Terra Tints SPF 8	Blaze	Beeswax, Calendula, Candelilla Wax, Carnauba, Castor Oil, Echinacea, Iron Oxides, Jojoba Oil, Lanolin, Mica, Oxybenzone, Padimate-O, Peppermint Oil, Titanium Dioxide, Tocopherol, Tocopheryl Acetate,
Bonne Bell	Lip Smacker	Melon Memories	Acetylated Lanolin Alcohol, Beeswax, Candelilla Wax, Carnauba Wax, Castor Oil, Cetyl Acetate, Flavor, Hydrogenated Soy Glycerides, Mineral Oil, Ozokerite, Polybutene, Sesame Oil
		Sugared Plum Dreams	
Burt's Bees	Lip Shimmer	Champagne	Burts Bees Lip Shimmer, Glycine Soja (Soybean) Oil, Mentha Piperita (Peppermint) Oil, Theobroma Cacao (Cocoa) Seed Butter, Candelilla Cera (Euphorbia Cerifera, Cire De Candelilla) Wax, Canola Oil (Huile De Colza), Cera Alba (Beeswax, Cire D'abeille), Cera Carnauba (Copernicia Cerifera, Cire De Carnauba) Wax, Helianthus Annuus (Sunflower) Seed Oil, Lanolin, Limonene, Ricinus Communis (Castor) Seed Oil, Rosmarinus Officinalis (Rosemary) Leaf Extract, Tocopherol **May Contain**: Iron Oxides, Mica, Titanium Dioxide, Caramine, Tin Oxide
		Rhubarb	
Chap-Ex	Tropicals	Bahama Berry	Aloe Vera, Cetyl Alcohol, Flavor, Isopropyl Lanolate, Isopropyl Myristate, Methylnaraben, Mineral Oil, Octinoxate, Oxybenzone, Propylparaben, Stearic Acid, Vitamin E , Waxes
Mary Kay	Tinted Lip Balm	Rose	Ascorbyl Palmitate, Bis-Diglyceryl Polyacyladipate-2, Butylene Glycol, Butyrospermum Parkii (Shea Butter), C10-30 Cholesterol/Lanosterol Esters, C30-50 Alcohol, Copernicia Cerifera (Carnauba) Wax,
		Poppy	
		Apricot	

		Blush	Euphorbia Cerifera (Candelilla) Wax, Hyaluronic Acid, Iron Oxides, Lanolin, Microcrystalline Wax, Octinoxate, Octocrylene, Octyldodecanol, Oxybenzone, Pentaerythrityl Tetraisostearate, Phytantriol, Red 7 Lake, Retinyl Palmitate, Simmondsia Chinensis (Jojoba) Seed Oil, Sorbitol, Tiliroside, Titanium Dioxide, Tocopherol, Tocopheryl Acetate, Triethoxycaprylylsilane, Trihydroxystearin, Ubiquinone, Vanillin, Zinc Oxide **May Contain**: Ricinus Communis (Castor) Seed Oil, Mica, Red 40 Lake, Red 30 Lake, Red 27 Lake, Red 33 Lake, Red 6 Lake, Yellow 5 Lake, Blue 1 Lake, Carmine,Tin Oxide
		Natural	
Neutrogena	Moistureshine tinted lip balm	30 Sunny	Octyldodecanol, Aloe Barbadensis Leaf Extract, Aluminum Hydroxide, Candelillawax (Euphorbia Cerifera), Carnauba Wax (Copernicia Cerifera), Flavor, Glyceryl Stearate, Isopropyl Jojobate, Jojoba Alcohol, Jojoba Ester, VP/Hexadecene Copolymer, Caprylic/Capric/Myristic/Stearic Triglyceride, Castor Seed Oil (Ricinus Communis), C12-15 Alkyl Benzoate, Trioctyldodecyl Citrate, Polyethelene, Ascorbyl Glucoside, Ascorbyl Palmitate, BHT, Tocopheryl, Tocopheryl Acetate, Octinoxate, Ozokerite, Petrolatum, Phenyl Trimethicone, Polybutene, Saccharin, Stearic Acid, Titanium Dioxide, Trimethylolpropane Triisostearate
Pallido	Herbal Tinted Lip balm	Orange	Polybutene, Octyldodecanol Caprylic/Capric Triglyceride, Ozokerite, Synthetic Wax, Microcrystalline Wax, Butyrospermum Parkii (Shea Butter) Fruit, Cetyl Lactate, Beeswax, Myristyl Lactate, Zea Mays (Corn) Starch, Silica, Helianthus Annuus (Sunflower) Seed Oil, Prunus Amygdalus Dulcis (Sweet Almond) Oil, Aluminum Hydroxide, Propylparaben, BHT, Tetradibutyl Pentaerithrityl Hydroxyhydrocinnamate, Benzotriazolyl Dodecyl P-Cresol, Persea Gratissima (Avocado) Oil, Wheat Germ Glycerides, Ricinus Communis (Castor) Seed Oil, Vanillin, Tocopherol, Ascorbyl Palmitate, Tocopheryl Acetate, Retinyl Palmitate, Panax Ginseng Root Extract, Camellia Sinensis Leaf Extract, Ginkgo Biloba Leaf Extract, Chamomilla Recutita (Matricaria) Flower Extract, Aloe Barbadensis Leaf Extract
Topps	Push Pop Flavored Lip Balm	Cherry	Not Available
		Watermelon	
		Blue Raspberry	
		Strawberry-Watermelon	

RESULTS AND DISCUSSION

In our previous study on lipsticks, all samples were found to be fluorescent when excited with the 532 nm laser. Fluorescence was also frequently encountered in lip balm and gloss samples, especially in the more colored samples. Most clear lip cosmetics, however, were not strongly fluorescent and could be analyzed by both the 532 and 780 nm laser sources. Figure 1 compares Raman spectra obtained using excitation with both the 532 and 780 nm laser for a weakly fluorescent sample. Overall, the spectra coincide. A higher baseline between 2000 and 2500 cm^{-1} was noticed with the 532 nm excitation and is most likely due to fluorescence. As with the lipstick samples, the 780 nm laser minimized fluorescence contributions and should be considered the preferred wavelength for analysis.

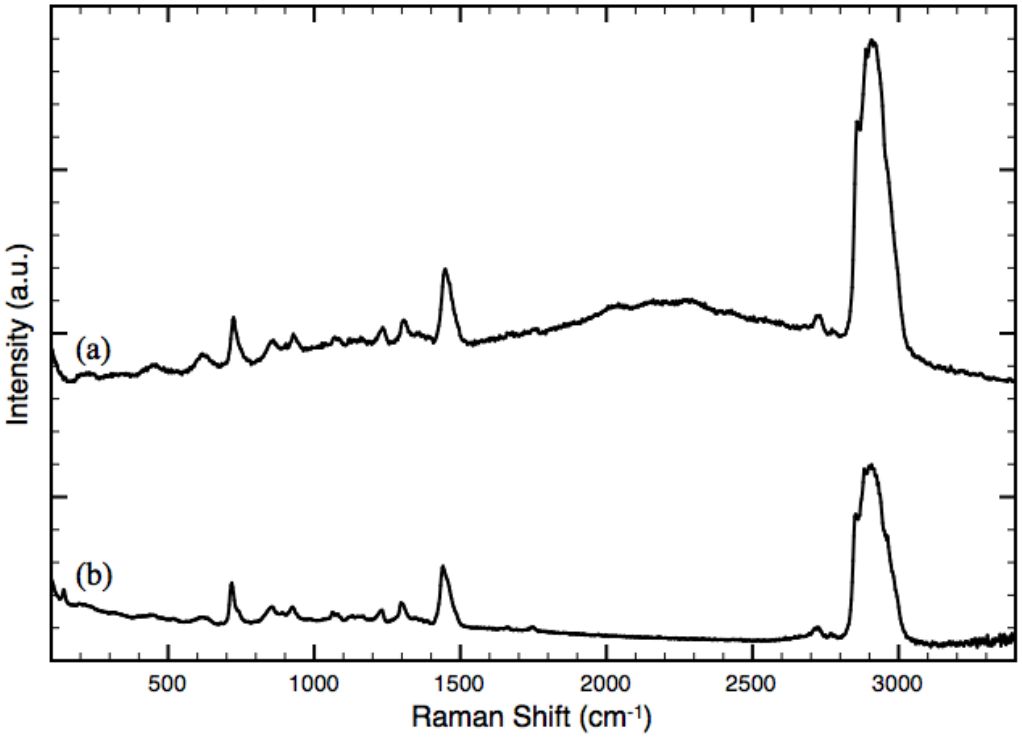

Figure 1 Raman spectra of white Claire's Cosmetics lip gloss using the (a) 532 and (b) 780 nm laser sources.

A typical lip gloss spectrum is shown in Figure 2. As was common in lipsticks [10], peaks were in one of three intervals: peaks below 800 cm^{-1}, peaks between 1000–1700 cm^{-1} as well as a series of overlapping bands between 2800–3000 cm^{-1} which are consistent with various C–H vibrations. The peaks found at 396, 515 and 640 cm^{-1} were reconciled with titanium dioxide (anatase) and the peaks at 225, 294 and 410 cm^{-1} were reconciled with iron oxide [11]. These oxides were both commonly observed in lipsticks [10] and were seen less frequently in lip glosses and lip balms. Castor seed oil was one

of the most commonly listed ingredients, appearing in 92% of lip balms and 22% of lip glosses that listed ingredients. Its bands were typically masked in the examined lip glosses. However, as can be seen in Figure 3, Alba Botanica's Terra Tints Blaze lip balm exhibits many peaks that could be attributed to this oil. Because of the quantity of different oils and waxes it was generally difficult to identify specific organic components.

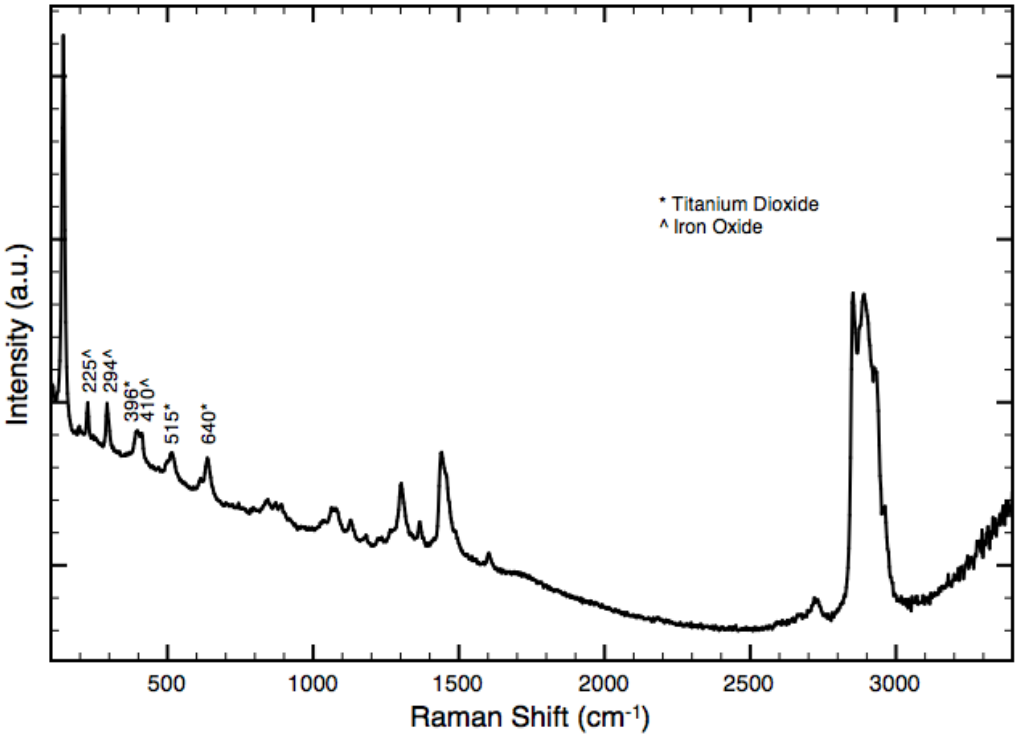

Figure 2 Raman spectrum of Clarins Rouge Prodige lip gloss in the color Grenedine, demonstrating a typical lip gloss spectrum.

It should be noted that in our previous study on lipsticks, no intra-sample variability was observed, and in a limited check of lip glosses and lip balms, this was also true. In order to further demonstrate that this holds true in this study, two spectra of Mary Kay's Nourishine Lip Gloss Bronze Bliss were collected on different days. As can be seen in Figure 4, no demonstrable differences were observed.

In the case of a typical lip balm sample, shown in Figure 5, it was less common to see peaks below 800 cm^{-1}. This is most probably due to fewer contributions from inorganic pigments. Commonly observed peaks at 1132, 1295, 1440, 2727, and 2882 cm^{-1} could be attributed to a combination of different waxes: candelilla wax, carnauba wax, lanolin, ozokerite and beeswax, all of which were commonly listed ingredients [12-14]. Carnauba wax and beeswax are also shown in Figure 5 and are often contributors to the

spectra of lip cosmetics. While there were some peaks more commonly seen in lip glosses, lip balms or lipsticks, none were identified that could potentially be used to differentiate between the three product classes.

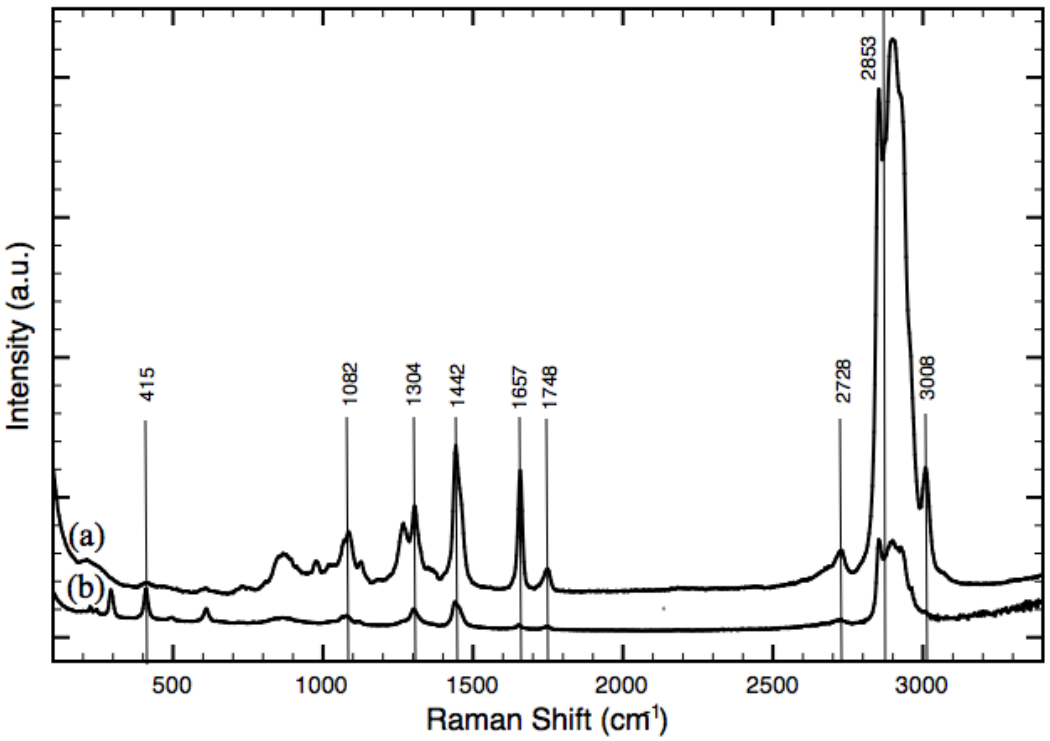

Figure 3 Raman spectra of (a) Castor Seed Oil which is an ingredient in the lip balm, and (b) Alba Botanica Terra Tints Blaze.

Colorants heavily influence Raman spectra as they can produce differing spectra even when samples are visually consistent [15, 16]. In lipsticks, this allowed for discrimination between samples in the same product line but restricted the possibility of identifying a specific brand of lipstick using its spectrum [10]. However, due to weak or non-existent contributions from colorants, the differentiation between lip glosses and lip balms from the same product line was more complicated. This was the case in samples from Claire's Cosmetics lip glosses, shown in Figure 6. The colors in the packaging appeared as a transparent blue, yellow, purple, orange or pink, allowing for visual differentiation, but the Raman spectra produced were indistinguishable.

This was also true for several lip balm samples including the Lip Smacker brand lip balms seen in Figure 7. Discrimination within a product line was only possible when the samples were heavily colored as with Clinique Glosswear lip gloss, shown in Figure 8. None of the samples examined had identical spectra to a sample from a different brand or a different class of product. Discrimination between brands and product lines within

the same brand was possible within this sample pool. For example, while the three clear lip glosses from different brands shown in Figure 9 share many characteristics, it is still possible to differentiate between them despite their visually similar color. Since lip balms are meant to soothe chapped lips in addition to imparting a visual effect and therefore tend to have a greater amount and variety of ingredients, it is not surprising that clear lip balms, as shown in Figure 10, were more easily distinguished than clear lip glosses.

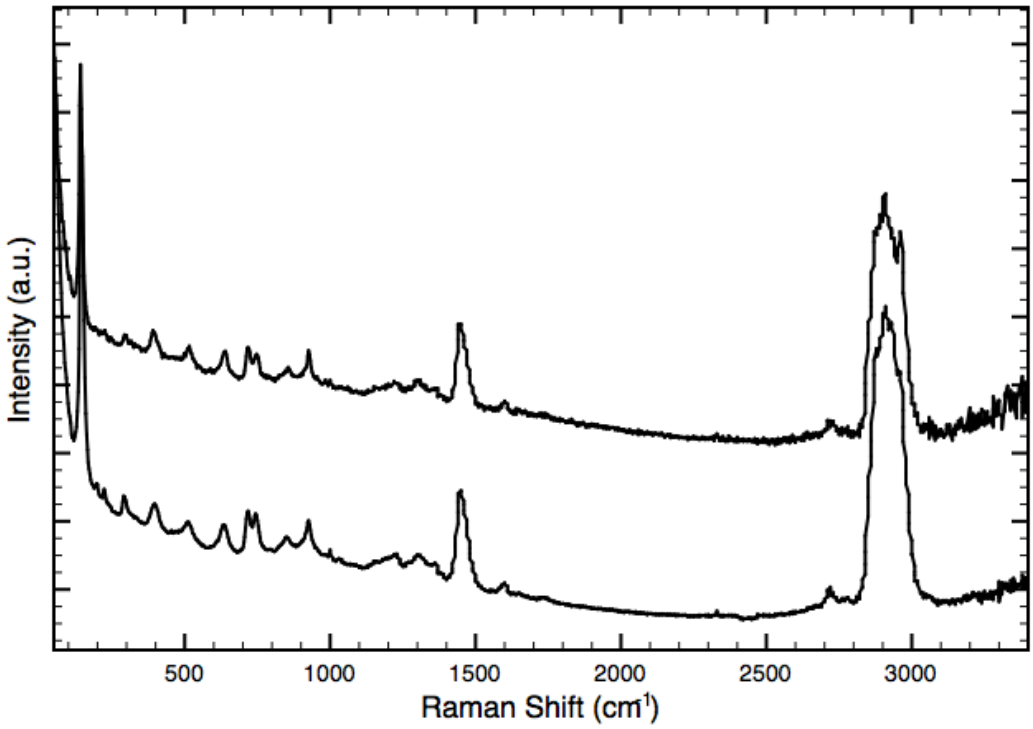

Figure 4 Raman spectra of Mary Kay's Nourishine Lip Gloss Bronze Bliss taken on successive days.

The three most listed colorants were Red 7 Lake, Yellow 5 Lake and Blue 1 Lake. In products listing Red 7 Lake, it was common to see the colorant's strongest three peaks, 1368, 1494 and 1606 cm^{-1} [17], but some or all of the minor peaks were either missing or masked. The same was true for Yellow 5 Lake which has strong peaks at 1602, 1505, 1126 and 1343 cm^{-1} [17]. Blue 1 Lake which has weak Raman peaks at 918, 1176, 1222, 1425 and 1621 cm^{-1} could not be confirmed in any spectra [17]. Due to the quantity of colorants used in lip cosmetic products and their similarities in composition, it was difficult to definitely confirm individual constituents.

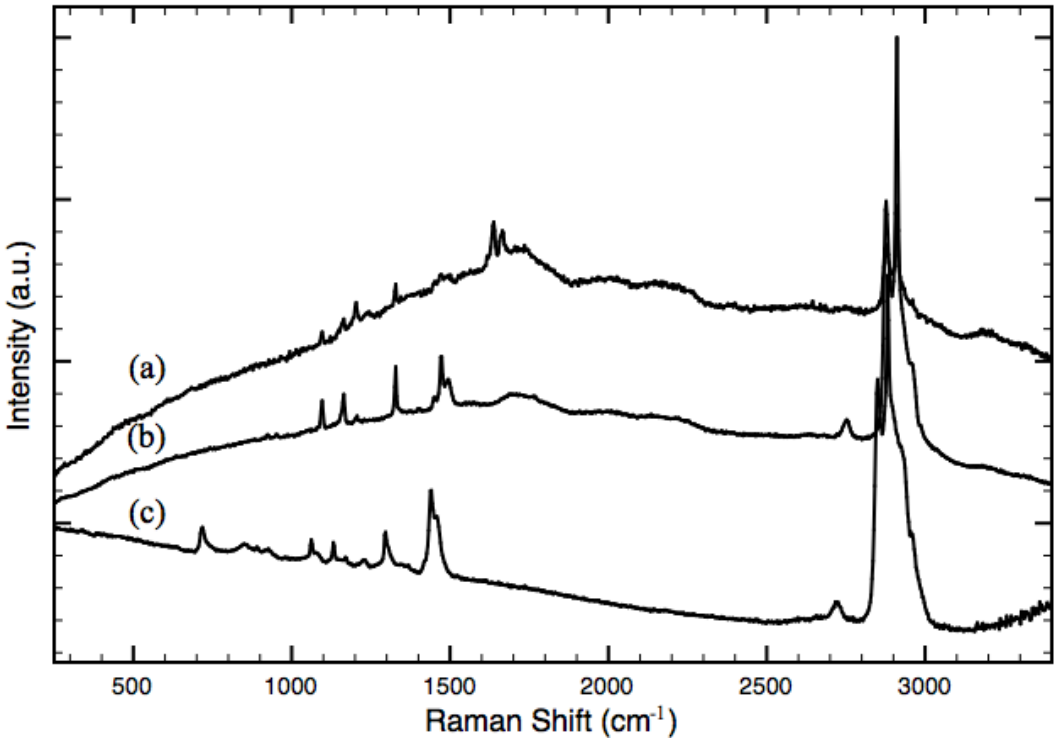

Figure 5 Raman spectra of (a) Carnauba Wax, (b) Beeswax and (c) Topp's Push Pop Watermelon lip balm, a typical lip balm spectrum.

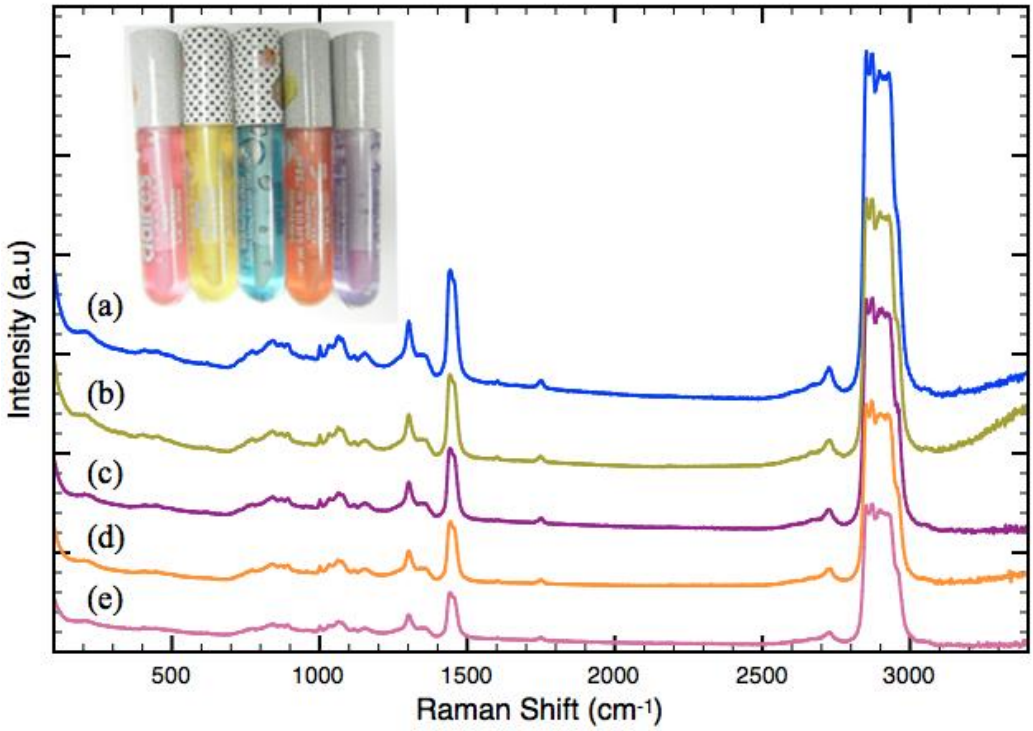

Figure 6 Raman spectra of Claire's Cosmetics lip glosses in (a) blue, (b) yellow, (c) purple, (d) orange and (e) pink, appear indistinguishable between different colors of the same product.

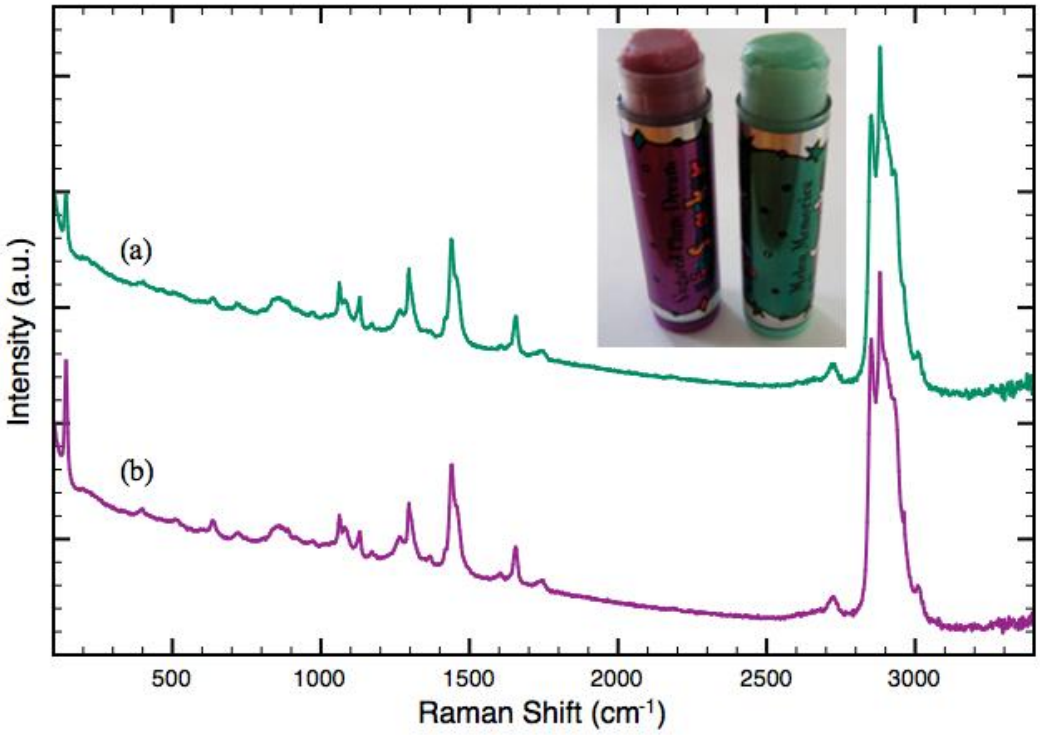

Figure 7 Raman spectra of Lipsmacker lip balm in the colors (a) Melon Memories and (b) Sugared Plum Dreams, lip balm spectra which appear consistent despite visually differing colors.

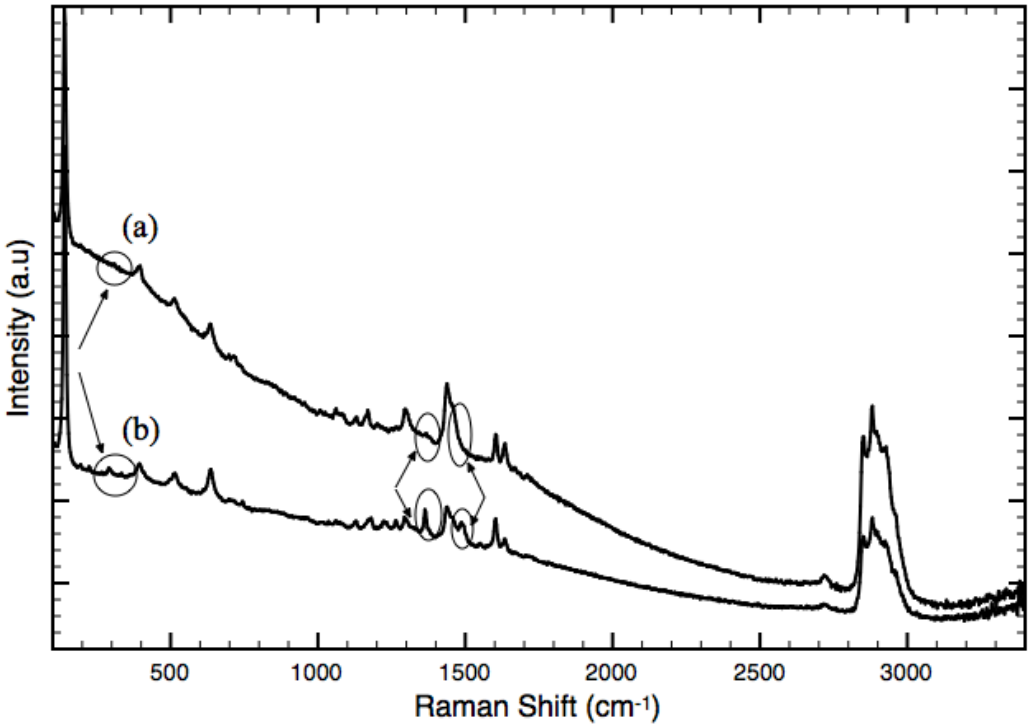

Figure 8 Raman spectra of Clinique Glosswear lip gloss in colors (a) Air Kiss and (b) Raspberry Jam, which differ within the product line.

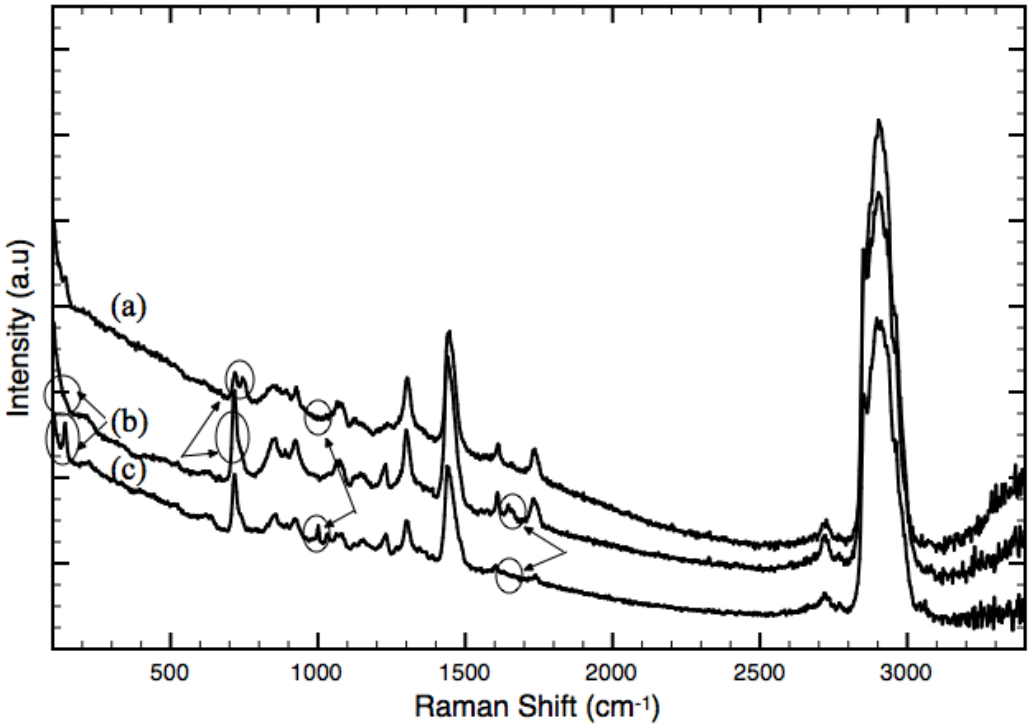

Figure 9 Raman spectra of (a) Revlon LeGloss Nude Touch, (b) Maybelline Shinylicious Lolly Pink and (c) NYX Sheer Gloss, clear lip glosses that can be differentiated between brands.

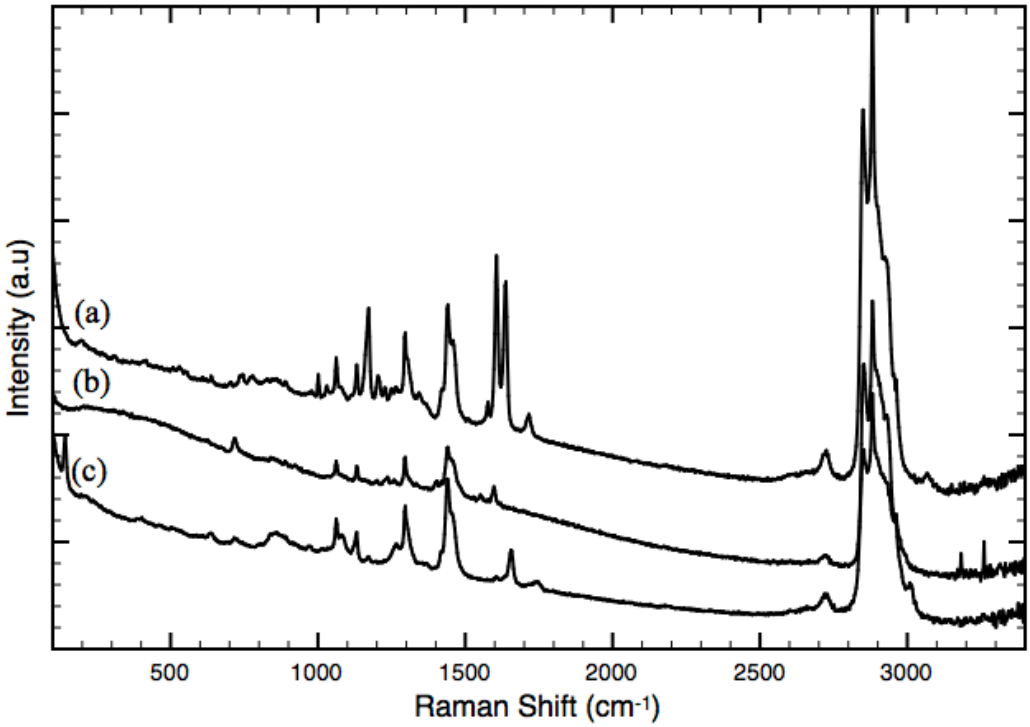

Figure 10 Raman spectra of (a) Chap Ex Tropicals Bahama Berry, (b) Push Pop Cherry and (c) Lipsmackers Melon Memories, three clear lip balms that can be easily differentiated.

CONCLUSION

In addition to the analysis of lipstick, Raman spectroscopy can be used to differentiate between lip glosses and lip balms. The 780 nm laser source was preferred for analysis as the 532 nm source hindered analysis of more highly fluorescing components. Since the 780 nm laser source was only available on our benchtop Raman, no microscopic examinations of the samples were performed. Trends within a brand were more likely to be influenced by base composition instead of color additives since lip glosses and lip balms typically appear clear on application. However, in the cases of products designed to impart color, different shades of the same product had different spectra, a trend that was also observed in lipsticks. No trends were found which could classify a sample as to the particular type of lip cosmetic (lip gloss, lip balm, or lipstick).

As the samples were used, it is possible that they may have been affected by environmental factors such as heat, saliva, and age. In the future, it would be useful to examine the effects of aging and contaminated samples, as these are more likely to be encountered in casework. Additionally, combination with another technique such as GC/MS may be used to better identify individual components such as wax components in the cosmetics.

Raman analysis allows data to be obtained in a matter of minutes, is non-destructive, and can provide good discriminatory power within lip cosmetics. Different classes of lip cosmetics could be treated using the same procedure during Raman analysis and this technique would be most useful in the comparison of questioned and known samples.

ACKNOWLEDGEMENTS

We would like to thank HORIBA scientific for providing a spectrum of Castor Seed Oil.

REFERENCES

[1] Choudhry MY. Comparison of Minute Smears of Lipstick by Microspectrophotometry and Scanning Electron-Microscopy Energy Dispersive Spectroscopy. Journal of Forensic Sciences. 1991;36:366-75.

[2] Ehara Y, Marumo Y. Identification of Lipstick Smears by Fluorescence Observation and Purge-and-Trap Gas Chromatography. Forensic Science International. 1998;96:1-10.

[3] Andrasko J. Forensic Analysis of Lipsticks. Forensic Science International. 1981;17:235-51.

[4] Reuland D, Trinler W. A Comparison of Lipstick Smears by High Performance Liquid Chromatography. Journal of the Forensic Science Society. 1980;20:111-20.

[5] Rodger C, Broughton D. The In-Situ Analysis of Lipsticks by Surface Enhanced Resonance Raman Scattering. Analyst. 1998;123:1823-6.

[6] Russell L, Welch AE. Analysis of Lipsticks. Forensic Science International. 1984;25:105-16.

[7] Salahioglu F, Went MJ. Differentiation of Lipsticks by Raman Spectroscopy. Forensic Science International. 2012;223:148-52.

[8] Seguí MA, Feucht MM, Ponce AC, Pascual FAV. Persistent Lipsticks and Their Lip Prints: New Hidden Evidence at the Crime Scene. Forensic Science International. 2000;112:41-7.

[9] Gordon A, Coulson S. The Evidential Value of Cosmetic Foundation Smears in Forensic Casework. Journal of Forensic Sciences. 2004;49:1244-52.

[10] Gardner P, Bertino MF, Weimer R, Hazelrigg E. Analysis of Lipsticks Using Raman Spectroscopy. Forensic Science International. 2013;232:67-72.

[11] Hanesch M. Raman Spectroscopy of Iron Oxides and (Oxy) Hydroxides at Low Laser Power and Possible Applications in Environmental Magnetic Studies. Geophysical Journal International. 2009;177:941-8.

[12] Jehlicka J, Edwards HGM, Villar SEJ, Pokorny J. Raman Spectroscopic Study of Amorphous and Crystalline Hydrocarbons From Soils, Peats and Lignite. Spectrochimica Acta Part A: Molecular and Biomolecular Spectroscopy. 2005;61:2390-8.

[13] Edwards HGM, Falk MJP. Fourier-Transform Raman Spectroscopic Study of Unsaturated and Saturated Waxes. Spectrochimica Acta Part A: Molecular and Biomolecular Spectroscopy. 1997;53:2685-94.

[14] Jehlicka J, Edwards HGM, Villar SEJ. Raman Spectroscopy of Natural Accumulated Paraffins from Rocks: Evenkite, Ozokerite and Hatchetine. Spectrochimica Acta Part A: Molecular and Biomolecular Spectroscopy. 2007;68:1143-8.

[15] Zięba-Palus J, Michalska A, Wesełucha-Birczyńska A. Characterisation of Paint Samples by Infrared and Raman Spectroscopy for Criminalistic Purposes. Journal of Molecular Structure. 2011;993:134-41.

[16] Zięba -Palus J, Was-Gubala J. An Investigation into the Use of Micro-Raman Spectroscopy for the Analysis of Car Paints and Single Textile Fibres. Journal of Molecular Structure. 2011;993:127-33.

[17] Palenik CS, Palenik S, Herb J, and Groves E. Fundamentals of Forensic Pigment Identification by Raman Microspectroscopy: A Practical Identification Guide and Spectral Library for Forensic Science Laboratories. US Department of Justice, 2011: www.ncjrs.gov/pdffiles1/nij/grants/237050.pdf

Steven Stone,[1] M.S.

Flexible Sealants – An Analysis

ABSTRACT:

An encounter with flexible sealants during casework led to the purchase and analysis of three different brands of the aerosolized sprays.

KEYWORDS: Flexible Sealants, IR, SEM, Py-GC-MS, PLM

INTRODUCTION

Recently, a case was examined that involved footwear impressions in what was described as "Flex Seal paint" a product typically sold through TV advertisements. The ads indicate that it is an aerosolized spray that can be used to fill any cracks, seals, or other areas of damage around the house. After searches at various retail stores, three different brands of this type of "paint" were acquired: PMI Technology's Flex Seal®, Rust-Oleum's® LeakSeal™, and Home Armor's™ Flexible Sealer (Figure 1). The Safety Data Sheets for these products show that they all contain large amounts of hydrocarbons along with other extenders and compounds in varying amounts such as calcium carbonate, barium sulfate, and hydrogen sulfide.[1,2,3] The following is an analysis of these three different sealant products.

PROCEDURE

Each of the three brands was sprayed onto individual microscope slides and allowed to dry. Material from each slide was sampled with a scalpel and placed onto two additional slides. On one of the slides the sample was smeared to form a thin film and on the other slide the sample was dissolved in xylenes in order to separate the extenders from the binder for microscopy. Both slides were then observed with a Polarized Light Microscope (PLM, Olympus BH, mounting medium MeltMount™ refractive index 1.662).

The flexible sealants were further analyzed on a Fourier Transform Infrared Spectrometer (IR, two separately prepared samples for each compound , Nicolet Thermo Nexus 760, Diamond Anvil Cell), a Scanning Electron Microscope with Electron Dispersive X-Ray Spectroscopy attachment (SEM-EDX, Hitachi S-4000 (SEM), EDAX (EDX), multiple runs on one prepared sample focusing on specific particles), and Pyrolysis Gas Chromatograph Mass Spectrometer (Py-GC-MS, two separately prepared samples for each compound, CDS 5250 Pyroprobe (Py) (Method: 750°C for 15 seconds), Agilent

[1] Washington State Patrol Crime Laboratory, 2203 Airport Way S. Bldg A. Ste 250 Seattle, WA 98134

7890A Gas Chromatograph (GC) (Split Ratio: 50:1, Column: 5% phenyl methyl siloxane, Method: 50°C for 1 minute, then 6°C/minute to 100°C, hold at 100°C for 1 minute, then 8°C/minute to 140°C, hold at 140°C for 1 minute, then 16°C/minute to 220°C, then hold at 220°C for 15.67 minutes), Agilent 5975C Mass Spectrometer (MS).

Figure 1 – The three brands analyzed

OBSERVATIONS

The texture of the dried sealants varied between the cans after spraying (Figure 2), but each appeared as a black coating (alternatively, some of the brands come in a white version as well). While spraying, it was noted that the sealants were emitted from the cans at differing amounts of force (nozzle design or other factors) which may account for the variance.

When sampled with a scalpel, the Flex Seal® and Flexible Sealer were both viscous. The LeakSeal™ sampled like a "typical" paint, peeling away. Both the Flex Seal® and the

Flexible Sealer smeared easily onto the microscope slides. The LeakSeal™ was more problematic and less prone to smearing, resulting in a thicker sample.

Figure 2 – Flex Seal®, LeakSeal™, and Flexible Sealer after drying.

PLM analysis of the smears showed opaque particles along with several dispersed birefringent particles of various sizes for each brand (Figure 3).

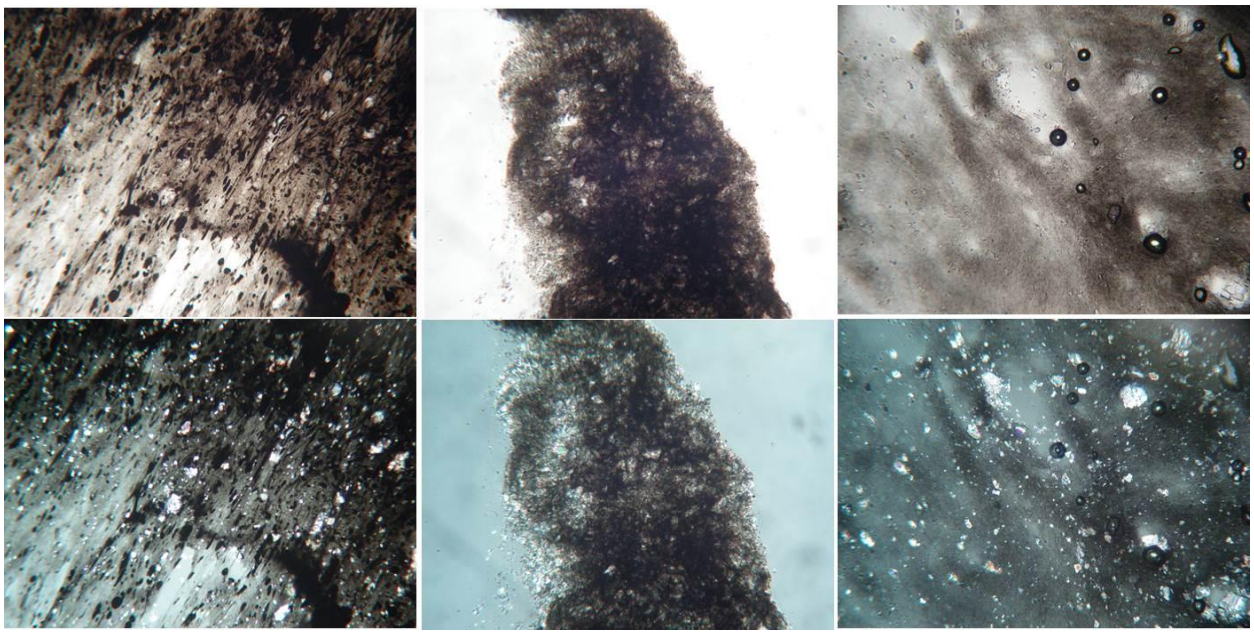

Figure 3 – Left to Right, PLM images of the smears of Flex Seal®, LeakSeal™, and Flexible Sealer. The top image is in polarized light; the bottom image is with slightly-uncrossed polars.

Calcite crystals of varying sizes were observed within the xylene dissolved samples (Figure 4). These were characterized by observing the striations on the crystal face and then noting that at one extinction value the crystal had high relief (in accordance with the nε of 1.48)[4] and at the other extinction had low relief (in accordance with the nω of 1.60)[5]. When viewed in high relief, the characteristic striations are observed in many of the crystals. Calcite was later confirmed with the IR.

Figure 4 – Calcite crystal example as seen in LeakSeal™ sample. Shown in high relief with characteristic striations.

IR spectra of the three brands showed similarities between the Flex Seal® and Flexible Sealer. The LeakSealTM had a noticeably different spectrum. All three brands had calcite bands (2515 cm^{-1}, 1797 cm^{-1}, 1424 cm^{-1}, 876 cm^{-1}) as well as styrene bands (a slightly shifted 760 cm^{-1} band as well as 700 cm^{-1}). The LeakSeal™ bands appeared to have a higher intensity of calcite than the other two. A rising baseline was observed in the spectra which was most likely due to carbon black (Figure 5).

Analysis with the SEM-EDX showed greater similarity in elemental composition between the Flex Seal® and the LeakSeal™ than with the Flexible Sealer, because of the detection of magnesium and aluminum (Figure 6). LeakSeal™ was shown to have a much higher prevalence of calcium. When an analysis was conducted focusing on specific particles, it was not possible to locate a particle in the LeakSeal™ that did not contain calcium. In contrast, particles without calcium were found in the in the Flex Seal® and Flexible Sealer. These are likely silicates. The element peaks for barium and sulfur were not observed in any of the samples which are in contrast to their being listed in at least one of the Safety Data Sheets.

Analysis with the Py-GC-MS showed similarities between all three brands due to the large styrene component and styrene pyrolysis byproducts that were observed (Figure 7). There were several differences in the ratios of the more intense peaks between the compounds but these were all determined to be styrene byproducts. From a comparison standpoint the only differences of note occur in the ratios of some of the more prevalent peaks, and in the data post twenty minutes.

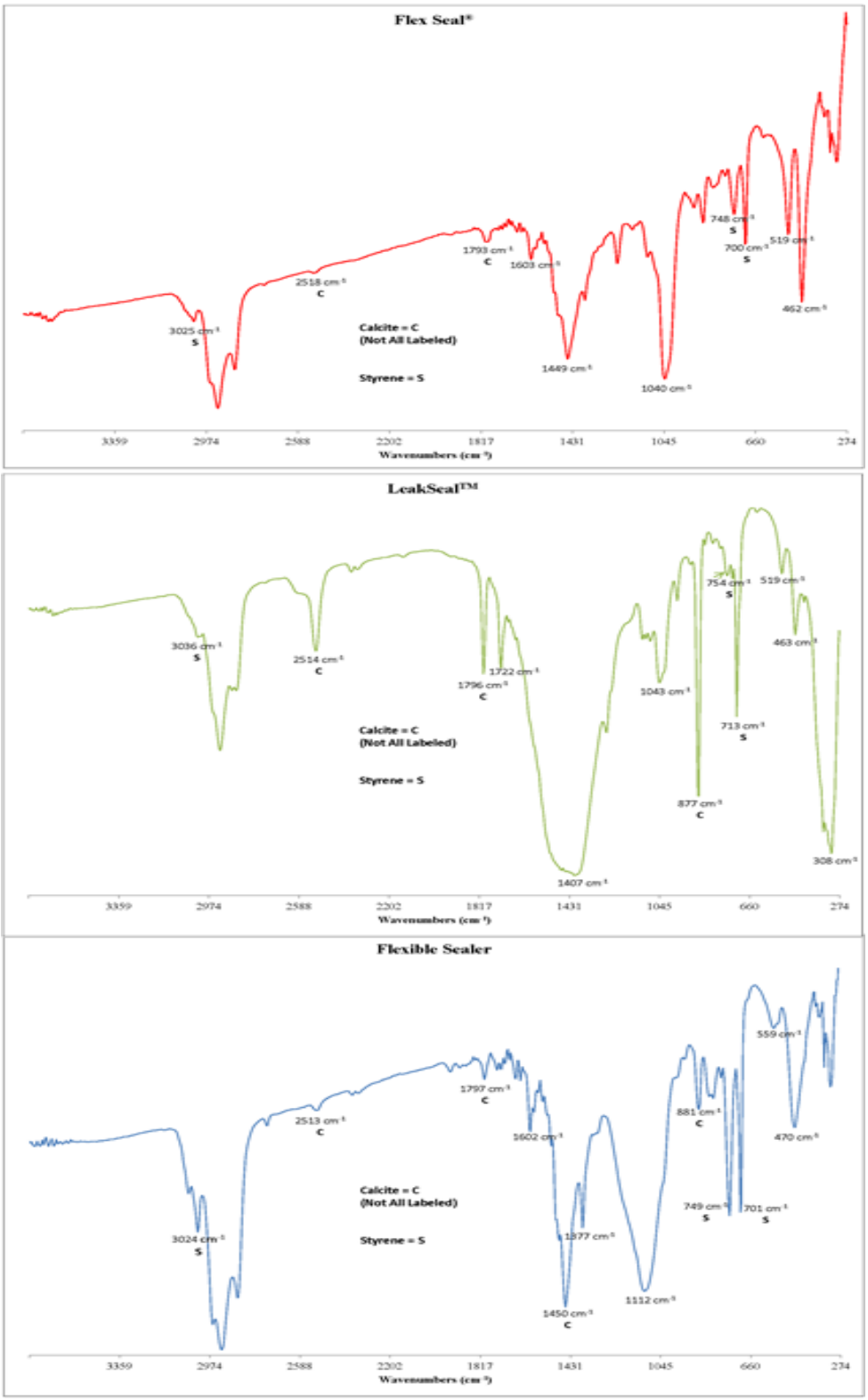

Figure 5 – IR spectra of Flex Seal®, LeakSeal™, and Flexible Sealer.

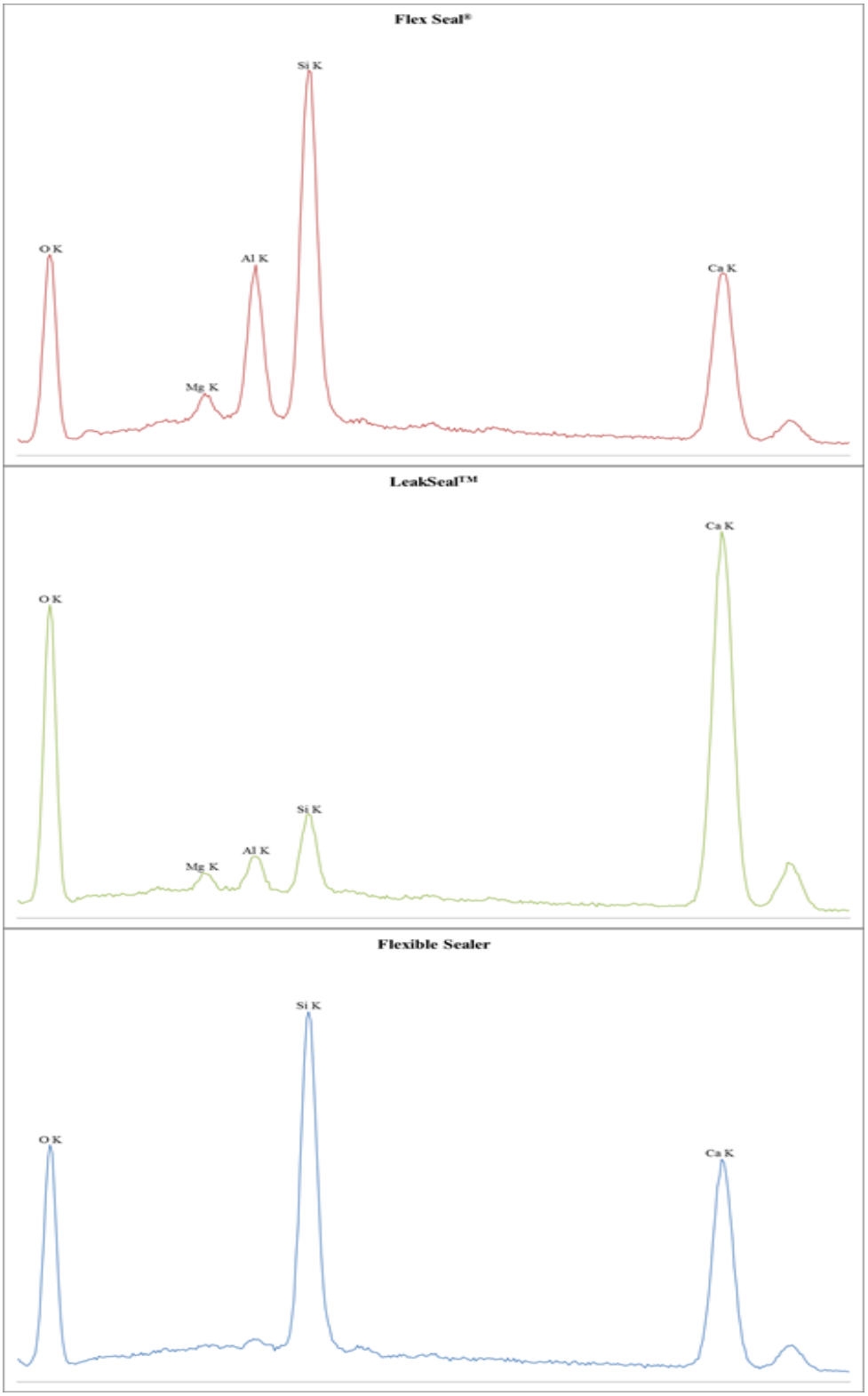

Figure 6 – Overall SEM-EDX of Flex Seal®, LeakSeal™, and Flexible Sealer. These spectra have been cropped to show the only peaks observed.

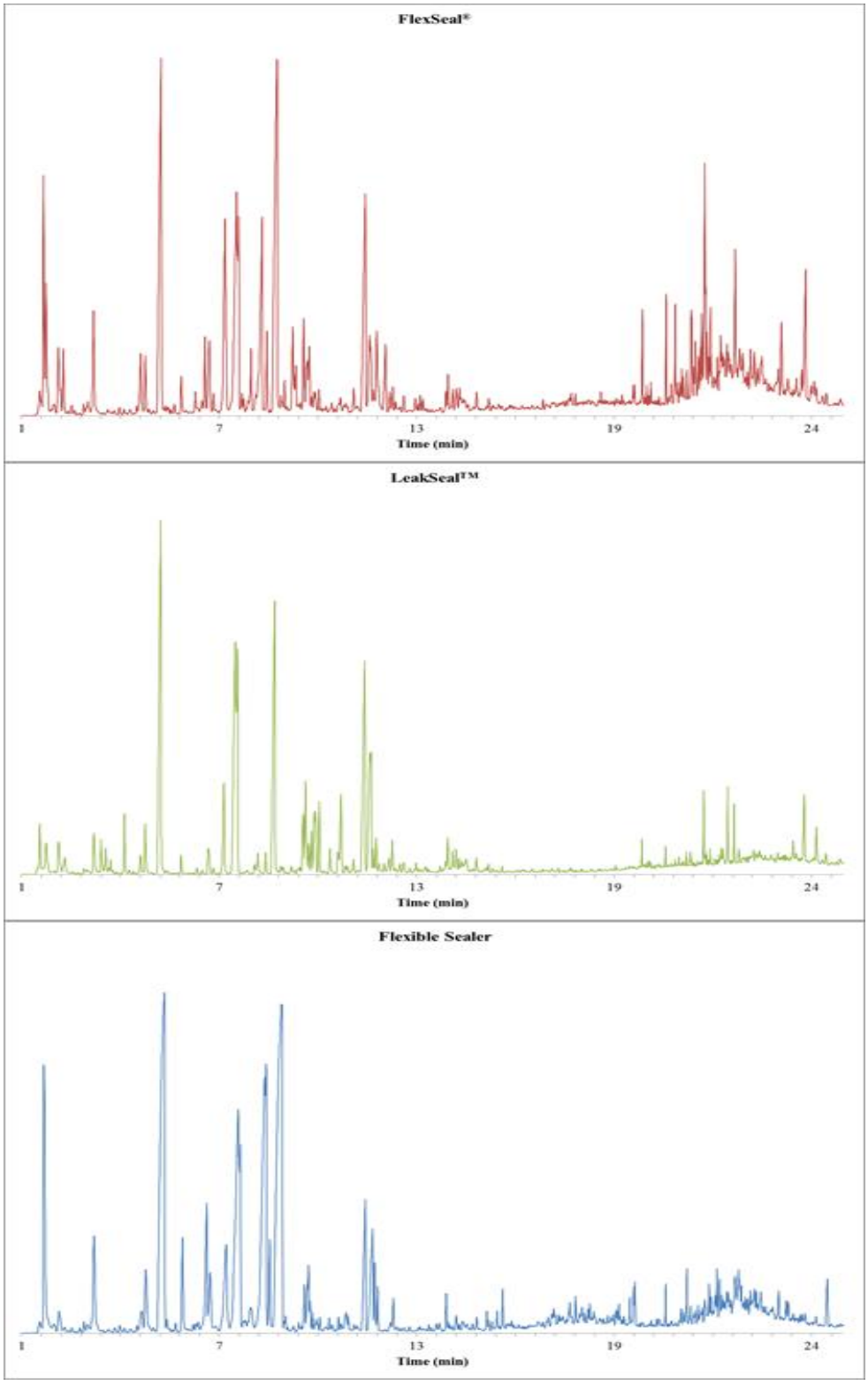

Figure 7 – Pyrogram of Flex Seal®, LeakSeal™, and Flexible Sealer (Styrene is the predominant peak just past five minutes in each of the spectra)

CONCLUSIONS

Analysis of the three brands of sealants showed that they consist of styrene, carbon black, calcite, silicates, and other various extenders. It is noted that compounds on some of the Safety Data Sheets such as barium sulfate, and hydrogen sulfide were not observed. Further analysis may reveal these compounds as they may be overshadowed by the extensive amounts of calcium carbonate. Based on the instrumental and optical analysis, it was possible to differentiate these three flexible sealants. LeakSeal™ displayed readily apparent differences from the other two sealants, while Flex Seal® and Flexible Sealer displayed more subtle differences from each other. These sealants are readily available and could be found in forensic examinations such as in this case or during an architectural paint comparison. Further studies could include investigations into their durability and chemical components over time and after being exposed to the environment.

REFERENCES

1. Flex Seal; Petrochem Manufacturing Inc.: Carlsbad, CA, March 14, 2006. http://pmitechnology.com/wp-content/uploads/2010/03/FlexSeal-NC-MSDS.pdf (accessed June 24, 2014).

2. LeakSeal; Rust-Oleum: Vernon Hills, IL, August 29, 2013. http://www.rustoleum.com/MSDS/ENGLISH/265495.PDF (accessed June 24, 2014).

3. Home Armor Flexible Sealer; W.M. Barr: Memphis, TN, October 15, 2013. http://www.homearmor.com/uploads/general/HA_Flexible_Sealer_Black.pdf (accessed June 24, 2014).

4. Winchell, Alexander Newton; Winchell, Horace. 1964. The Microscopical Characteristics of Artificial Inorganic Solid Substances: *Optical Properties of Artifical Minerals*. 3rd Edition. Chicago, IL (USA).

THE MICROSCOPE • Vol. 61:2, pp 51–60 (2013)

Plumbum Microraptus: Definitive Microscopic Indicators of a Bullet Hole in a Synthetic Fabric*

Christopher S. Palenik[1], Skip Palenik[1]
Microtrace, LLC
Peter Diaczuk[2]
John Jay College of Criminal Justice and the CUNY Graduate Center

KEYWORDS

Ammunition, backscattered electron imaging, bullets, energy-dispersive X-ray spectroscopy, fabrics, fibers, firearms, forensic science, Fourier transform infrared microspectroscopy, lead, primer gunshot residue, polarized light microscopy, secondary electron imaging, scanning electron microscopy

ABSTRACT

A central question in a criminal forensic investigation involved a hole (later termed a "defect") observed in a garment and whether it was produced by a bullet or some other means. The individual wearing the item was known to have fired or been in the vicinity of a firearm that was discharged, rendering the presence or absence of gunshot residue on the garment irrelevant. The micromorphology and elemental composition of the severed fiber ends in a series of exemplar bullet holes were characterized to identify specific physical indicators of the bullet-garment interaction on a microscopic scale. This study confirms prior research indicating that fiber failure, due to the high-energy transfer from a bullet to a synthetic fabric, is consistent with a high-speed tensile fracture mechanism, which results in characteristic fiber-end micromorphology due to partial melting. In addition, scanning electron microscopy (SEM) imaging and elemental analyses by energy-dispersive X-ray spectroscopy (EDS) provide direct evidence of the capture of detectable microscopic lead particles both on and within the melted fiber ends, a process termed here as plumbum microraptus (microscopic lead capture). These lead particles are observed primarily as planar abrasion fragments but also as spherical particles, the latter of which further illustrates the high-energy transfer. Through the study of individual broken fibers from within a suspected bullet hole, these characteristic indicators provide a minimally invasive and direct means to definitively associate or (equally important) dissociate a fabric defect with a bullet perforation.

INTRODUCTION

The question of whether or not a bullet has perforated a fabric is a discrete question with relevance to the field of forensic science. In many instances, the presence of secondary evidence such as blood, tissue or an associated wound can render such a question trivial. In close range events, the presence of primer gunshot residue (pGSR) on a fabric can provide strong evidence of a ballistic association. At greater distances, a dark ring of debris, called "bullet wipe," is often observed (Figure 1) or can be detected (even on dark clothing) and has been stated to consist of traces of bullet metal, lubricant and residue from the gun barrel (1, 2) (Figure 2). In some cases, bullet wipe may not be visible or the presence of pGSR on a garment may not be sufficient to provide a definitive answer as to the origin of a particular hole. For example, in the event that an alleged bullet hole was located on a garment worn by a person who fired or was in the vicinity of a discharged firearm, such ancillary evidence may not be

* Originally presented at Inter/Micro 2011, Chicago.

[1] 790 Fletcher Drive, Suite 106, Elgin, IL 60213; cpalenik@microtracescientific.com
[2] 524 W. 59th Street, New York, NY 10019; pdiaczuk@jjay.cuny.edu

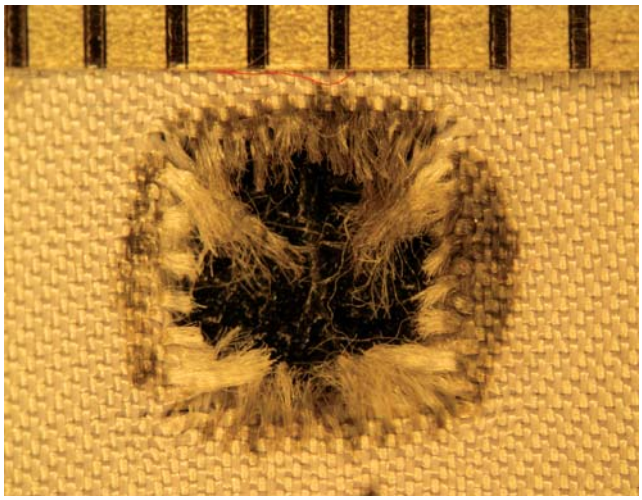

Photo courtesy of Peter Diaczuk

Figure 1. This hole in a woven cotton fabric was made by a 7.62 mm full metal jacket bullet. The discoloration at the perimeter of the hole is an example of "bullet wipe," the deposition of bullet and barrel material transferred as the bullet perforated the fabric. Shown is the entry side of the hole, which has the greatest concentration of deposited material and can be more closely examined microscopically to assess fiber failure mechanisms and spectroscopically to identify the foreign material. The presence of lead can also be determined at such a site by using the classic sodium rhodizonate test. Each line on the scale equals 1/16 inch.

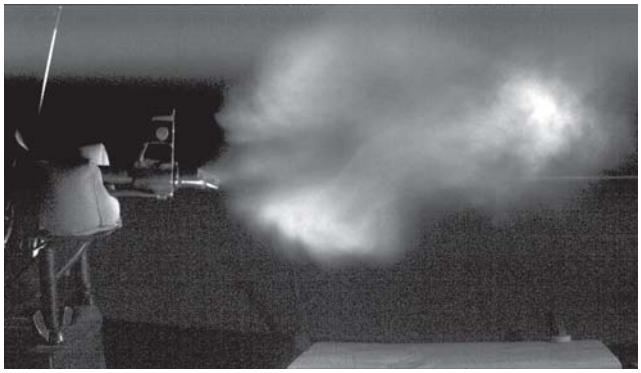

Photo courtesy of Peter Diaczuk

Figure 2. Gases shown were emitted at the muzzle of an AK-47 rifle one millisecond after the bullet exited the barrel. This plume contains a rich supply of lead, which originates from both the primer (containing lead styphnate) and the base of the bullet that is not enclosed by the jacket, thus exposing the lead core (seen in Figure 3) to the hot gases impinging on the base. When the firing sequence begins, the firing pin strikes the primer, creating a shower of sparks that ignites the smokeless powder, which burns rapidly, generating a huge volume of hot gas. Some of the exposed lead is vaporized by the hot gases impinging on the base of the bullet and results in the heavy contribution of lead in the plume exiting the muzzle. A portion of this vaporized lead is left behind in the barrel and condenses inside the barrel circumference when the temperature cools, so when the next bullet travels down the barrel it can carry with it lead from prior discharges.

conclusive. In such cases, we have demonstrated that a direct microscopical examination of the hole, often termed the "defect area" (in contrast to the area surrounding the hole), can provide a definitive answer to this question.

This approach is based on a fundamental principle of forensic science, which suggests a strong likelihood of transfer between objects that come into contact with each other. In the case of a bullet that perforates a synthetic fabric, at least two possible types of transfer are hypothesized to occur at the interface of the bullet and fabric. The first is a transfer of energy, which results in fiber (and fabric) failure; the second is a transfer of material from the bullet to the broken ends of the fibers (or the transfer of polymer to the bullet).

The energy transfer resulting in high-speed synthetic fiber breakage, due to an event such as a bullet perforation, has been mechanically classified as a "high-speed tensile break" (3) or "rapid shear." Physically, such a break can be understood by considering the brief interaction of a fired bullet as it passes through a synthetic fabric whereby a portion of the kinetic energy is transferred from the bullet to individual fibers of the fabric. This tension mechanism stretches and eventually breaks the fiber. The energy transfer is sufficient to melt the stretched portion of the thermoplastic polymer comprising the fiber. This result has been observed in several forensic research efforts specifically involving the perforation of synthetic (nylon or polyester) textiles by a bullet (4, 5). This mechanism does not apply to cellulose-based fibers such as cotton or rayon, which do not melt (6).

It is also anticipated that particle transfer will occur during the bullet-fiber contact period, resulting in the presence of firearms-related particles around this area and embedded in the molten fiber. While SEM/EDS and atomic absorption spectroscopy have been used to identify lead (Figures 3 and 4) and primer particles (Figure 5) in the vicinity of bullet holes (7), it is hypothesized that such particles will also be found on and embedded within the broken fiber ends. Although the distinction between "around" and "embedded within" is minor, the latter provides definitive evidence that the fiber end was created by a high-speed lead or lead-laden object and eliminates the argument of in-

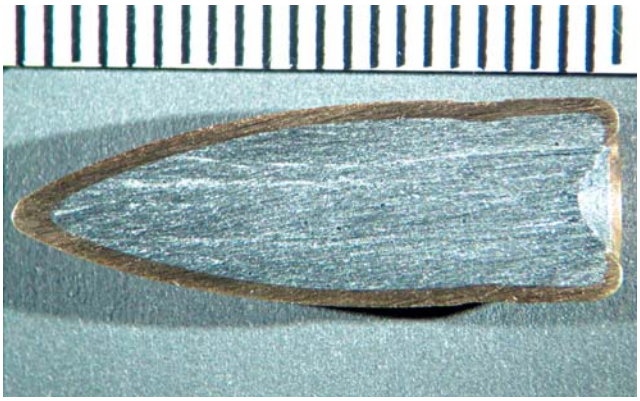

Photo courtesy of Peter Diaczuk

Figure 3. A full metal jacket bullet that was removed from a 7.62 x 39 mm cartridge has been cut in half lengthwise to reveal its construction. Despite the name "full metal jacket," the base of the bullet is not jacketed and, therefore, the exposed lead is susceptible to attack by the energetic gases generated by the burning propellant. These gases impinge upon the exposed lead, some of which is volatilized, allowing it to migrate to the outside surface of the bullet's jacket; it can also condense on the inside of the gun barrel. This lead becomes one source of material that can be deposited at the perimeter of a bullet hole. (Scale is in millimeters.)

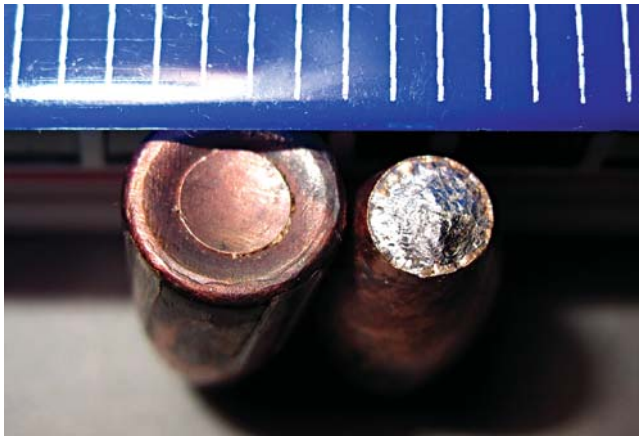

Photo courtesy of Peter Diaczuk

Figure 4. Two unfired 7.62 mm soft-point bullets, one is base up (left) and the other is base down (right). The base-up bullet reveals that the jacket material continues around the bullet's base, sealing off the lead core. The base-down bullet shows that the jacket does not extend fully to the tip, leaving exposed lead to interact with the object that the bullet impacts (therefore, the name "soft point" bullet). Similar to the mechanism described in Figure 3, this lead becomes one source of material that can be deposited at the perimeter of a bullet hole. (Scale is in sixteenths of an inch.)

advertent contamination from non-GSR sources, e.g. airbags (8), fireworks (9), brake pads (10), etc. Confirmation of this hypothesis in conjunction with the distinct fiber-end morphology, as demonstrated in this research, provides a simple and definitive means to confirm or refute the statement that a hole was produced by a bullet using microanalytical methods readily available in most forensic laboratories.

EXPERIMENTAL

The bullet holes were initially examined by stereomicroscopy with Leica EZ-4D and Wild M5 stereomicroscopes using a combination of transmitted, oblique and co-axial illumination. Isolated individual fibers were mounted on glass microscope slides in various refractive index oils (n=1.520 and n=1.660 at 20° C). The preparations were then examined by transmitted polarized light microscopy using an Olympus BH2 microscope. Fibers were mounted on carbon tabs on aluminum stubs, which were then gold-coated for SEM analysis. SEM analysis was conducted using a JEOL 6490LV SEM with a Thermo Noran System Six Silicon Drift Detector at 20keV with a spot size that varied from 20 to 65 (nominal value) with backscattered electron (BSE) and secondary electron (SE) imaging detectors.

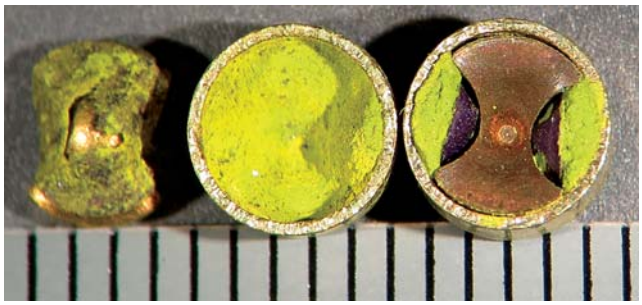

Photo courtesy of Peter Diaczuk

Figure 5. Ammunition primer removed from an unfired cartridge is shown intact on the right. A similar primer is disassembled to reveal its two main components, the anvil (left) and the cup (center). The yellow mustard color is a result of the lead styphnate initiator. When struck by the firing pin, the impact-sensitive composition is crushed between the inside of the cup and the anvil, igniting it and sending a shower of sparks into the body of the cartridge to then ignite the smokeless powder. These sparks contain combustion by products of the lead styphnate, thus contributing lead to the system. Even if the jacket seals off the lead core of the bullet (as in Figure 4), the lead contribution from the primer will present a source of lead that can be carried with the bullet to the impact site. (Scale is in millimeters.)

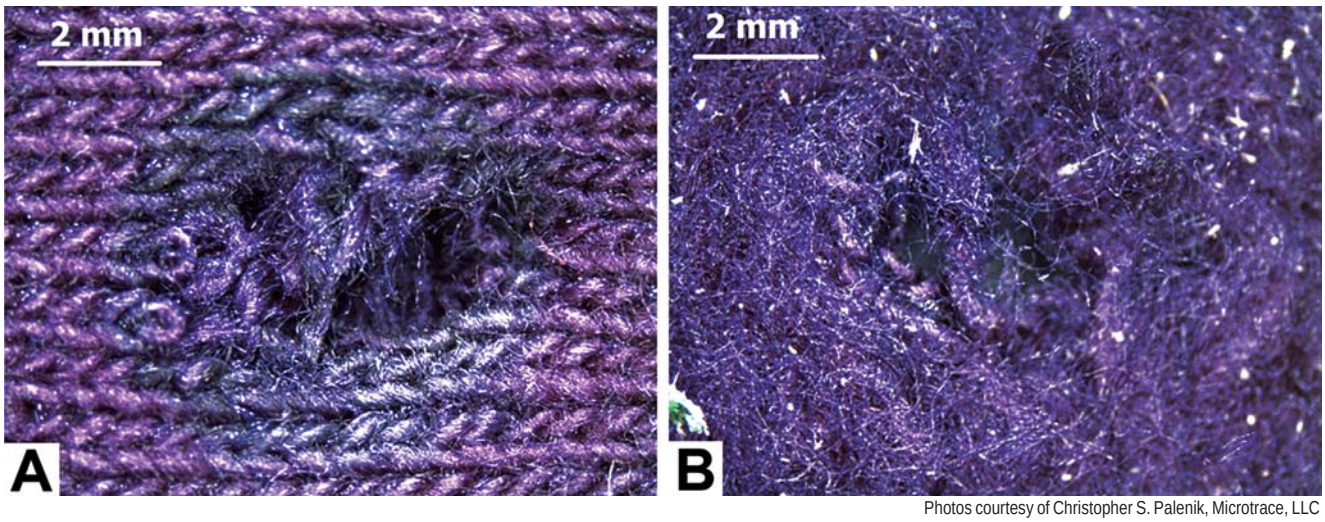

Photos courtesy of Christopher S. Palenik, Microtrace, LLC

Figure 6. The entry (6A) and exit (6B) sides of a single-bullet perforation in a cotton-polyester blended fabric. The entry side (6A) shows a ~2 mm wide annular discoloration that surrounds the hole, which is generally referred to as "bullet wipe."

RESULTS AND DISCUSSION

Exemplar Preparation

An exemplar fabric containing multiple entry and exit points was prepared for this examination by firing Wolf ammunition (7.62 x 39 123 GR. SP, steel jacketed, lead bullet) from an AK-47 rifle at a distance of 3.5 meters normal to the target at an air temperature of 30° C through a 70% cotton and 30% polyester (polyethylene terephthalate) dyed sweatshirt fabric. The fiber composition was confirmed by polarized light microscopy (PLM) and Fourier transform infrared microspectroscopy (FTIR) (6). The entry and exit side of one bullet perforation in the fabric is shown in Figure 6. The entry side of the hole (Figure 6A) shows a ~2 mm wide annular discoloration or staining that surrounds the hole, which is generally referred to as "bullet wipe" (4). Stereomicroscopy was used to determine and document the size of the holes (~0.5 cm), their relatively round shape and to observe a distinct directionality imparted to the broken threads, which are consistent with, though not definitively indicative of, the direction of bullet travel. (Fiber direction may vary in many cases due to removal of clothing and other factors.)

Fiber-End Isolation and Preparation

Once located by stereomicroscopy, a more detailed analysis of the frayed fibers was conducted at higher magnification by PLM and SEM. Prior to this, it was necessary to isolate individual fibers for analysis while tracking the end formed by the bullet. Depending on the sample and details of the case, specimens can be prepared in a variety of ways. For SEM, the simplest method is to excise a 2.5 x 2.5 cm fabric square containing the hole in question. In this way, it is possible to study an entire hole in the SEM. The drawbacks of this method are that the broken fibers are not ideally oriented in a direction that is optimal for imaging their ends, and in forensic casework, isolation of an area of this size is not generally an option due to evidence preservation requirements.

For these reasons, single fibers were individually isolated and studied. A single fiber of interest was located under the stereomicroscope and held with a pair of forceps approximately 5 mm from the broken tip (taking care not to touch the broken end). Prior to cutting off the thread from the garment, the fiber to be excised was marked (~10 mm from the broken tip) using a fine-tipped permanent marker while observing under a stereomicroscope. A cut was then made through the marker line, effectively isolating the fiber of interest. A benefit to this method is that the freshly cut ends (both that on the isolated fiber and the end remaining in the fabric) are both marked providing a semi-permanent indicator of the cut ends. This ensures that any future analysis is not confused by razor-cut fiber ends.

Fiber-End Characterization

Characterization of the isolated fibers by PLM was conducted using temporary mounts in refractive index oil (n=1.520). In this way, the generic class of the fiber can be easily identified by its optical properties (6) and, if necessary, washed in xylene, dried and

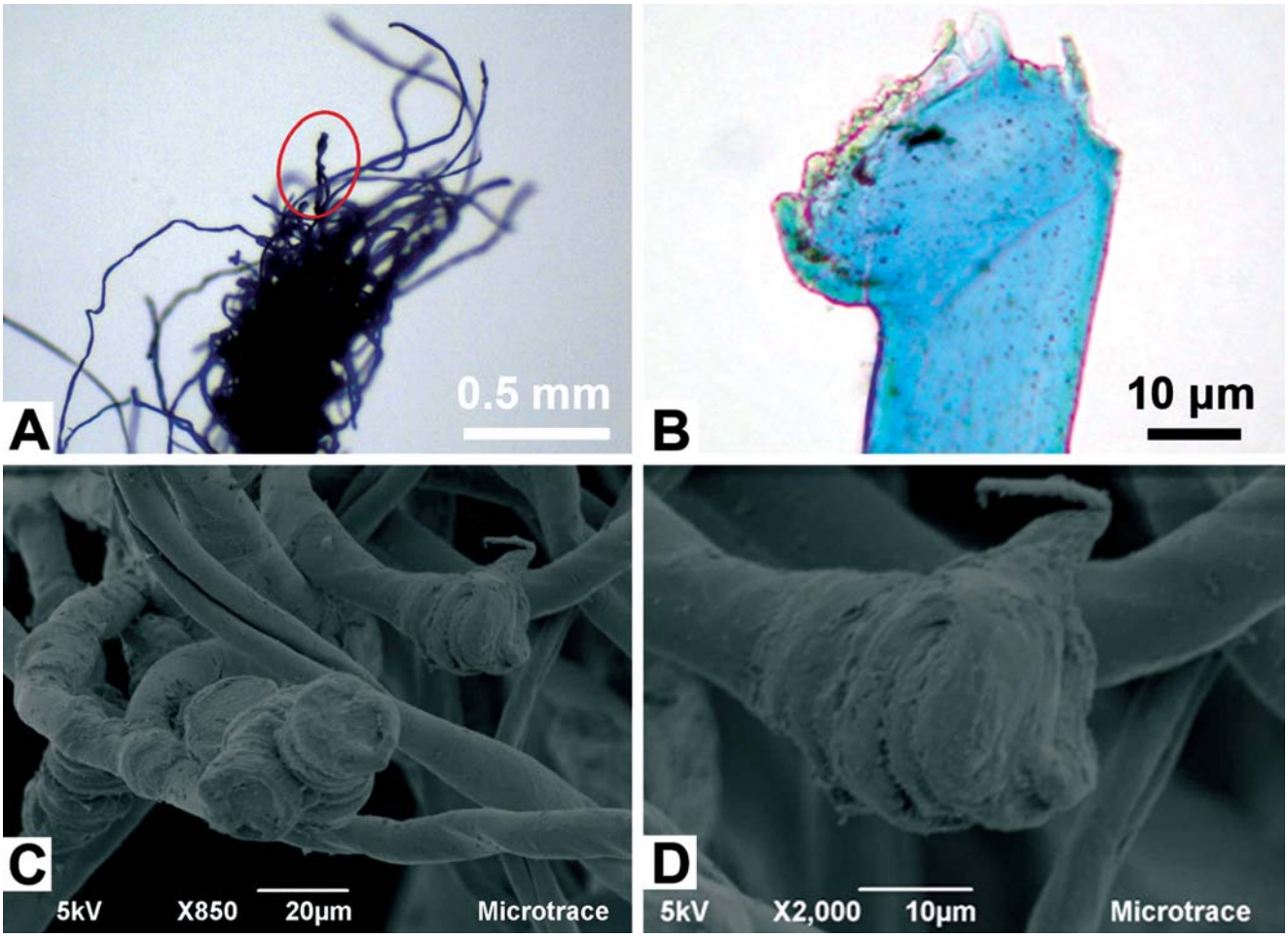

Photos courtesy of Christopher S. Palenik, Microtrace, LLC

Figure 7. 7A: A stereomicroscope image shows yarn composed of multiple fibers that were all severed by the bullet perforation. The red circle highlights a group of fibers that were fused together as a result of the high-energy transfer that occurred during perforation. 7B: A transmitted light image of a broken polyester fiber end shows the characteristic globular end resulting from a high-speed tensile fracture mechanism. 7C and 7D: Multiple fiber ends observed in secondary electron imaging; 7C shows fused fiber ends. 7D: The result of a stretch, fracture and recoil due to a high-speed, high-energy fiber break are captured in the morphology of a broken fiber end.

mounted for SEM analysis (though care should be taken with respect to fiber orientation because xylene will dissolve the orientation mark on the fiber).

SEM analysis was performed in various configurations using a JEOL 6490LV tungsten SEM. Uncoated fibers were successfully examined via backscattered electron imaging in variable pressure mode at 5–20 kV (30–50 Pa). While serviceable, fibers still charged at times under these conditions make the highest quality documentation difficult. For the purposes of publication, fibers were gold coated and observed without issue in both BSE and SE imaging modes. The gold coated fibers were generally preferable for study, documentation and elemental analysis. Despite the thin gold coating, metallic particles of interest (e.g. lead, chromium, iron *etc.*) were easily located in BSE imaging and readily characterized by EDS (as demonstrated here).

Morphology

Indicators of high temperature alteration are visible even at relatively low magnifications obtainable by stereomicroscopy, such as the fusing of multiple fibers shown in Figure 7A. In Figure 7B, the bulbous end typical of a severed fiber resulting from the rapid shear mechanism is shown as observed by PLM. Based on the failure mechanism, which results in partial melting and recoil of the elongated fiber prior to cooling, this characteristic end morphology has been

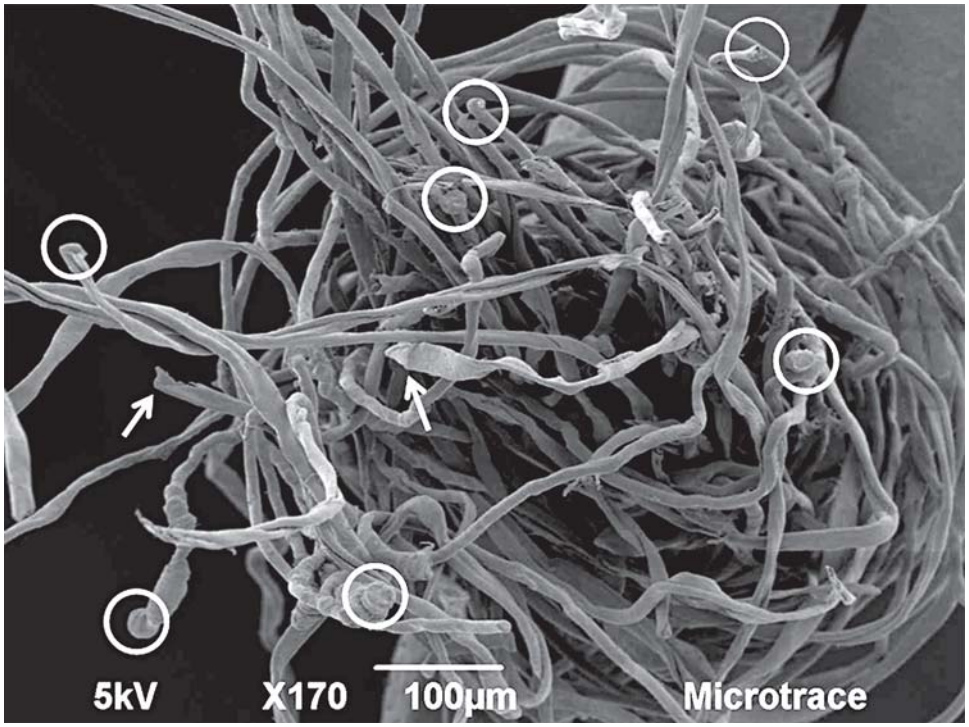

Photo courtesy of Christopher S. Palenik, Microtrace, LLC

Figure 8. A SE-SEM image of a single severed yarn shows numerous polyester ends (circled) all of which have globular ends characteristic of a high-speed, high-energy fracture mechanism. Arrows point to broken cotton fibers, which do not have globular ends.

termed a "globular" end. In general, the globular ends of the fibers show remarkably decreased birefringence when observed between crossed polarizers, which are consistent with prior findings (4, 5). This is expected, due to the loss of orientation when the newly formed fiber ends melt and rapidly cool without any specific means of reorientation.

While indications of globular ends can be observed by PLM, secondary electron imaging in the SEM provides more definitive evidence of the melting, stretching and rebounding that occurs when a thermoplastic fiber undergoes rapid shear. Figure 7C shows the melted globular ends of several fibers. In Figure 7D, the stretch, fracture and recoil resulting from a high-speed, high-energy fiber break are captured in the morphology of a broken fiber end as illustrated by the roughly annular compression marks near the globular end. Cotton (and other cellulosic) fibers do not melt and would not be expected to show such features, which are characteristic of a thermoplastic fiber. However, such fibers, which are often blended with synthetics in a fabric, are readily identified by PLM or SEM by their optical properties and morphology.

A SE-SEM image of a single, entirely severed thread (composed of many twisted fibers) isolated from the bullet hole is shown in Figure 8. Examination of this particular thread by stereomicroscopy, PLM and SEM shows that all of the broken polyester fiber ends in this cluster are globular. In total, more than 90% of the severed synthetic fiber ends counted in these bullet holes show distinct globular ends.

Particle Transfer

By transmitted light, visible discoloration in the form of dark opaque debris on the severed fibers in the bullet hole is apparent (Figure 7B). By reflected light, these same fragments show a dull metallic luster, which is consistent with the appearance of fine lead particles. This surface debris has a more irregular particle size distribution and is clearly distinguishable from the smaller, transparent TiO_2 inclusions that are added to many synthetic fibers as a delustrant.

Because it was anticipated that these metallic particles were related to bullet lead, they were studied by BSE imaging. Figure 9A shows the distribution of lead particles on the severed fiber end where lead-rich particles are indicated by their high contrast (white) against the lower average atomic number of the fiber and background of the image. Elemental analysis by EDS confirms that all of these particles are lead-rich. Figure 9B shows one particle that contains additional detectable iron and chromium, indicating it is a stainless steel particle.

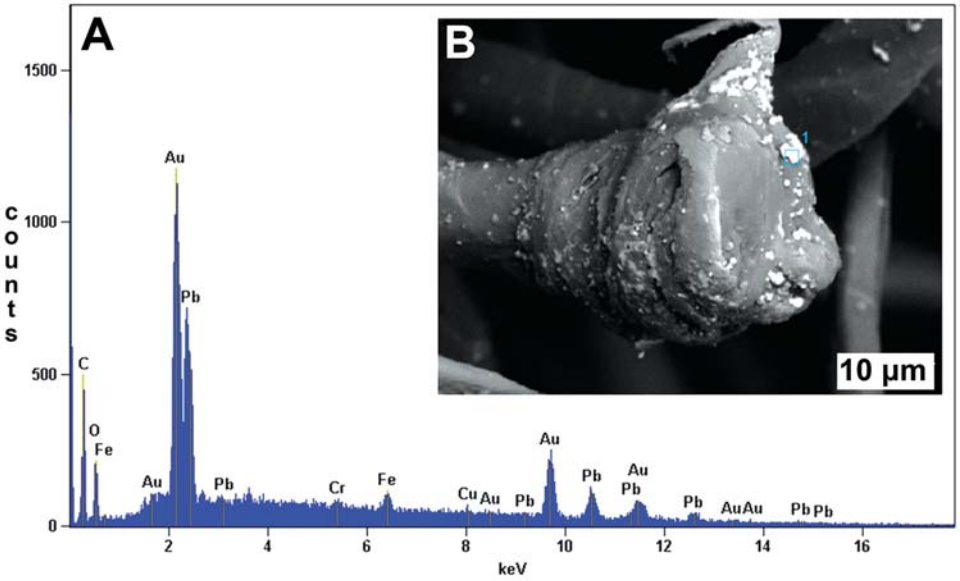

Figure 9. 9A: A BSE-SEM image shows the distribution of lead-rich particles on a broken polyester end. 9B: EDS spectrum of one of these particles also shows the presence of iron and chromium, suggesting the presence of stainless steel. The gold peaks are a result of the coating applied to improve image resolution.

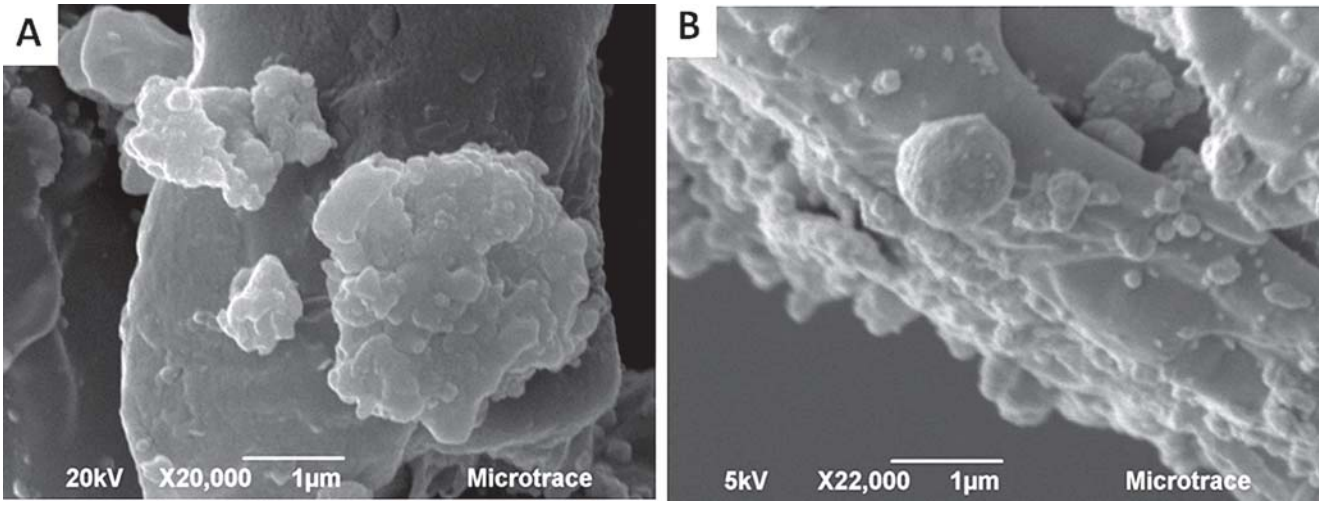

Photos courtesy of Christopher S. Palenik, Microtrace, LLC

Figure 10. SE-SEM images show 10A, lead plates abraded from the perforating bullet and 10B, a lead sphere resulting from aerosol deposition of molten lead. Both types of particles have similar elemental compositions.

Detailed examination of lead particles on these fiber surfaces show that most of them are platy or planar abrasion particles (Figure 10A), while occasional spherical particles are also observed (Figure 10B). Such spheres originate when molten lead cools and solidifies in air to a low surface energy (spherical) morphology. Both the spheres and plates have a similar elemental composition and are composed of lead, with minor antimony and copper (Figure 11). This composition is typical of a bullet lead alloy. None of the particles studied showed evidence of tri-component pGSR (Pb-Ba-Sb) particles (11).

The presence of fused fibers is shown at relatively low magnification in Figure 7A. The fusing of fibers, which was often observed among the fibers in each bullet hole studied, is shown in more detail in Figure 12. Detailed examination of these images shows two fused fibers at a variety of magnifications, which illustrate the extent of the fusing and the distribution of GSR particles on their surface. While lead particles are generally present in higher concentrations at the globular end of the fibers (and qualitatively decrease

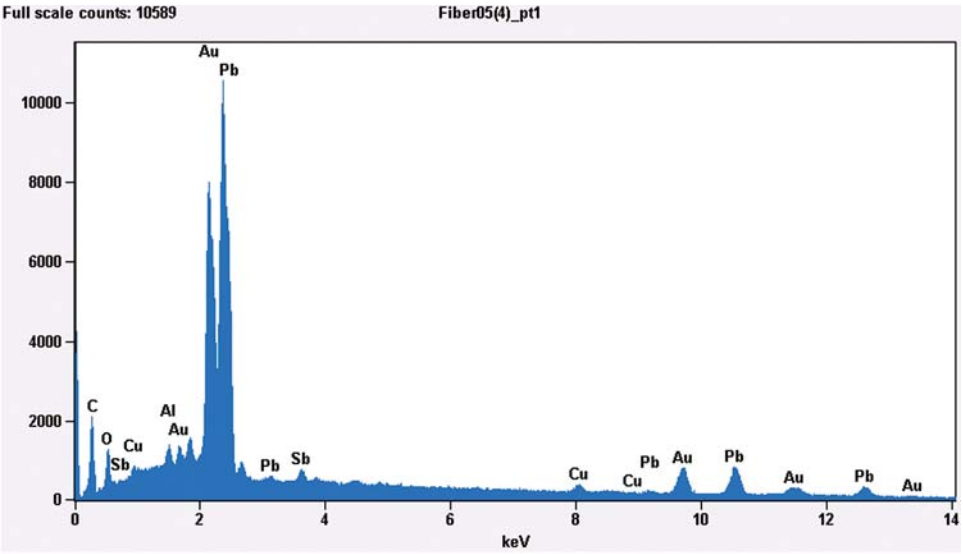

Figure 11. A typical EDS spectrum from a lead particle on the end of a severed fiber.

in number as the distance from the severed end increases), they are also present in high concentrations at the melted interface of the two fused fibers (Figure 12B and 12C). Examination of one of the fused areas also show that not only are the lead particles present on the surface of the fiber, but that they are also trapped within the fused areas, as confirmed by EDS and illustrated visually in the combined BSE/SE image shown in Figure 12D. These images illustrate the irrefutable link between a high-energy transfer and a lead-rich particle transfer, which can only originate from a ballistic event involving a lead or lead-laden projectile.

SUMMARY AND FORENSIC SIGNIFICANCE

These results indicate that a bullet hole from a jacketed soft point (exposed lead) bullet fired through a synthetic fabric can be definitively identified by studying the severed broken ends within a hole to identify the presence of globular ends and the presence of adhering and/or embedded lead particles.

Under certain circumstances, the issue may be raised as to whether certain variables may affect the formation or residence time (persistence) of the characteristic features noted above. Such variables may include environmental factors (such as weather), handling factors, fiber type, ammunition type, speed and firing distance.

Because the physical indicators of bullet perforation established above are subject to unknown and potentially disputed environmental variables (e.g. handling, washing, storage conditions and cross contamination) or firing variables (e.g. ammunition type and velocity), questions of persistence (i.e. residence time) will arise, particularly due to the similarities in particle size and composition shared by GSR. For example, a wealth of research into the affects of environmental conditions on the residence time of GSR particles has been conducted (11, 12) and many laboratories limit the collection of GSR to 24 hours or less after an incident due to concerns over residence and background contamination that may occur over longer periods (12). However, GSR is deposited by a distinctly different mechanism than metallic bullet fragments being transferred to severed fibers in a bullet hole. GSR is deposited *on* a surface at ambient conditions, while metallic ammunition particles transferred during partial melting of the fiber end are partially or entirely embedded *into* the fiber surface. This singular difference illustrates why metal particles associated with a bullet hole will have a distinctly longer residence time, regardless of handling conditions. Similarly, the characteristic globular ends are part of the fabric and are, therefore, not subject to any degradation beyond that expected for the garment as a whole. At ~20 μm in length, the globular end represents only a minor fraction of the total fiber length, which is generally at least 100x longer and physically anchored in the fabric. Therefore, both indicators of bullet perforation are expected to persist through harsh post-firing conditions.

While the exemplar in this work is composed of polyester fibers, many other types of fibers are used in the textile industry (e.g. nylon, polyolefin and rayon).

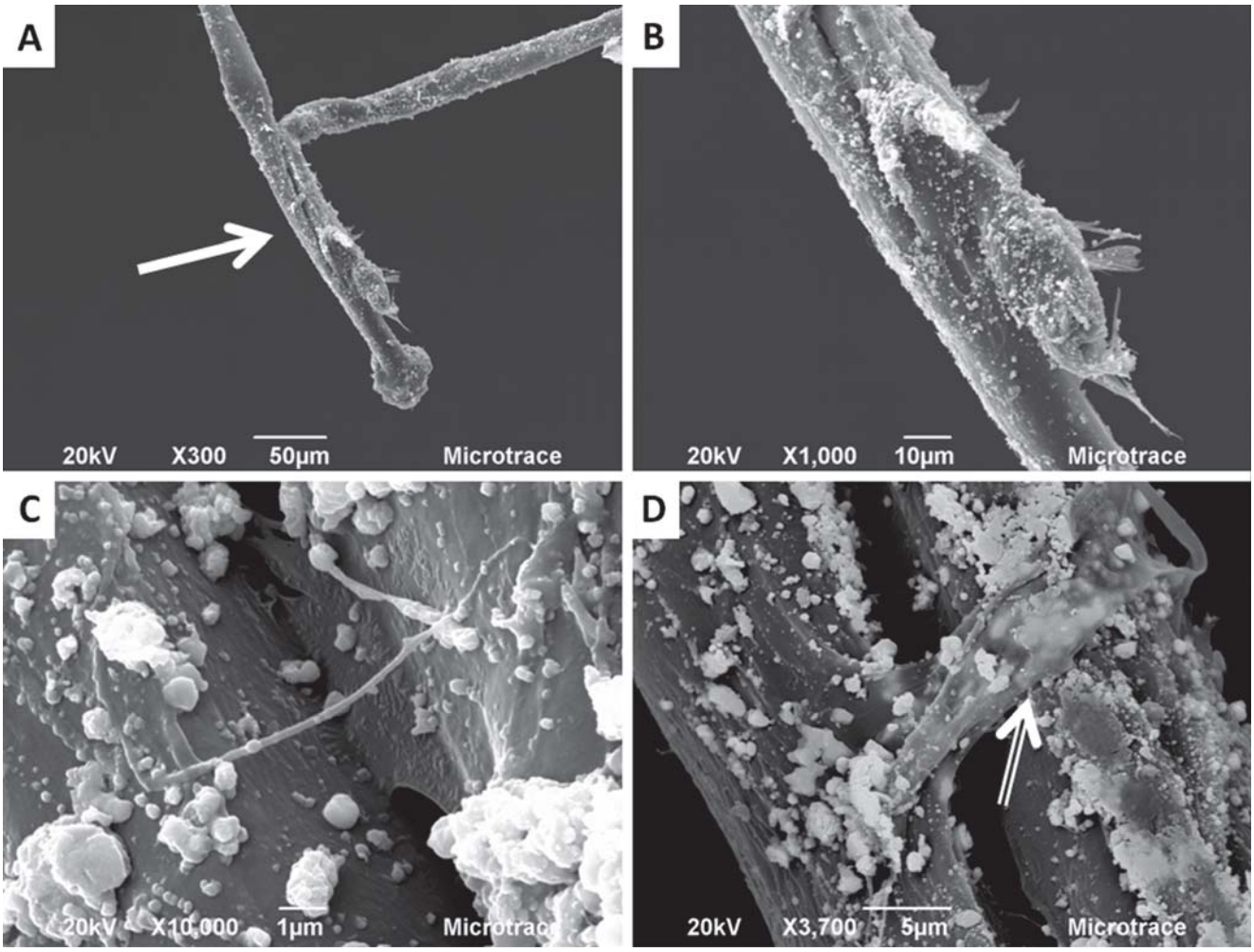

Photos courtesy of Christopher S. Palenik, Microtrace, LLC

Figure 12. 12A: An SE-SEM image shows two fibers that were thermally fused during the high-speed impact event. 12B: Close-up view of the area denoted by an arrow in part (12A) showing the presence of lead particles on the fused fibers (SE-SEM). 12C: Highest magnification image of the same fused fibers at the melted interface showing individual, discrete lead particles abraded from the bullet during impact (SE-SEM). 12D: Mixed SE-BSE SEM image shows that lead particles are actually embedded within the melted polymer (arrow).

The mechanism of high-energy tensile fracturing also occurs in other thermoplastic fibers such as nylon to produce similar globular ends (5). In contrast, cellulosic fibers (e.g. cotton, rayon and vegetable fibers) will not melt and, therefore, do not form globular ends. SEM examination of cotton fibers in our research confirms this (Figure 8), however, metal particles of lead were observed on the surface of the severed cotton fibers as well.

Ammunition type is another factor that will vary in casework. Ammunition and its jacketing are manufactured with various compositions. The detection of multiple metals on the globular ends by EDS in this work suggests that metals from bullets of different compositions and from different parts of the ammunition hold the potential to be transferred to a severed fiber. Conversely, the observation of specific lead alloys, GSR particles, copper, brass, stainless steel or other components can provide additional investigative information about the source of the impacting bullet.

Finally, the question of globular end formation may be challenged. The mechanism of globular end formation is directly related to the kinetic energy of the bullet passing through the fabric, which in turn is related to the velocity of the bullet. A prior study of globular ends produced in polyester and nylon fibers correlated to chronographed bullet velocities showed that various combinations of firearms and ammuni-

tion used to obtain velocities, ranging between 40 m/s and 823 m/s, all resulted in the production of globular ends (5). Microscopic features suggestive of other sources of fabric defect formation (e.g. "pinching" from scissors, tool marks from razor cuts, etc.) have also been studied (3) and have been shown to be different from those created by a bullet.

Therefore, in addition to proving a positive, the question may arise in certain contexts as to whether absence of such features can be used to state that a fabric "defect" was not produced by a bullet. Based on this research, both globular end formation and metallic particle capture would be expected to occur under all but the most extreme conditions. Therefore, it follows that the absence of such indicators is strongly suggestive of a negative conclusion — i.e. a bullet did not produce the hole.

ACKNOWLEDGEMENTS

The authors would like to thank Jason Beckert and Brendan Nytes of Microtrace, LLC for discussions and comments during the course of this research.

REFERENCES

1. J.A. Bailey. "Analysis of Bullet Wipe Patterns on Cloth Targets," *Journal of Forensic Identification,* Vol. 55, No. 4, pp 448–460, 2005.

2. P.R. DeForest, L. Rourke, M. Sargeant and P. A. Pizzola. "Direct Detection of Gunshot Residue on Target: Fine Lead Cloud Deposit," *Journal of Forensic Identification,* Vol. 58, No. 2, pp 265–276, 2008.

3. J. Hearle, B. Lomas and W. Cooke, Eds. *Atlas of Fibre Fracture and Damage to Textiles*, 2nd ed., The Textile Institute, CRC Press, Woodhead Publishing Limited, 1998.

4. L. Haag, in *Shooting Incident Reconstruction*, Elsevier Academic Press, pp 37–39, 2006.

5. C. Huemmer. "The study of rapid shear in synthetic fibers from ballistic impact to fabrics using polarized light microscopy" (MS thesis), John Jay College of Criminal Justice, City University of New York, 2007.

6. S. Palenik. "Microscopical Examination of Fibres," in *Forensic Examination of Fibres*, 2nd ed., J. Robertson and M. Grieve, Ed., Taylor and Francis: London, pp. 153–178, 1999.

7. M. Raverby. "Analysis of Long-Range Bullet Entrance Holes by Atomic Absorption Spectrophotometry and Scanning Electron Microscopy," *Journal of Forensic Sciences,* Vol. 27, No. 1, pp 92–112, 1982.

8. R. Berk. "Automated SEM/EDS Analysis of Airbag Residue I: Particle Identification," *Journal of Forensic Sciences,* Vol. 54, No. 1, pp 60–68, 2009.

9. P. Mosher, M. McVicar, E. Randall and E. Sild. "Gunshot Residue-Similar Particles Produced by Fireworks," *Canadian Society* of *Forensic Science Journal,* Vol. 31, No. 2, pp 157–168, 1998.

10. C. Torre, G. Mattutino, V. Vasino and C. Robino. "Brake Linings: A Source of Non-GSR Particles Containing Lead, Barium and Antimony," *Journal of Forensic Sciences,* Vol. 47, No. 3, pp 494–504, 2002.

11. ASTM E1588 – 10e1. Standard Guide for Gunshot Residue Analysis by Scanning Electron Microscopy/Energy Dispersive X-ray Spectrometry, ASTM International: West Conshohocken, PA.

12. R. Berk, S. Rochowicz, M. Wong and M. Kopina. "Gunshot Residue in Chicago Police Vehicles and Facilities: An Empirical Study," *Journal of Forensic Sciences,* Vol. 52, No. 4, pp 838–841, 2007.

Forensic Fiber Examination Guidelines: Infrared Analysis of Textile Fibers

Scientific Working Group for Materials Analysis (SWGMAT)

1.0. Scope

If polymer identification is not readily apparent from optical data alone, an additional method of analysis should be used such as microchemical tests, melting point, infrared (IR) spectroscopy, or pyrolysis gas chromatography. Infrared analysis offers the advantage of being the least destructive of these methods.

IR spectroscopy is a valuable method of fiber polymer identification and comparison in forensic examinations. The use of IR microscopes coupled with Fourier transform infrared (FTIR) spectrometers has greatly simplified the IR analysis of single fibers, thus making the technique feasible for routine use in the forensic laboratory.

Attenuated Total Reflectance (ATR) accessories for FTIR spectrometers, as well as stand-alone ATR instruments and diamond anvil cells with a beam condenser, enable the analyst to collect infrared spectra from manufactured textile fibers with minimal sample preparation.

This guideline is intended to assist individuals and laboratories that conduct forensic fiber examinations and comparisons in the effective application of infrared spectroscopy to the analysis of fiber evidence. Although this guide is intended to be applied to the analysis of single fibers, many of its suggestions are applicable to the infrared analysis of small particles in general.

2.0. Reference Documents

SWGMAT Trace Evidence Quality Assurance Guidelines (January 2000)

SWGMAT Trace Evidence Recovery Guidelines (October 1999)

SWGMAT Forensic Fiber Examination Guidelines (April 1999)

ASTM E1492-11 Standard Practice for Receiving, Documenting, Storing, and Retrieving Evidence in a Forensic Science Laboratory

ASTM E131-10 Standard Terminology Relating to Molecular Spectroscopy

ASTM 1421-99(2009) Standard Practice for Describing and Measuring Performance of Fourier Transform Mid-Infrared (FTIR) Spectrometers: Level Zero and Level One Tests

ASTM E2224-10 Standard Guide for Forensic Analysis of Fibers by Infrared Spectroscopy

3.0. Terminology

Absorbance (A): the logarithm to the base 10 of the reciprocal of the transmittance, (T).

$A = \log_{10}(1/T) = -\log_{10} T$

Absorption Band: A region of the absorption spectrum in which the absorbance passes through a maximum.

Absorptivity (a): Absorbance (A) divided by the product of the sample pathlength (b) and the concentration of the absorbing substance (c). a = A/bc

Absorption Spectrum: A plot, or other representation, of absorbance or any function of absorbance, versus wavelength, or any function of wavelength.

Attenuated Total Reflection (ATR): An instrumental method of FTIR spectrum collection in which an infrared beam is reflected within an optically dense crystal (e.g., diamond), creating a wave that extends beyond the crystal's exterior surface into a sample that is placed in direct contact with the crystal.

Background: Apparent absorption caused by anything other than the substance being analyzed.

Cellulosic Fiber: Fiber composed of polymers formed from glucose.

Evanescent wave: a wave that is created when a beam of infrared light is reflected within an optically dense crystal. This evanescent wave extends beyond the surface of the crystal and into an adjoining sample.

Far-Infrared: Pertaining to the infrared region of the electromagnetic spectrum with wavelength range from approximately 50 to 1,000 µm (wavenumber range 200 to 10 cm^{-1}).

Fourier Transform (FT): A mathematical operation that converts a function of one independent variable to that of a different independent variable. In Fourier transform infrared (FTIR) spectroscopy, the Fourier transform converts a time function (the interferogram) to a frequency function (the infrared absorption spectrum). Spectral data is collected through the use of an interferometer, which replaces the monochromator found in a dispersive infrared spectrometer.

Fourier Transform Infrared (FTIR) Spectrometry: A form of infrared spectrometry in which an interferogram is obtained. This interferogram is then subjected to a Fourier transform to obtain an amplitude-wavenumber (or wavelength) spectrum.

Generic Class: A group of fibers having similar, but not necessarily identical, chemical composition. A generic name applies to all members of a group and is not protected by trademark registration. Generic names for manufactured fibers include, for example; rayon, nylon, and polyester. Generic names used in the United States for manufactured fibers were established as part of the Textile Fiber Products Identification Act enacted by Congress in 1954.

Infrared: Pertaining to the region of the electromagnetic spectrum with wavelength range from approximately 0.78 to 1,000 µm (wavenumber range 12,820 to 10 cm^{-1}).

Infrared Spectroscopy: Pertaining to spectroscopy in the infrared region of the electromagnetic spectrum.

Manufactured Fiber A class name for various families of fibers produced from fiber-forming substances, including synthetic polymers, modified or transformed natural polymers and glass.

Mid-Infrared: Pertaining to the infrared region of the electromagnetic spectrum with wavelength range from approximately 2.5 to 50 µm (wavenumber range 4,000 to 200 cm^{-1}).

Near-Infrared: Pertaining to the region of the electromagnetic spectrum with wavelength range from approximately 0.78 to 2.5 µm (wavenumber range 12800 to 4,000 cm^{-1}).

Spectrometer: Photometric device for the measurement of spectral transmittance, spectral reflectance, or relative spectral emittance.

Subgeneric Class: A group of fibers within a generic class that shares the same polymer composition. Subgeneric names include, for example; nylon 6, nylon 6,6, and poly(ethylene terephthalate).

Transmittance (T): The ratio of radiant power transmitted by the sample, (I), to the radiant power incident on the sample, (I_o). $T = I/I_o$

Wavelength: The distance, measured along the line of propagation, between two points that are in phase on adjacent waves.

Wavenumber: The number of waves per unit length, in a vacuum, usually given in reciprocal centimeters (cm^{-1}).

4.0. Summary of Guidelines

This guideline covers identification of fiber polymer composition by interpretation of absorption spectra obtained by infrared spectroscopy. It is intended to be applicable to a wide range of infrared spectrometer and microscope configurations. Spectra may also be obtained by a variety of alternative IR techniques not covered in this document.

This analytical method covers the analysis of manufactured textile fibers (with the exception of inorganic fibers). Although natural fibers may also be analyzed by IR spectroscopy, light microscopy is the preferred method for the identification of natural fibers.

5.0. Significance and Use

Fiber samples may be prepared and mounted for infrared analysis by a variety of techniques. Infrared spectra of fibers are obtained using an IR spectrometer coupled with an IR microscope, ATR accessory, or diamond compression cell with beam condenser. Fiber polymer identification is made by comparison of the fiber spectrum with reference spectra.

Consideration should be given to the potential for additional compositional information that may be obtained by IR spectroscopy over PLM alone (see the Microscopy chapter of SWGMAT's Forensic Fiber Examination Guidelines). The extent to which IR spectral comparison is indicated will vary with specific sample and case evaluations.

IR analysis should follow visible and fluorescence comparison microscopy, polarized light microscopy, and UV or visible spectroscopy. However, it should be conducted before dye extraction for thin-layer chromatography due to the semi-destructive nature of the technique. Because of the large number of subgeneric classes, forensic examination of acrylic and modacrylic fibers is likely to benefit significantly from IR spectral analysis. Useful distinctions between subtypes of nylon and polyester fibers can also be made by IR.

6.0. Sample Handling

The general handling and tracking of samples should meet or exceed the requirements of ASTM 1492-05 (14).

The quantity of fiber used and the number of fiber samples required will differ according to the following:
-Specific technique and sample preparation,
-Sample homogeneity,
-Condition of the sample, and
-Other case-dependent analytical conditions, concerns, or both.

Sample preparation should be similar for all fibers being compared. Except when using ATR, fibers should be flattened prior to analysis in order to obtain the best quality spectra. Flattening the fiber alters the morphology, and therefore, the minimum length of fiber necessary for the analysis should be used. Flattening the fibers can alter the crystalline/amorphous structure of the fiber and result in minor differences in peak frequencies and intensities. This must be taken into consideration when making spectral comparisons. Leaving the fiber unflattened, while allowing crystallinity-sensitive bands to be observed unaltered, results in distortion of peak heights due to variable pathlengths. In certain situations, a combination of both approaches may be advisable. Fibers analyzed via Attenuated Total Reflectance (ATR) do not require flattening prior to analysis. During ATR analysis, sample fibers are flattened by a hand-operated press when the sample is mounted against the diamond surface.

The flattened fiber may be mounted across an aperture, on an IR window, or between IR windows. It is important that the longitudinal plane (flattened surface) of the fiber be as nearly parallel to the IR window or other mount as possible. Common IR window materials used for this purpose include, but are not limited to, KBr, CsI, BaF_2, ZnSe, and diamond. The choice of window material should not reduce the effective spectral range of the detector being used. Where the fiber is mounted between two IR windows, a small KBr crystal should be placed next to the fiber. The background spectrum should be acquired through this crystal to avoid interference fringes that would arise if the spectrum were acquired through the air gap between the two IR windows.

Where several fibers are mounted on or in a single mount, they should be well separated (physically) so that their positions can be unambiguously documented for later retrieval, reanalysis, or both, and to prevent spectral contamination from stray light that might pass through another fiber.

7.0. Analysis

A mid-infrared spectrometer and an infrared microscope that is compatible with the spectrometer or diamond compression cell with beam condenser are recommended. The lower frequency cutoff varies with the microscope detector used (preferably no higher than 750 cm^{-1}).

Useful sample preparation accessories include, but are not limited to, sample supports, infrared windows, presses, dies, rollers, scalpels, and tungsten probes.

7.1. Equipment Readiness
All spectrometer and microscope components should be turned on and allowed to reach thermal stability prior to commencement of calibration and operational runs. It should be noted that some FTIR instruments are designed to work best when left on or in the standby mode 24 hours a day.

Analysts should refer to the manufacturer's guidelines for the optimum performance of their instruments.

7.2. Instrument Performance and Calibration
It is essential that instrument performance and calibration be evaluated routinely, at least once a month, in a comprehensive manner.

The preferred performance evaluation method is in accordance with ASTM 1421-99(2009). In brief, this includes evaluating system throughput, single-beam spectrum, 100% T line, and polystyrene reference spectrum.

Instrument performance records should be maintained on hard copy, computer disk, electronically or all of the above. Case documentation may vary by laboratory but should include the date, the operator, the system parameters, and the original instrumental output data.

7.3. Sample Illumination and Detector Measurement Apertures
The apertures that control the areas (fields) of sample illumination and detector measurement in an IR microscope may be of fixed or variable size and may be either rectangular or circular in shape. Variable rectangular apertures are recommended because they can be more closely matched to the fiber shape. Light throughput, stray light reduction, and aperture focus in the sample image plane are some of the considerations in selecting aperture parameters and positioning. Fiber width, length, flatness, and linearity will usually limit the size of the illumination and detector apertures used for analysis. In general, the illuminating and detector fields should lie within the boundaries of the fiber edges.

7.4. Objective and Condenser Adjustment
The objective, condenser, or both should be optimized, if possible, for any IR window that lies between the optic and the sample in the beam path. This compensation reduces spherical aberration and permits more accurate focus.

7.5. Polarization Bias of the Infrared Spectrometers and Microscopes
Infrared spectrometers and microscopes exhibit a polarization bias. It is essential that fiber alignment be consistent throughout an analysis.

7.6. Focusing
Samples should be focused as close to the center of the sample volume as possible and centered on the optical axis of the system. The condenser should be focused and re-centered if necessary. This is best accomplished using a circular field aperture.

The detector measurement aperture width should be adjusted to just slightly less than the width of the fiber but preferably not less than 10 µm. The aperture length may vary with sample geometry but should not be so great as to allow the detector to be saturated when acquiring a background spectrum. The illuminating field aperture should be adjusted so that the image of its edges coincide with those of the detector measurement aperture. The size and position of the apertures should not vary between sample and background data acquisition for a given analysis.

7.7. Background Spectrum
A background spectrum refers to a reference absorption spectrum, which includes the absorbance contributions of all system components except the sample of interest. The IR window or windows with KBr crystal are all considered part of the system. The system parameters for background spectra should be identical to the parameters used for sample spectra (with the possible exception of gain and number of scans). These parameters include resolution,

mirror velocity, and spectrometer aperture size. Because the apertures are adjusted to fit the sample, it is usually most convenient to acquire the sample spectrum prior to acquiring the background spectrum.

7.8. Resolution

Resolution should be set at 4 cm^{-1} (one data point every 2 cm^{-1}). Higher resolution may be used. The additional data points, however, typically yield no further analytical information for polymer samples.

7.9. Spectral Quality and Data Storage

The quality of a spectrum is dependent on the focus, size of the window, thickness of the fiber, nature of the fiber, delustrant, etc.. A spectrum should be repeated, for example, if the baseline is noisy, or diffraction effects and/or interference fringes are pronounced. These hamper the identification of fibers and comparison of spectra.

It is generally useful to save all data after it is generated and prior to any modification.

7.10. Identification of Fiber Polymers by IR Spectra

Successful identification of fiber polymers by IR spectra depends on experience and familiarity with fiber reference spectra. Spectral identification is accomplished by comparison with spectra of known reference standards. A library of reference IR spectra is essential. A library of reference fiber IR spectra obtained using the same technique used for the unknown fiber is desirable. It is also desirable to have available authenticated reference samples of the fibers.

For identification, the positions of the absorption bands according to wavelength or wavenumber and their relative intensities must be compared with those of a known reference spectrum. The generic class of manufactured textile fibers can be unequivocally identified with the exception of cellulosic generic classes (these may be differentiated by their optical properties). The subgeneric class of synthetic manufactured fibers may be identified.

8.0. Examination Documentation

Similarity or dissimilarity in the IR spectra should be noted when making a fiber comparison. The examination documentation should contain sufficient detail to support conclusions.

9.0. References

Bartick, E. G. Considerations for fiber sampling with infrared microspectroscopy. In: *The Design, Sample Handling, and Applications of Infrared Microscopes, ASTM STP 949.* Ed., P. B. Roush. American Society for Testing and Materials, Philadelphia, 1987, pp. 64-73.

Bartick, E. G., Tungol, M. W., and Reffner, J. A. A new approach to forensic analysis with infrared microscopy: Internal reflection spectroscopy, *Analytica Chimica Acta* (1994) 288:35-42.

Carlsson, D. J., Suprunchuk, T., and Wiles, D. M. Fiber identification at the microgram level by infrared spectroscopy, *Textile Research Journal* (1977) 47:456-458.

Cook, R. and Paterson, M. D. New techniques for the identification of microscopic samples of textile fibres by infrared spectroscopy, *Forensic Science International* (1978) 12:237-243.

Federal Trade Commission Rules and Regulations Under the Textile Products Identification Act, Title 15, U. S. Code Section 70, et seq. 16 CFR 303.7.

Fox, R. H. and Schuetzman, H. I. The infrared identification of microscopic samples of man-made fibers, *Journal of Forensic Sciences* (1968) 13:397- 406.

FTIR Spectroscopy, Attenuated Total Reflectance (ATR), Technical Note; PerkinElmer Life and Analytical Sciences; Shelton, CT., 2005.

Gál, T., Ambrus, I., and Urszu, S. Forensic analysis of textile fibres by Fourier transform infrared diamond cell technique, *Acta Chimica Hungarica* (1991) 128:919-928.

Garger, E. F. An improved technique for preparing solvent cast films from acrylic fibers for the recording of infrared spectra, *Journal of Forensic Sciences* (1983) 28:632-637.

Grieve, M. C. Another look at the classification of acrylic fibres: Using FTIR microscopy, *Science and Justice* (1995) 35:179-190.

Grieve, M. C. and Kotowski T. M. Identification of polyester fibres in forensic science, *Journal of Forensic Sciences* (1977) 22:390-401.

Hartshorne, A. W. and Laing, D. K. The identification of polyolefin fibres by infrared spectroscopy and melting point determination, *Forensic Science International* (1984) 26:45-52.

Hatch, K. L. *Textile Science.* West Publishing, Minneapolis/St. Paul, 1993, pp. 84.

Messerschmidt, R. G. Minimizing optical nonlinearities in infrared microspectrometry. In: *Infrared Microspectroscopy: Theory and Applications.* Eds. R. G. Messerschmidt and M. A. Harthcock. Marcel Dekker, New York, 1988, pp. 1-19.

Read, L. K. and Kopec, R. J. Analysis of synthetic fibers by diamond cell and sapphire cell infrared spectrophotometry, *Journal of the Association of Official Analytical Chemists* (1978) 61:526-532.

Tungol, M. W., Bartick, E. G., and Montasser, A. Forensic examination of synthetic textile fibers by microscopic infrared spectrometry. In: *Practical Guide to Infrared Microspectroscopy.* 2nd. ed. Ed., H. Humecki. Marcel Dekker, New York, 1995.

Tungol, M. W., Bartick, E. G., and Montaser, A. The development of a spectral data base for the identification of fibers by infrared microscopy, *Applied Spectroscopy* (1990) 44:543-549.

Forensic Fiber Examination Guidelines: Fabric and Cordage

***Scientific* Working Group for Materials Analysis (SWGMAT)**

1.0 Scope

These guidelines are intended to assist individuals and laboratories that conduct examinations of fabric and cordage for the purposes of identifying types of fabric, cordage and damage, as well as potentially associating such damage with the implement that caused it.

2.0 Reference Documents

SWGMAT Trace Evidence Quality Assurance Guidelines (January 2000)

SWGMAT Trace Evidence Recovery Guidelines (October 1999)

ASTM Standard E2225-10, "Standard Guide for Forensic Examination of Fabrics and Cordage," ASTM International, West Conshohocken, PA, 2010, www.astm.org.

3.0 Terminology

Braid: The intertwining (not twisting) of 3 or more strands to make a rope/cord.

Cordage: Any type of rope, string, twine, etc. made from twisting or braiding yarns together to produce a long strand either with a single ply or multiple plies.

Cord: A thin rope made of several strands braided or twisted together with an overall diameter less than 3/16".

Core: Fibers, one or more filaments, or other material running lengthwise through the center of a rope or other cordage.

Course: The row of loops or stitches running across a knit fabric, corresponding to the weft in woven fabrics.

Crown: The raised portion of a strand in twisted cordage.

Knit fabric: A structure produced by interlooping one or more ends of yarn or comparable material.

Filament: A single continuous fiber extruded to an indefinite length.

Fusing: Uniting together as by melting together.

Nonwoven: Fabrics made directly from fibers held together by mechanical, chemical and/or thermal means.

Pitch: The number of crowns per inch along the length of the cordage.

Ply: One of the individual yarns that are twisted together to form a cord.

Rope: A heavy, strong cord made from natural or manufactured fibers with an overall diameter greater than 3/16".

Selvage: The narrow edge of woven fabric that runs parallel to the warp. It is made with stronger yarns in a tighter construction than the body of the fabric to prevent unraveling.

Staple: Natural fibers or manufactured fibers cut into short lengths.

Strand: The largest individual element used in the final rope making process and obtained by joining and twisting together several yarns or groups of yarns

Thermoplastic: A synthetic material that is semi-permanently fusible or softens at high temperatures.

Thread: A slender, strong strand or cord made by plying or twisting yarns, typically used for stitching.

Tracer: A yarn or yarns different in color, size and/or composition from that of the basic cordage found within or alongside a ply, strand or braid.

Twine: Two or more twisted strands or a single-strand yarn with an overall diameter less than 4 millimeters, made from natural fibers.

Twist, Direction of: The direction of twist in yarns is indicated by the capital letters S and Z. A yarn has an S-twist if, when it is held vertically, the spirals around its central axis slope in the same direction as the middle portion of the letter S, and Z-twist if they slope in the same direction as the middle portion of the letter Z.

Wale: A column of loops lying lengthwise in a knit fabric, corresponding to the warp in woven fabric.

Warp: The set of yarns in all woven fabrics that runs lengthwise and parallel to the selvage and is interwoven with the weft.

Weft (Filling): In a woven fabric, the yarn running from selvage to selvage at right angles to the warp.

Woven fabric: Generally used to refer to fabric that is formed by the perpendicular interlacing (weaving) of warp and weft (filling) yarns.

Yarn: A general term for a continuous strand of textile fibers, filaments or material in a form suitable for intertwining to form a textile structure via any one of a number of textile processes (e.g. knitting, weaving)

4.0 Summary of Guide

Due to their general availability, fabrics and cordage are often encountered by forensic scientist~~s~~, who examine, identify and compare these types of evidence. Structural details such as design, construction, and composition can provide information that may assist the examiner in reaching a conclusion.

5.0 Significance and Use

The construction, composition and color of textiles contain useful comparative characteristics for forensic examinations. Textiles may appear in a variety of constructions: woven, knit, nonwoven or in combination. The range of colors in which textiles are offered in the marketplace is vast and constantly changing due to styles and seasons. A complete characterization of the fabrics, including their construction, and other materials used in the assemblage of a textile (e.g., sewing thread) is a critical component of a comprehensive forensic fabric or cordage examination.

6.0 Sample Handling

Photography of the item prior to conducting any analyses in order to provide documentation of original condition is recommended. Prior to textile analysis, other evidence (e.g., hair, blood, paint) that may require additional examination should be documented and collected. Any physical damage (e.g., worn, cut, broken, frayed) should also be documented at this time.

A questioned material (e.g., a piece of fabric, yarn, tuft of fibers) must not be brought in contact with the known fabric from which it is suspected to have originated until a preliminary examination of the questioned specimen has been performed.

The condition of a questioned material (e.g., shape, position, layers or relation of one yarn to another) should not be altered before a preliminary examination for damage has been conducted.

A sample to be used for composition testing should not be cut from ends of yarn or edges of fabric if there is a possibility of physically matching a questioned item to a known item. It is recommended that the known sample be collected away from the existing edge(s) and the location marked.

All data collected on questioned and known samples should be placed into, or referenced within, the specific case file.

The information contained on tags in textiles should be recorded, especially the Registered Number (RN) and the Woolen Products Label number (WPL) when applicable. These refer to the manufacturer of the textile and can assist the examiner with tracking a particular textile or garment.

7.0 Analysis

Prior to any analysis of the fibers comprising a fabric or cordage, the fabric or cordage should be examined for physical matches, pattern evidence, damage such as thermoplastic fusions, cut/tear marks, etc. Any adhesives or other material used in bonding fabrics, carpet backings, etc., should also be noted.

7.1 Physical Match. Physical matches should be considered if two pieces of fabric or cordage having cut or torn ends are to be compared. A physical match must be documented by photography, sketching or through a thorough description of the condition of corresponding threads and their relative positions in the damaged areas on the questioned and known pieces (“longs and shorts”).

If a physical match is not possible, comparison of the color, pattern, construction and composition of the items in question should be undertaken to determine if they are similar and if the items could have originated from the same source.

7.2 Fabric. A fabric examination is primarily a process of deconstructing the fabric by dissecting its constituent elements. Each of these elements can have a number of sub-elements, all of

which must be characterized to complete the examination for comparison purposes. These elements include, but are not limited to, the following:

- Overall
  - Construction (woven, knit, nonwoven)
  - Yarn counts in warp and weft direction
  - Color(s) and design
  - Type of dyeing or printing
  - Sewing threads, buttons, decorations, etc.

- Yarns
  - Staple or filament fibers in yarns
  - Diameter
  - Yarn twist
  - Number of plies
  - Direction of twist of each ply
  - Number of filaments in each ply, if feasible
  - Composition of yarn
  - Blend of two or more types of fibers within each ply

7.3 Cordage. A cordage examination is primarily a process of deconstructing the rope or cordage by dissecting its constituent elements (see figure 1). Each of these elements can have a number of sub-elements, all of which must be characterized to complete the examination for comparison purposes. These elements include, but are not limited to, the following:

- Overall
  - Diameter
  - Braided or plied
  - Direction of twist
  - Number of crowns or turns per inch
  - Number of plies/strands/braids
  - Core, if any
  - Color(s)
  - Coatings, if any
  - Tracers, if any

- Plies / Strands / Braids
  - Staple or filament fibers
  - Twisted or non-twisted
  - Direction of twist for each
  - Crowns or turns per inch for each
  - Number of filaments in each, if feasible

After the construction has been established, then the constituent fibers should be analyzed with the appropriate microscopical and instrumental techniques. Additional characteristics may be used if necessary to adequately describe the cordage.

7.4 Fabric impressions

An impression made from an item of clothing, for example, in a vehicular accident or other situation may provide valuable evidence. The weave or knit pattern of a fabric impressed onto another surface or into blood, grease, etc. can be compared to the garment in question. Fabric impressions of a known fabric can be made with impression material used for footwear impressions and then transferred onto a piece of paper or digitally reproduced onto a clear sheet of plastic to use as an overlay for direct comparison with the evidence impression. Portions of a

garment that were stitched or have other identifying features may help align the patterns. The count of the warp and weft yarns per inch and any other identifying construction indicators must be comparable between the impression and the fabric. Fibers left in the impression should be recovered and examined further as they may add additional significance to the overall fabric and fiber examination.

7.5 Thermoplastic fusions
Fiber fusions may occur between textiles and various plastic or polymer coated surfaces due to the heat caused by the friction of impact, such as from high-speed impacts with a vehicle. Partially fused fibers may be found in a fabric impression on a vehicle hood, interior of a car, etc. Photographs with a scale should be taken prior to removing any fused fibers to preserve the impression. Care must be taken not to damage the impression when attempting to remove fibers partially fused to the surface. The removed fibers can then be compared to a known sample and, if necessary, the thermoplastic properties can be assessed (e.g., melting point).

7.6 Cut/Tear Fabric Damage
Examination of the cuts and tears in fabrics can offer information as to the implement that may have produced the damage. Analysis and documentation of the shape, pattern, and dimensions of the damage is followed by analysis of the edges of the cut/torn yarns. The analysis should be both visual and with the aid of magnification, either with a microscope or magnifying lens, to determine if the individual yarns of the fabric are cut or torn. A scanning electron microscope may add further detail to the examination of the cuts and tears of the individual fibers.

Test cuts may be made with questioned implements to see if they make cuts or tears that are consistent with the shape, pattern and dimensions of those found on the evidence. These test cuts should be made after all other forensic examinations, such as DNA and latent fingerprint analyses, have been conducted on the item. Test cuts are made in an undamaged portion of the item corresponding to where the damage originally was noted or, if it is too damaged, in a similar type of fabric or garment. The fabric should be placed on an appropriate substrate prior to producing the test cuts/tears. Examples of suitable substrates include cardboard boxes of sufficient strength to withstand the insertion of a blade or other cutting implement, styrofoam, gel blocks and body replicas. In addition to comparing the test cuts/tears to those found in the evidence, the orientation of a knife in relation to the cut mark may be determined. This can be done if a single-edged blade was used, by finding the characteristic “V” shaped notch at one end of a cut/tear mark, which corresponds to where the flat portion of the blade entered the fabric. It should be noted that the dimension of the test cut/tear may not correlate on a one-to-one basis with the knife due to fabric stretch.

8.0 Report Documentation

If a physical match is found, it should be reported in a manner that will indicate that the two or more pieces of material were at one time a continuous piece of fabric or cordage. If no physical match is possible/found, a complete fabric/cordage comparison, including construction and composition, can be performed. If, during this examination, the items are found to be the same in all tested characteristics, then the examiner reports that the two objects exhibit the same color, construction, and composition and are consistent with originating from the same source.

Fabric impressions associated to a known sample should be reported as consistent in all points of comparison between the questioned and known impressions; however, the results should not be limited to that specific garment as having produced the impression due to the bulk manufactured nature of textile material. It is rare that a positive identification can be made for fabric impression evidence and care should be taken to account for possible fabric stretch or distortion. Fabric impressions without fiber transfer associations generally do not rise to the same level of significance as those with a transfer.

In fabric damage cases, when comparing test cuts/tears to documented damage, and an association is found, the report wording should be limited to a statement that the cut/tear marks are consistent in size, shape and general appearance with having been made by that weapon or another implement of similar characteristics and dimensions. If a transfer of fibers has been found on the weapon, the significance of the conclusion in the report may be strengthened. However, the report wording concerning the fabric damage should still be limited to the cut/tear analysis wording without overstating the results or precluding other possible weapons of similar nature from having produced the damage.

9.0 Bibliography

Budworth G, *Knots and Crime*, London, UK: Police Review Publishing Co., 1985.

Complete Textile Glossary. Charlotte, NC: Celanese Acetate LLC. 2001.

Griffin, H "Glass Cuts in Clothing" 2007 Trace Evidence Symposium http://projects.nfstc.org/trace/docs/final/Griffin_paper_GlassCuts.pdf

Hatch KL, *Textile Science*. Minneapolis, MN: West Publishing Company, 1993.

Hearle, J.W.S., Lomas, B., Cooke, W.D. and Duerden, I.J., *Fibre failure and wear of materials - An atlas of fracture, fatigue and durability*. New York, NY: John Wiley and Sons, Inc., 1989.

Himmelfarb D, *The Technology of Cordage Fibres and Rope*, Metuchen, NJ: Textile Book Service, 1957.

-, The Cordage Directory.

-, *RN/WPL Encyclopedia*, New Providence, NJ: Reed Reference Publishing, 1996.

-, *Davison's Textile Blue Book*, Nealy BW (ed), Concord, NC: Davison Publishing Company, 1996.

Jochem, G. "Fiber-Plastic Fusions and Related Trace Material in Traffic Accident Investigation" in *Trace Evidence Analysis - More Cases in Mute Witnesses*, ed. Houck,MM, Elsevier 2004.

Koch, SL and KL Deaver, "The Effects of Scavenging and Weathering on Fabric Damage" 2007 Trace Evidence Symposium http://projects.nfstc.org/trace/docs/Trace%20Presentations%20CD-2/koch.pdf

Mahall K, *Quality assessment of textiles - Damage detection by microscopy*. New York, NY: Springer-Verlag, 1993.

Masakowski, S. et al, Fiber-Plastic Fusions in Traffic Accident Reconstruction*, Journal of Forensic Sciences*, 1986, pp.903-912.

Monahan, DL and HWJ Harding, "Damage to Clothing – Cuts and Tears," *Journal of Forensic Sciences*, 35/4 (901-912).

Oelsner GH, *A Handbook of Weaves*, New York, NY: Dover Publications, Inc., 1952.

Pelton, WR, "Distinguishing the Cause of Textile Fiber Damage Using the Scanning Electron-Microscope (SEM)," *Journal of Forensic Sciences*, 1995, 40/5, (874-882).

Taupin, JM, “Testing Conflicting Scenarios – A role for simulation experiments in damage analysis of clothing,” *Journal of Forensic Sciences*, 1998, 43/4 (891-896).

Taupin, JM, F-P Adolf and J Robertson “Examination of Damage to Textiles” *Forensic Examination of Fibres 2nd Ed,* Robertson and Grieve, eds. London: Taylor and Francis Publishing, 1999.

Taupin, JM, Cwiklik, C. *Scientific Protocols for Forensic Examination of Clothing*. Boca Raton: CRC Press, 2011.

Wiggins, K., Recognition, Identification and Comparison of Rope and Twine, *Science and Justice*, 1995, 35(1), pp. 53-58.

Figure 1: Fiber Rope Components and Constructions

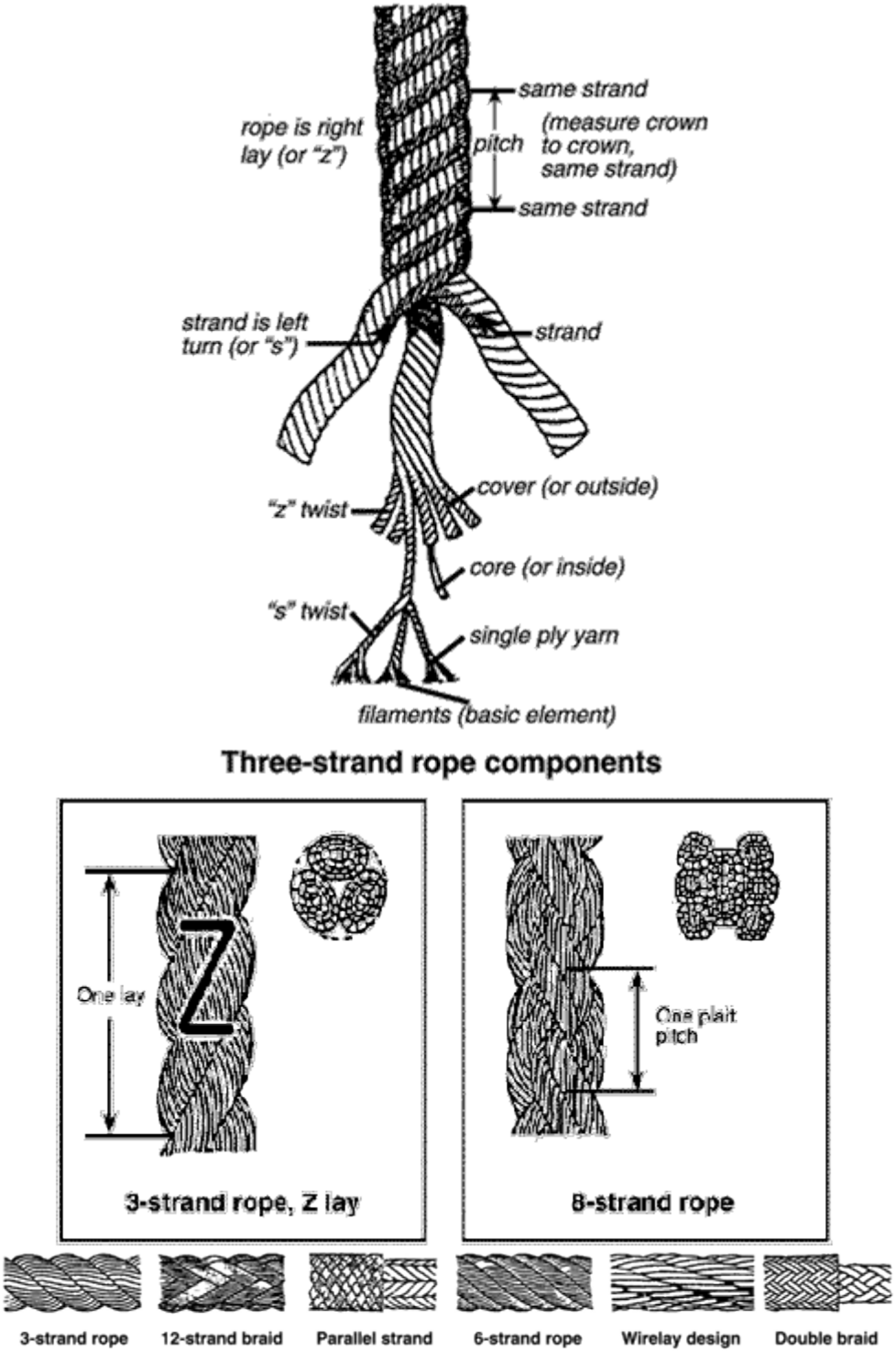

Note: From *The Cordage Directory*, published by The Cordage Institute, Hingham, Massachusetts, 1998.